

A NEW PARADIGM: LIGNIN TO POLYMER NETWORKS BY DECATUNGSTATE PHOTO- CATALYZED PARTIAL DEPOLYMERIZATION

HONGYAN WANG

A dissertation
submitted to the Faculty of
the department of chemistry
in partial fulfillment
of the requirements for the degree of
Doctor of Philosophy

Boston College
Morrissey College of Arts and Sciences
Graduate School

Jun 2024

A NEW PARADIGM: LIGNIN TO POLYMER NETWORKS BY DECATUNGSTATE PHOTOCATALYZED PARTIAL DEPOLYMERIZATION

Hongyan Wang

Advisor: Ph.D. Dunwei Wang, Professor of Chemistry and Chairperson; Margaret A. and Thomas A. '53 Vanderslice Chair in Chemistry

As an inedible component of biomass, lignin features rich functional groups that are desired for chemical syntheses. How to effectively depolymerize lignin without compromising the more valuable cellulose and hemicellulose has been a significant challenge. Existing biomass processing procedures either induce extensive condensation in lignin that greatly hinders its chemical utilization or focus on fully depolymerizing lignin to produce monomers that are difficult to separate for subsequent chemical synthesis. Here, we report a new approach to selective partial depolymerization, which produces oligomers that can be readily converted to chemically recyclable polymer networks. The process takes advantage of the high selectivity of photocatalytic activation of the β -O-4 bond in lignin by decatungstate catalysts (DT). In the photocatalytic system, DT works as both catalyst and oxidant, leading to two different reaction pathways, slow and steady bond cleavage pathway, and fast but limited oxidation pathway. The availability of exogenous electron mediators or external oxidants promotes cleavage or oxidation of this bond, respectively, enabling high degrees of control over the depolymerization and the stoichiometry of a key functional group, C=O, in the products. The resulting oligomers can then be readily utilized for the synthesis of polymer networks through reactions between C=O and branched $-NH_2$ as a dynamic covalent cross-linker. Importantly, the resulting polymer network can be recycled to enable a circular economy of materials directly derived from biomass.

TABLE OF CONTENTS

Table of Contents	iv
List of figures	v
Table of abbreviations	viii
Acknowledgements	x
1 Chapter 1 Introduction	1
1.1 Lignocellulose.....	1
1.2 Technical lignin and its utilization	5
1.3 Lignin-first strategy and monomerization studies	8
1.4 The scope of this thesis	18
1.5 Reference	20
2 Chapter 2 Photocatalytic depolymerization of native lignin toward chemically recyclable polymer networks	26
2.1 Introduction	26
2.2 Methods.....	29
2.3 Results	36
2.3.1 Proposed reaction mechanisms.....	36
2.3.2 Photocatalytic depolymerization of model compounds with β -O-4 motif	40
2.3.3 Photocatalytic depolymerization of native lignin	47
2.3.4 Polymerization of lignin oligomers.....	53
2.4 Discussion.....	57
2.5 Reference	58
3 Chapter 3 Large scale native lignin photocatalytic upcycling toward polyimine networks via oligomers with adjustable functionalities	63
3.1 Introduction	63
3.2 Methods.....	66
3.3 Results	69
3.3.1 Optimization of photocatalytic system	69
3.3.2 Kinetics in controllable lignin photocatalytic depolymerization	73
3.3.3 Promotion of lignin oxidation reaction.....	80
3.3.4 Lignin polymerization from lignin oligomers with varied C=O stoichiometry	85
3.4 Discussion.....	87
3.5 Reference	87
4 Chapter 4 Conclusion	93

LIST OF FIGURES

Figure 1.1	1
Figure 1.2	3
Figure 1.3	3
Figure 1.4	4
Figure 1.5	4
Figure 1.6	5
Figure 1.7	6
Figure 1.8	7
Figure 1.9	9
Figure 1.10.....	10
Figure 1.11.....	12
Figure 1.12.....	14
Figure 1.13.....	16
Figure 1.14.....	17
Figure 1.15.....	19
Figure 2.1	28
Figure 2.2	28
Figure 2.3	31
Scheme 2.1.....	33
Scheme 2.2.....	35
Figure 2.4	37
Figure 2.5	38
Figure 2.6	38
Figure 2.7	39
Figure 2.8	39
Figure 2.9	40

Figure 2.10.....	41
Figure 2.11.....	41
Figure 2.12.....	42
Figure 2.13.....	43
Figure 2.14.....	44
Figure 2.15.....	45
Figure 2.16.....	47
Figure 2.17.....	48
Figure 2.18.....	49
Figure 2.19.....	49
Figure 2.20.....	51
Figure 2.21.....	51
Figure 2.22.....	52
Figure 2.23.....	52
Figure 2.24.....	53
Figure 2.25.....	54
Figure 2.26.....	55
Figure 2.27.....	56
Figure 2.28.....	56
Figure 3.1.....	70
Figure 3.2.....	70
Figure 3.3.....	71
Figure 3.4.....	72
Figure 3.5.....	73
Figure 3.6.....	75
Figure 3.7.....	76
Figure 3.8.....	77
Figure 3.9.....	77
Figure 3.10.....	79
Figure 3.11.....	79
Figure 3.12.....	81
Figure 3.13.....	82
Figure 3.14.....	83

Figure 3.15	84
Figure 3.16	84
Figure 3.17	86

TABLE OF ABBREVIATIONS

2D-HSQC	2-dimensional heteronuclear single-quantum coherence spectroscopy
AAEMA	(2-acetoacetoxy)ethyl methacrylate
AC	acetone
AIBN	azobisisobutyronitrile
AN	acetonitrile
Ar-OMe	aryl methoxy
BDE	bond dissociation energy
DCM	dichloromethane
DI water	deionized water
DIPEA	diisopropylethylamine
DMA	dynamic mechanical analysis
DMBQ	2,6-dimethoxybenzoquinone
DMSO	dimethyl sulfoxide
DPA	9,10-diphenyl anthracene
DPN	dynamic polymer networks
DSC	differential scanning calorimetry
DT	decatungstate
EA	ethyl acetate
GC-MS	gas chromatography and mass spectrometry
GPC	gel permeation chromatography
HAR	hydrogen atom return
HAT	hydrogen atom transfer
Hex	hexanes
Jeffamine	trimethylolpropane tris[poly(propylene glycol), amine terminated] ether
LMCT	ligand-to-metal charge transfer
MeOH	methanol

MMA	methyl 2-methylprop-2-enoate
M_n	number average molecular weight
NaDT	sodium decatungstate
NHPI	N-hydroxyphthalimide
NMR	nuclear magnetic resonance
PCET	proton-coupled electron-transfer
PDMS	polydimethylsiloxane
PHBA	p-hydroxybenzoic acid
PPone	2-phenoxy-1-phenylethanone
PPol	2-phenoxy-1-phenylethanol
PUR/PIR	polyurethane/polyisocyanurate
PTFE	polytetrafluoroethylene
RCF	reductive catalytic fractionation
RD-RCD	reactive distillation-reductive catalytic deconstruction
RDS	rate-determining step
SCS	spin-center shift
SEC	size exclusion chromatography
TAEA	tris(2-aminoethyl)amine
TBA ⁺	tetrabutylammonium
TBAB	tetrabutylammonium bromide
TBADT	tetrabutylammonium decatungstate
THF	tetrahydrofuran
TLC	thin layer chromatography

ACKNOWLEDGEMENTS

Five years of graduate student life have passed by in a flash. Looking back on these years, I feel a significant growth. It is difficult to express in words how I felt when my thesis was about to be completed.

First of all, I would like to express my sincerest thanks to my advisor, Professor Dunwei Wang, for his invaluable work from the beginning to the end of my five years as a graduate student. He recognizes me when I work hard and encourages me when I am depressed. He acts as an alarm when I am complacent and a beacon when I am confused. On the occasion of my graduation, I would like to say that it's my fortune to get Prof. Dunwei Wang as my advisor.

Secondly, I would like to express my gratitude to my committee members, Prof. Matthias Waegele, Prof. Lucas Bao, and Prof. Alexis Grimaud. During the past five years, I learnt a lot from them.

Next, I would like to express my gratitude to my second mentor, Dr. Rong Chen. When I felt down and confused after getting hurt by my first mentor, she stood out and pulled me out of abyss, and kept warming me with her heat. I really cherish the time worked with her, and I really appreciate her selfless help during that.

Then, I would like to express my gratitude to my collaborator, Mr. Gavin Giardino and Prof. Jia Niu. The experiments of polymerization, polymer recycling and characterization were performed by Gavin Giardino and advised by Prof. Jia Niu. Their expertise in polymer science helped us a lot in the whole project, and their timely replies made the cooperation much more efficient. I also cherish the time worked with them.

Besides, I would like to express my gratitude to my colleagues in Wang lab, and my friends. Working with you was really happy, and your ideas inspired me a lot. I learnt a lot from you in different perspectives.

Finally but not the last, I would like to express my gratitude to my parents. They supported me during the pandemic and inflation, which enabled me focus on research. They also comforted me when I was struggling because they understood the difficulty in the PhD study.

In the end, I want to thank myself. I successfully overcame the challenge in mental health instead of getting beaten by it. I wouldn't see the scenery on the other side if I chose not to pursue the highest degree. Thanks for staying there, myself.

Hongyan Wang
May 2024

CHAPTER 1: INTRODUCTION

1.1 LIGNOCELLULOSE

Biomass has attracted increasing research attention as a renewable resource to replace petroleum for the production of chemicals¹ and plastics.² As an inedible and abundant biomass source that features rich chemical structures, lignocellulose is a predominant starting material in biomass upcycling.³ It contains three major components, cellulose, hemicellulose, and lignin,⁴ the last of which makes up 15-40%⁵ of the total biomass (**Figure 1.1**).

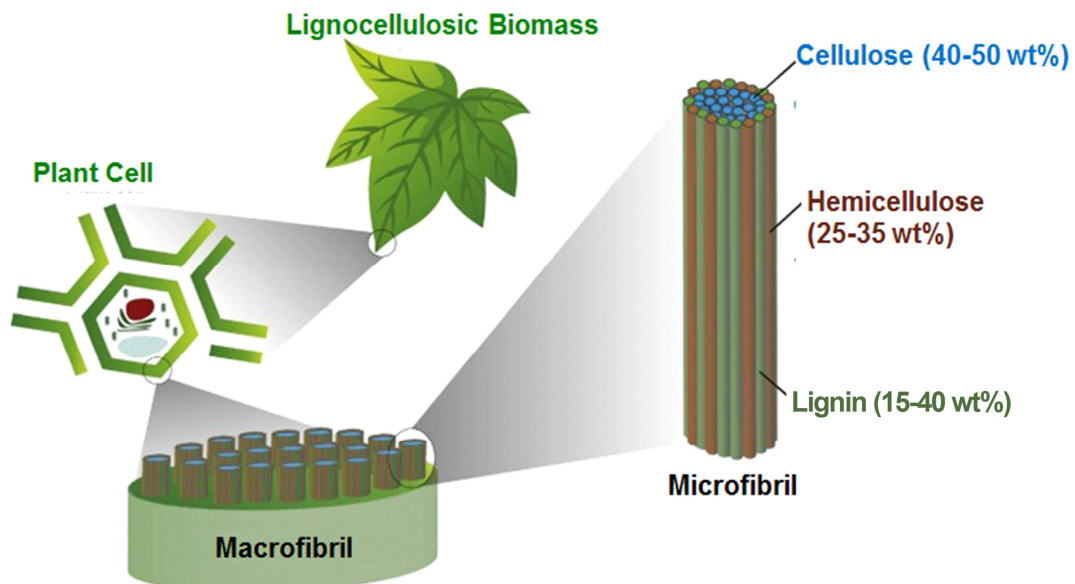


Figure 1.1 The composition of lignocellulosic biomass.⁴

Of them, cellulose and hemicellulose have been the center of previous attention in biomass utilization.⁶⁻⁸ Cellulose and hemicellulose are already widely valorized in the pulping industry;⁶⁻⁷ besides, due to the consistent and relatively easily hydrolysable glycosidic bonds, these polysaccharides are also used in bio-ethanol⁸ production as a sustainable fuel, as well as in the biomaterials and biomedical industry.⁹ However, as the most important source of renewable aromatic compounds, lignin is kept underutilized in this “cellulose-first” strategy. During the delignification process in pulp industry, separated lignin has been largely discarded as a waste or burned to just retrieve its thermal energy.^{5, 10-11}

One important reason is the complicated and heterogeneous chemical structure of lignin¹² (**Figure 1.2**). Lignin is a highly complex aromatic biopolymer which is mainly composed of three phenolic monomers: sinapyl, coniferyl, and p-coumaryl units, all of which share a central aromatic core and differ in the methoxyl substitutions.¹³ On the one hand, lignin is rich with oxygen-containing functional groups, including methoxyl, hydroxyl, carbonyl, and carboxylic ester groups.¹⁴ These features make lignin highly attractive as a feedstock for synthetic purposes. On the other hand, due to the radical mechanism in lignin biosynthesis process (**Figure 1.3**),¹⁵ different ways of lignin monomer radicals' coupling lead to different linkage between them: C–C (β -5, 5-5, β - β , β -1) and C–O–C (β -O-4, 4-O-5, α -O-4) ether bonds with different bond dissociation energies (BDE) (**Figure 1.4-1.5**),¹⁶ which increases the difficulty of lignin depolymerization toward monomers.

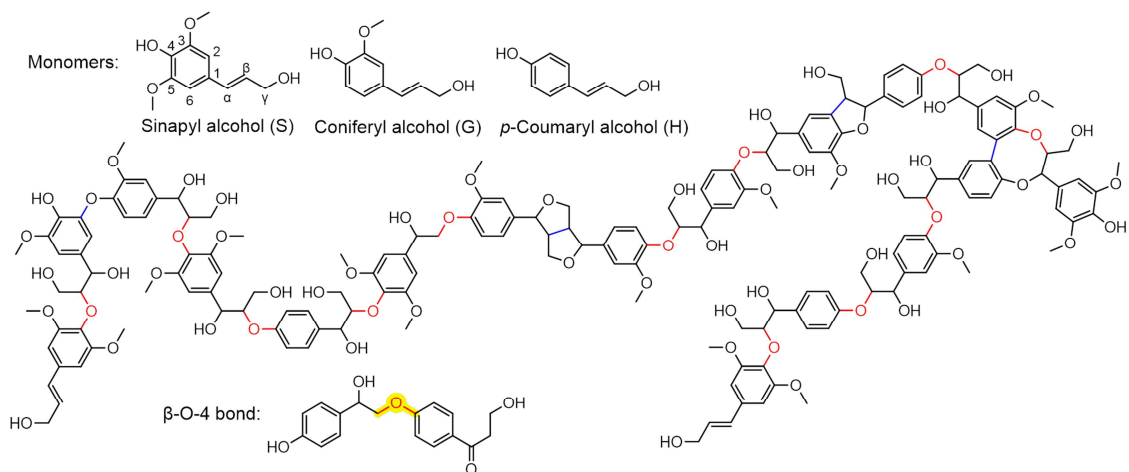


Figure 1.2 The monomers and overall structure of lignin with the β -O-4 bond highlighted.¹²

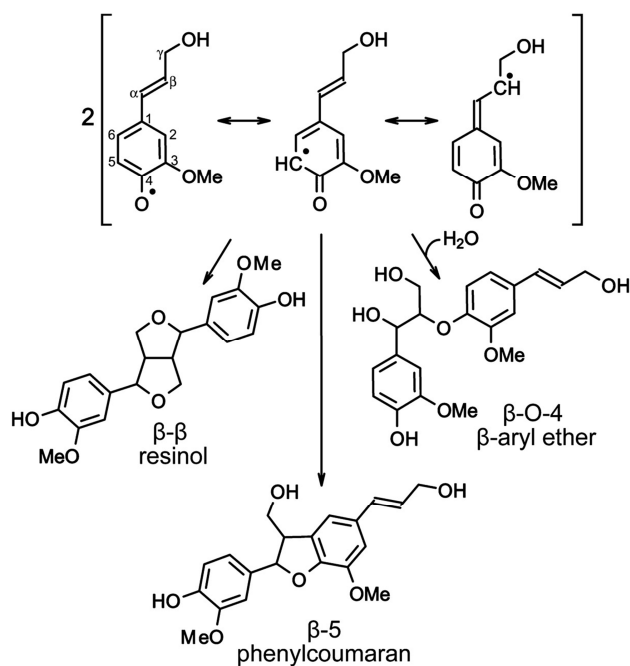


Figure 1.3 The radical mechanism of C-C (β -5, β - β) and C-O-C (β -O-4) motif formation in lignin biosynthesis.¹⁵

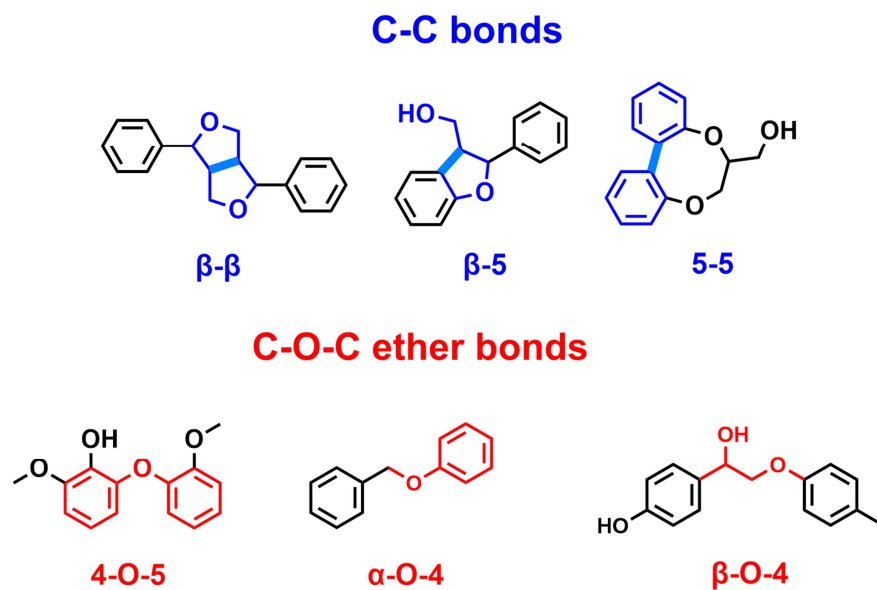


Figure 1.4 Schematics of C-C and C-O-C motifs in native lignin.

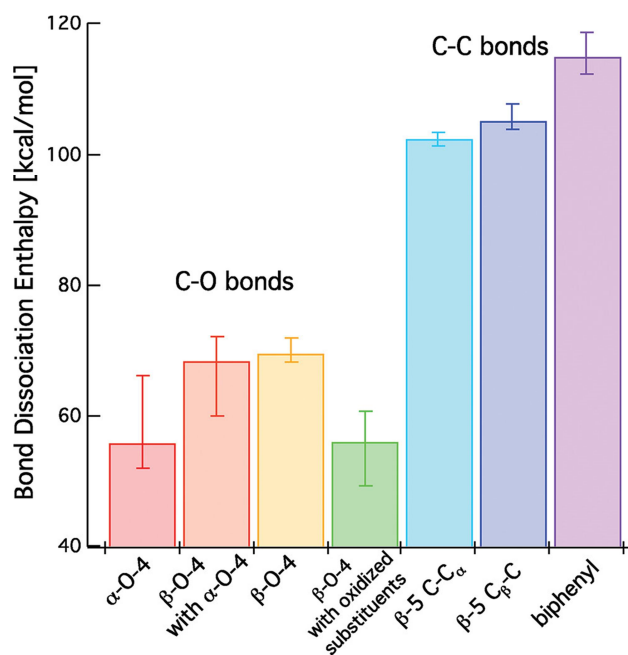


Figure 1.5 Different BDEs of C-C and C-O-C motifs in native lignin.¹⁶

On the other hand, underutilization of lignin may be attributed to the process by which cellulose and hemicellulose are extracted. Delignification process called “pulping”

is a key pretreatment step in the paper production industry and generates technical lignin as the main byproducts, distinguished with original native lignin.⁵ It often involves extended heating and/or highly alkaline or acidic conditions, leading to significant condensation reactions that produce C–C crosslinking at the expense of the more labile C_α-OH groups in the β-O-4 ether motifs,¹⁷ which are the key in the cleavage of β-O-4 ether bonds. For example, Kraft lignin is obtained via pretreatment with sodium hydroxide and sodium sulfide at elevated temperatures.¹⁸ Phenolic hydroxyl group can be deprotonated with the help of alkaline catalyst, and then a quinone methide is formed by C_α-OH dehydroxylation. This reactive intermediate will soon react with another aromatic ring in another part on lignin structure and form a recalcitrant C–C bond.⁵ Similar condensation reactions take place when acidic catalysts are used, albeit through a different mechanism (**Figure 1.6**).

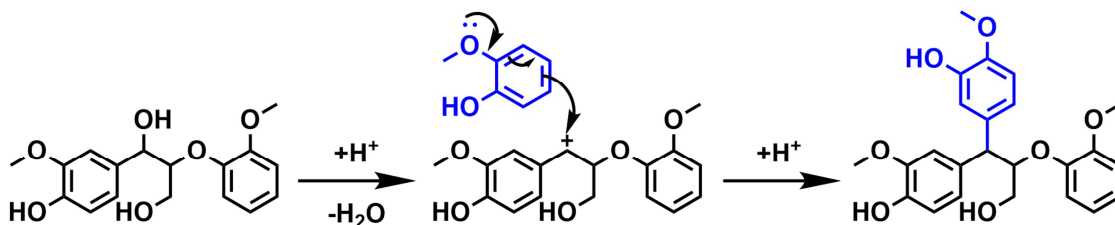


Figure 1.6 Condensation mechanisms that eliminate the abundant and labile β-O-4 linkages in paper production industry.

1.2 TECHNICAL LIGNIN AND ITS UTILIZATION

Due to the harsh conditions in technical lignin generation, many functional groups and properties of lignin are significantly altered.¹⁹ For instance, these processes often lead

to the formation of the more robust α -5 C-C bonds as well as a decrease in hydroxyl concentration (**Figure 1.7**).²⁰ Pyrolysis and gasification could break the stable C–C bonds but require high temperatures (400-1000 °C).^{17, 21-22} Furthermore, those pretreatments often cause the average molecular weight of lignin to change, as the result of decomposition and condensation reactions.²³ These conditions greatly increase the cost of capital expenditures and make the process too expensive to be practical for large-scale implementations. As a result, it is often challenging to decompose technical lignin to lignin monomers for further chemical synthesis.²⁴ Existing applications of technical lignin have been focused on producing materials (**Figure 1.8**), which will be briefly discussed below.¹²

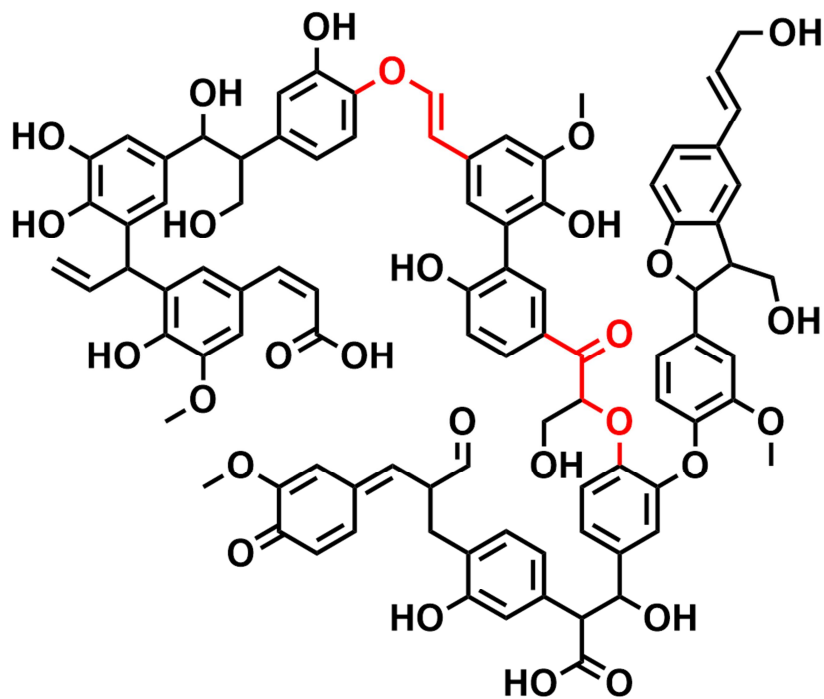


Figure 1.7 The model chemical structure of softwood Kraft lignin.²⁰

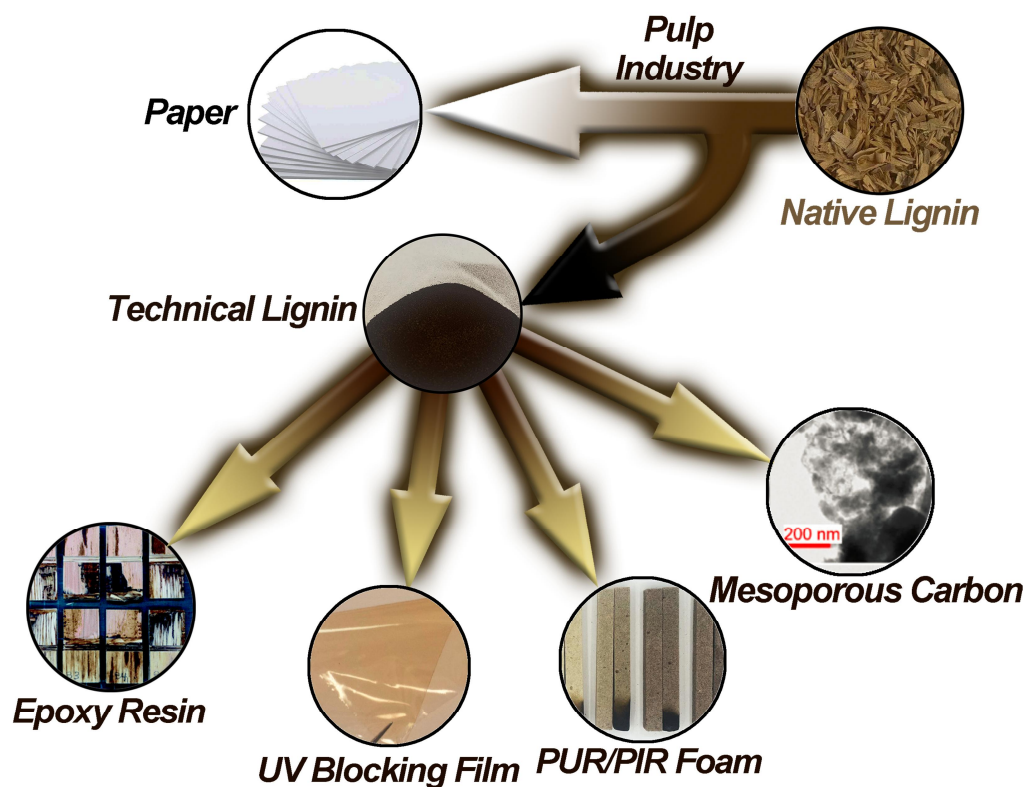


Figure 1.8 Different potential applications of technical lignin.²⁵⁻²⁸

Technical lignin can be incorporated into epoxy resins for the improvement of material properties with its hydroxyl and aromatic functionalities.^{25, 29-30} To generate epoxy networks with lignin incorporated,²⁹ alkali lignin was reacting with a cyclic anhydride resulting in the generation of a pendant carboxylic acid on lignin, for subsequent reaction with epoxy monomers in one-pot. Recently, Kraft lignin has been incorporated into epoxy vitrimers;³⁰ with the help of epichlorohydrin and poly(ethylene glycol) bis(carboxymethyl ether), the constructed vitrimers had the ability to use infrared light to activate the self-healing ability of the material via dynamic crosslinking.

Technical lignin has also been demonstrated for use in construction materials. By oxidizing Kraft lignin by potassium hydroxide for a higher carboxylic acid content,³¹ it

was found that lignin was able to adsorb to cement particles better, resulting in improved fluidity of cement pastes. Additionally, the compression strength of the cement was improved and the amount of water used in cement was reduced. Alternatively, due to its high aromaticity and UV absorbing properties,²⁶ organosolv lignin was incorporated into poly(vinyl alcohol) films to exhibit UV blocking properties.³² Besides, kraft lignin, without further modification, could be incorporated into polyurethane/polyisocyanurate (PUR/PIR) foams for the replacement of toxic polyols for better fire resistance.²⁷ Foams containing Kraft lignin showed improvements in respect to burn time compared to the commercial polyol counterparts.

While a variety of materials including resins, biocomposites, foams, and porous materials have been constructed from technical lignin, there are still limitations with this type of material that could be improved upon.³³ For example, the chemical structures of technical lignin are often poorly defined and difficult to characterize, so they are not suitable as feedstocks for downstream synthesis of value-added products. Furthermore, technical lignin generally requires further purification using methods such as precipitation, filtration, and extraction to remove contaminants from the pulping process. These contaminants include additives and left-over carbohydrates that can affect the properties of downstream applications if not removed.

1.3 LIGNIN-FIRST STRATEGY AND MONOMERIZATION STUDIES

For better valorization of lignin, direct transformation of native lignin has emerged as an attractive alternative to the route that involves the formation of technical lignin.^{14, 34-}

³⁶ Also known as a lignin-first strategy, working on native lignin ensures access to the rich, original β -O-4 linkages, which are far easier to break than the C-C bonds that would replace the ether bond during the production of technical lignin,³⁷⁻³⁸ thereby representing a fundamentally new paradigm in biomass conversion, where lignin can be readily valorized. However, the chemical integrity of cellulose and hemicellulose must be preserved because their valorizing potential is much more than lignin, which prohibits us from using rigid conditions to fully decomposing lignin toward monomers through the cleavage of lignin C-C bonds with higher than 100 kcal/mol BDE.^{3, 35, 39} Existing processes for lignin-first strategies include reductive catalytic fractionation (RCF), oxidative, and redox-neutral pathways (**Figure 1.9**), which will be briefly discussed next.

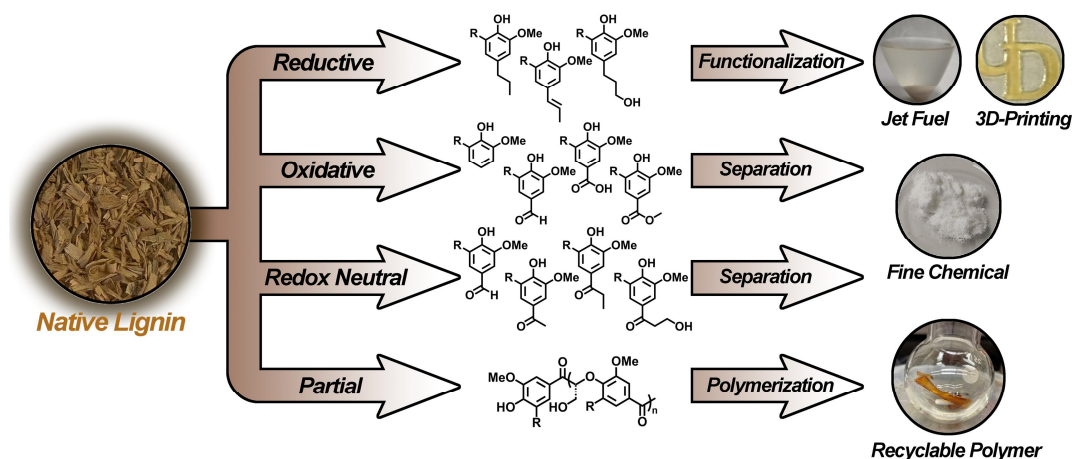


Figure 1.9 Different methods for processing native lignin and the consumer products that can be generated from the depolymerization products.¹²

Among all of these 3 pathways mentioned above in lignin-first strategy, RCF is the best-developed one.⁴⁰ RCF is an approach that focuses on the direct hydrogenation of lignocellulosic biomass under elevated temperatures and pressures in the presence of reductive catalysts for the generation of lignin mixtures.⁴¹⁻⁴² RCF combines both the

delignification of lignocellulosic biomass with the depolymerization of the extracted lignin, followed by stabilization to generate the product, lignin oil (**Figure 1.10**).⁴² RCF is the first scalable lignin valorization process within lignin-first strategy; a large scale processing of lignocellulose has been demonstrated to be feasible on scales ranging from 100 mL up to 50 L.⁴⁰ Although different scales were demonstrated to be feasible, little change in the outcome of the lignin extraction step was noted.

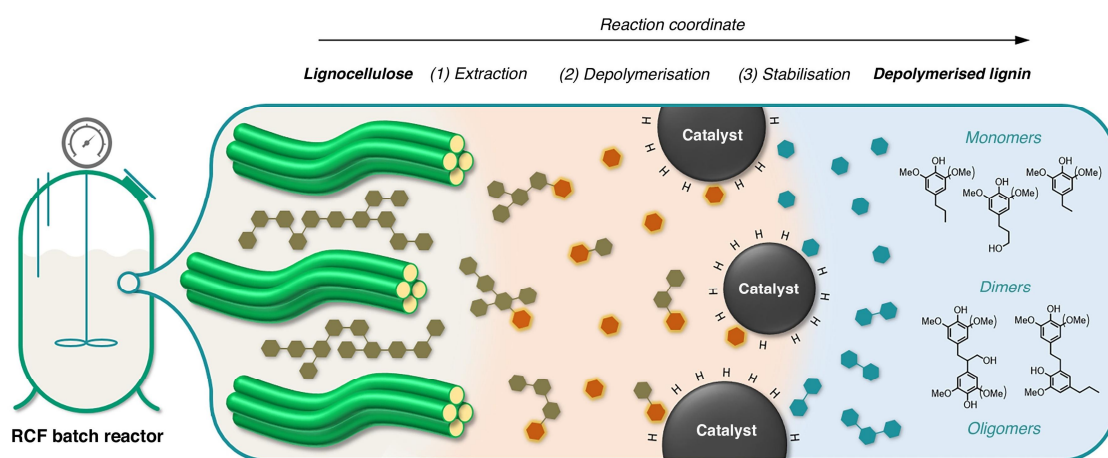


Figure 1.10 Schematic representation of RCF in batch reactor, with the three elementary steps: lignin extraction, depolymerisation and stabilisation.⁴²

The RCF process mainly cleaves the C-O-C ether bonds (mainly β -O-4, in addition to some 4-O-5 and α -O-4 bonds), for depolymerization.⁴³⁻⁴⁶ Under the given reaction conditions, the C-O-C ether linkages can be near quantitatively cleaved to maximize the monomer yield (**Equation 1.1**).^{43, 47} As the C-O-C ether motif in lignin is relatively abundant, accounting for ca. 60-70% of the linkers,^{5, 35, 48} RCF is effective in depolymerizing lignin in lignocellulosic biomass; however, due to the high BDE of C-C bonds (**Figure 1.5**),¹⁶ it's inevitable that there's a significant amount of lignin oligomers remained in the product mixture.⁴⁸ As a result, RCF of lignocellulosic biomass generates

a mixture named lignin oil, containing ca. 40 wt% phenolic monomers as well as ca. 60 wt% oligomers, whose lignol units are linked by C-C bonds.^{43, 47, 49}

$$\text{Maximum monomer yield} = [C - O - C]^2 \quad \text{(Equation 1.1)}$$

Where $[C - O - C]$ represents the concentration of breakable C-O-C motifs in all linkages, excluding the monomers with condensed C-C bonds.

Unique to hydrogenolysis is the fact that it tends to yield hydrogenated products that lack high-value functional groups, such as aldehydes and ketones, required for subsequent chemical utilizations.⁵⁰ As a result, additional post-treatments are required to convert lignin oil to platform chemicals or commercial products.⁵¹⁻⁵² Indeed, there have been few reports that have successfully used the functionalized lignin monomer compounds for further chemical synthesis. For example, corn stover lignin oil obtained from RCF has been used as a starting material for the production of terephthalic acid,² which is a key platform chemical for plastics in soft drink bottles. After RCF, a series of reactions including de-methoxylation, carbonylation, and oxidation resulted in the production of the valuable polyester feedstock, terephthalic acid, from a complex mixture of lignin oil derived monomers. Another notable example is the reactive distillation-reductive catalytic deconstruction (RD-RCD), which depolymerized technical lignin to its constituent monomers.⁵³ The monomers were then further chemically modified with a vinyl group to participate in photocurable three-dimensional (3D) printing. Furthermore, the lignin oil can be further hydrodeoxygenated to generate aromatic hydrocarbons as an alternative for sustainable aviation fuels. The phenolic hydroxyl groups and methoxyl groups are removed under 375 °C to meet the oxygen content requirement that's lower

than 0.5% in jet fuel.⁵⁴ While promising, the need for extra chemical functionalization steps is not ideal. Besides, there are also concerns that RCF not only delignifies, depolymerizes, and stabilizes lignin, but also has the ability to damage polysaccharides under the reaction conditions necessary for RCF to take place. Although the total sugar content is not significantly damaged, the hydrolysis of these chemically modified polysaccharides is easier to process,⁵⁵ which means the glycosidic bonds are somehow weakened, leading to unknown effect to the paper production industry. Within this context, there is a strong incentive to develop milder conditions for the delignification and depolymerization of lignocellulose biomass.

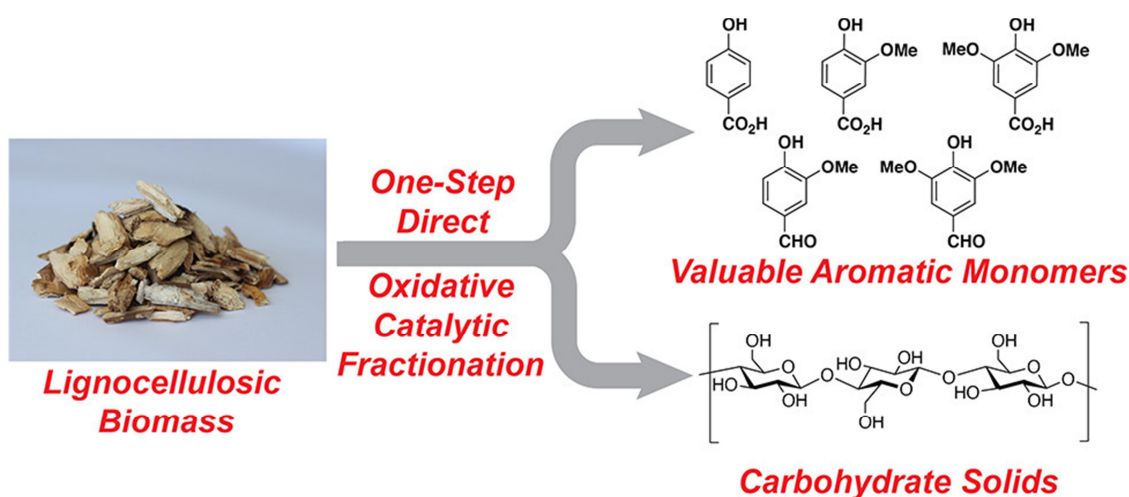


Figure 1.11 The oxidative approach for lignocellulosic biomass processing.³⁹

Recently, oxidative methods have been disclosed that focused on generating oxygenates, including carboxylic acids and aldehydes.⁵ These functional groups are promising handles for further functionalization and downstream utilization. With the presence of oxygen gas as oxygenate, native lignin from poplar wood was successfully fractionated to generate *p*-hydroxybenzoic acid, vanillic acid, syringic acid, vanillin, and

syringaldehyde (**Figure 1.11**) with relatively mild condition (less than 200 °C, less than 2.5 bar O₂), which preserved the integrity of polysaccharides better.³⁹ Similarly, it was proved possible to methoxylate the C_α-OH site on lignin during lignin fractionation of wood sawdust to avoid potential condensation reaction, and then depolymerize it in the presence of polyoxometalate acid catalysts to generate ketones, methyl esters, and aldehydes.⁵⁶ Other oxidative conditions involved the treatment of poplar sawdust with sodium hydroxide and exogenous oxygen.⁵⁷ This resulted in a mixture of carboxylic acids and aromatic aldehydes such as vanillin, syringaldehyde, vanillic acid, syringic acid, and p-hydroxybenzoic acid. In a more recent work, a slightly different approach was taken to valorize the mixture of dimers and oligomers from RCF.⁴⁸ It involved additional oxidation to further increase the utilization of lignin monomer-based products for desirable chemicals. More specifically, the mixture was subjected to oxidative conditions using Bobbitt's salt to generate 2,6-dimethoxybenzoquinone (DMBQ), a platform chemical for organic synthesis.

As a method for functionalizing and depolymerizing lignocellulosic biomass into smaller oligomers and monomers, oxidative treatment offers access to a wide range of oxygen-containing functionalized small molecules and oligomers. Although it is a good strategy for generating diverse molecules, the monomer yield is quite limited compared to the robust, nearly quantitative RCF methods.³⁹

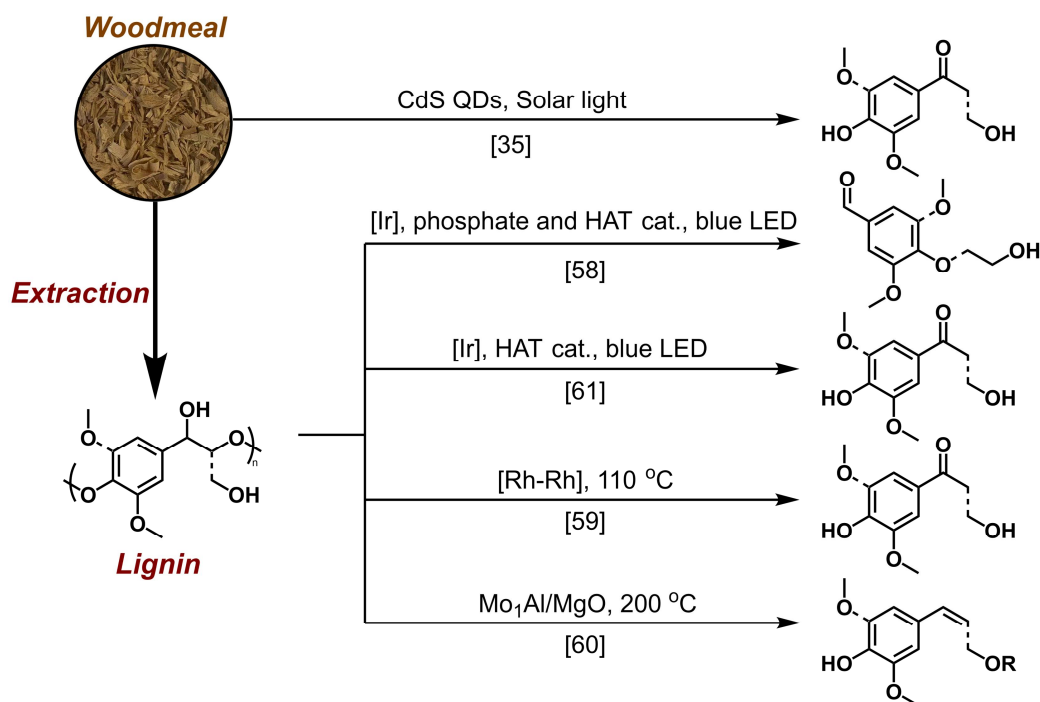


Figure 1.12 Various redox neutral methods for depolymerizing native lignin toward lignin monomers.¹²

Just as oxidative methods have shown to generate lignin oligomers and monomers with high functionality, redox-neutral methods have also been developed to do so as well (**Figure 1.12**). The redox-neutral approach generally avoids the use of stoichiometric oxidants or reductants. Comparing with RCF and oxidative methods, redox-neutral methods provide unique selectivity towards aldehydes and ketones, which can be used as key functional groups for the construction of valorized materials.^{35, 58} Researchers mainly used thermocatalysis and photocatalysis to generate redox-neutral products.¹²

For thermocatalysis perspective, it was demonstrated that a rhodium binuclear catalyst in the presence of base under elevated temperatures could degrade alkaline lignin and lignocellulose toward lignin monomers rich in carbonyls and phenolic alcohols,⁵⁹

without significant loss of total polysaccharides. Other methods involving the depolymerization of Eucalyptus lignin catalyzed by a combination of Mo centers with Al Lewis Acid sites that are on MgO substrates have been developed.⁶⁰ The work demonstrated that the β -O-4 bond could be cleaved at elevated temperatures ca. 200 °C, resulting in the production of coniferyl and sinapyl methyl ethers. Unique to this approach, the product lignin monomers contained side chains with unsaturated C=C bonds, which can be used as functional handles for further derivitization or transformations.

The benzylic C atom in native lignin can serve as a handle to generate reactive radical intermediates in photocatalysis. Indeed, it was shown that proton-coupled electron-transfer (PCET) could be utilized to activate benzylic alcohols in lignin with an iridium-based photocatalyst. In doing so, it led to the cleavage of C_{α} - C_{β} bonds in native lignin and produced small molecules with aldehyde functional groups.⁵⁸ This process was carried out with visible light as the illumination source. In a separate study, lignin oligomers from natural pine shavings were extracted with acidic dioxane and then photocatalytically degraded with the iridium-based catalyst and a cysteine-derived hydrogen atom transfer (HAT) catalyst that contained a disulfide linkage.⁶¹ This system cleaved β -O-4 bonds in native lignin and produced aryl ketones and phenols. The process was redox-neutral and demonstrated the utility of a spin-center shift (SCS). The SCS was proposed to generate a radical at the α -hydroxyl position which could promote an elimination reaction at the position adjacent to the radical followed by a shift in the radical. In yet another report, photocatalytic cleavage of native lignin was carried out after electrocatalytic oxidation.⁶² It involved the utilization of N-hydroxyphthalimide

(NHPI)/2,6-lutidine for benzylic oxidation. The products were treated with an iridium photocatalyst, diisopropylethylamine (DIPEA), and formic acid. This led to the depolymerization due to the cleavage of β -O-4 bonds, which was confirmed by reactions in model systems. This one-pot metal-free oxidation method followed by iridium photocatalysis was highly selective, paving the way for potential scale up usages.

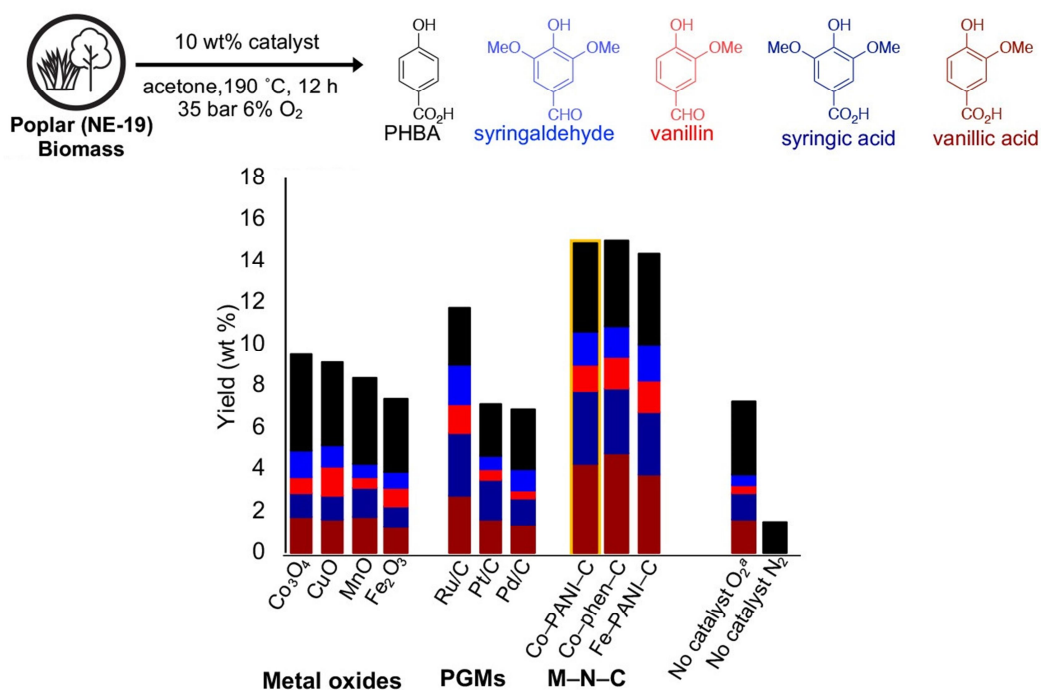


Figure 1.13 The distribution of oxidative lignin decomposition products.³⁹

However, those methods toward lignin monomers are facing some critical challenges. First, due to the richness of chemical structures in native and technical lignin, the resulting products are mixture of compounds including monomers that's uneconomical or even impractical to fully separate and purify; especially for the oxidative or redox-neutral methods, the selectivity towards different oxygenates without a main product (selectivity >50%) makes the separation step even more difficult (**Figure**

1.13).³⁹ Besides, the requirement of cellulose and hemicellulose preservation only allows us to use mild conditions to extract and cleave the lignin, resulting in a sacrifice in lignin monomer yield; the mild conditions only cleave relatively fragile C-O-C ether bonds, leaving the robust C-C bonds existing as the linkages in lignin oligomers, which is a predominant byproduct in the lignin decomposition mixture (**Equation 1.1, Figure 1.14**).^{43, 47-49} Due to the complicated structure of lignin oligomers, it's impossible to separate a specific lignin oligomer as platform chemical for subsequent modification or synthesis. Although there's report using lignin oligomers generated from RCF process for further oxidative decomposition,⁴⁸ the yield of lignin monomers is still limited.

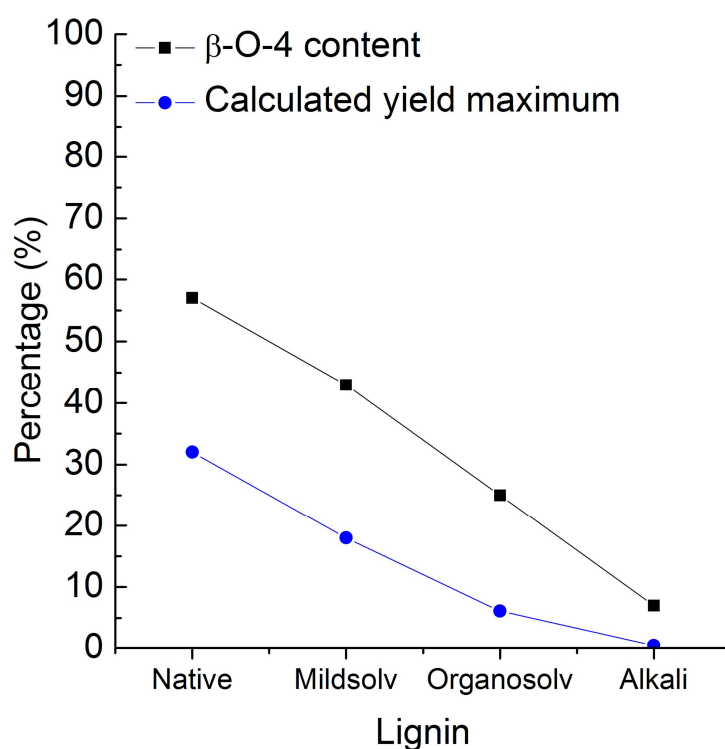


Figure 1.14 The influence on the content of β -O-4 motif and resulting maximum monomer yield in lignin-first strategy with differently pretreated lignin.²⁴

1.4 THE SCOPE OF THIS THESIS

The motivation of this thesis is to shift the paradigm of biomass valorization by enabling lignin conversion under mild conditions. Toward this goal, we make our efforts on a photocatalytic strategy for controlled depolymerization of lignin. Different from other similar efforts for lignin valorization, we focus on oligomers with desired molecular weight and stoichiometry of carbonyl functionalities. The resulting materials is readily utilized for the production of covalent dynamic polymer networks (DPNs), which can be chemically and mechanically recycled at the end of their life, enabling a circular economy of polymers that are derived from biomass.

This concept is proved in Chapter 2 (**Figure 1.15**).³ The process takes advantage of the high selectivity of photocatalytic activation of the β -O-4 bond in lignin by tetrabutylammonium decatungstate (TBADT). With the help of TBADT-based photocatalytic system, lignin-based oligomers are produced by selective partial depolymerization, which can then be readily utilized for the synthesis of polymer networks through reactions between C=O from lignin oligomers and polymer filler, and branched $-NH_2$ as a dynamic covalent cross-linker. The resulting polymer network can be recycled up to 3 times to enable a circular economy of materials directly derived from biomass.

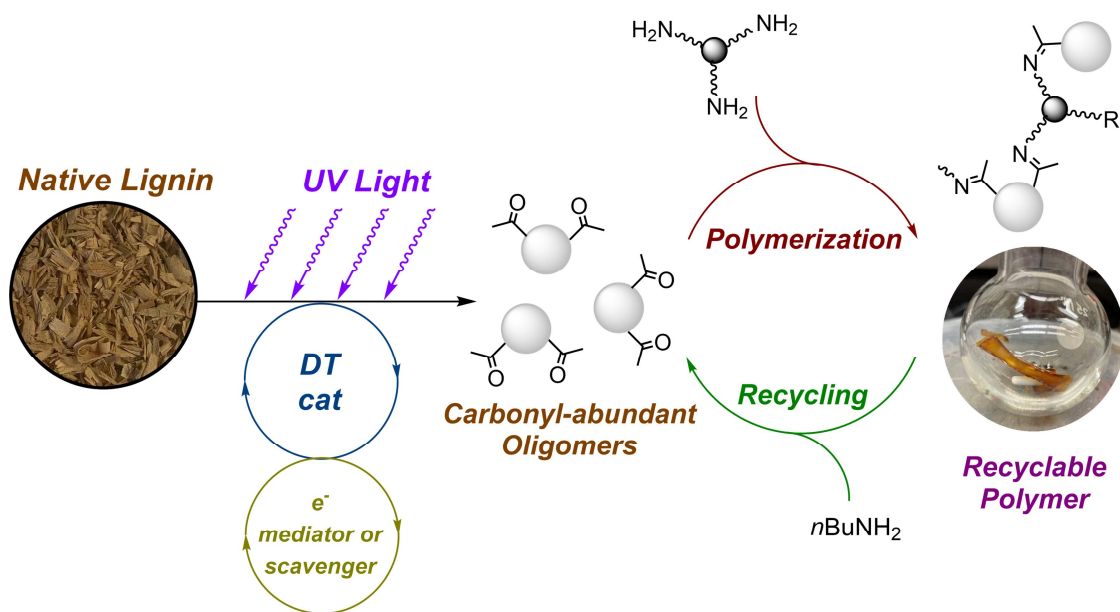


Figure 1.15 The concept of converting native lignin toward chemically recyclable polymer via carbonyl-abundant oligomers from partial photocatalytic depolymerization.³

In Chapter 3, we have successfully developed a process enabling high degrees of control over the number average molecular weight (M_n) and the concentration of a key functional group for subsequent polymerization, C=O, in the products. Due to the possible side reactions of tetrabutylammonium cation in TBADT photocatalyst, we turned our interest to sodium decatungstate (NaDT), which features better selectivity on β -O-4 motifs in native lignin. The purity and higher M_n of the resulting lignin oligomers lead to filler-free lignin-based polymer with significantly improved mechanical strength. We further explore the relationship between mechanical strength of the lignin-based polymer and the degree of polymerization, which can be fine-tuned by varying the C=O stoichiometry of the starting lignin oligomers.

1.5 REFERENCE

1. Jaswal, A.; Singh, P. P.; Mondal, T., Furfural—a versatile, biomass-derived platform chemical for the production of renewable chemicals. *Green Chemistry* **2022**, *24*, 510-551.
2. Song, S.; Zhang, J.; Gözaydın, G.; Yan, N., Production of terephthalic acid from corn stover lignin. *Angewandte Chemie International Edition* **2019**, *58*, 4934-4937.
3. Wang, H.; Giardino, G. J.; Chen, R.; Yang, C.; Niu, J.; Wang, D., Photocatalytic Depolymerization of Native Lignin toward Chemically Recyclable Polymer Networks. *ACS Central Science* **2022**, *9*, 48-55.
4. Bertella, S.; Luterbacher, J. S., Lignin functionalization for the production of novel materials. *Trends in Chemistry* **2020**, *2*, 440-453.
5. Schutyser, W.; Renders, a. T.; Van den Bosch, S.; Koelewijn, S.-F.; Beckham, G.; Sels, B. F., Chemicals from lignin: an interplay of lignocellulose fractionation, depolymerisation, and upgrading. *Chemical society reviews* **2018**, *47*, 852-908.
6. Cheng, F.; Wang, H.; Chatel, G.; Gurau, G.; Rogers, R. D., Facile pulping of lignocellulosic biomass using choline acetate. *Bioresource technology* **2014**, *164*, 394-401.
7. Johansson, A.; Aaltonen, O.; Ylinen, P., Organosolv pulping—methods and pulp properties. *Biomass* **1987**, *13*, 45-65.
8. Gupta, A.; Verma, J. P., Sustainable bio-ethanol production from agro-residues: a review. *Renewable and sustainable energy reviews* **2015**, *41*, 550-567.
9. Abeer, M. M.; Mohd Amin, M. C. I.; Martin, C., A review of bacterial cellulose-based drug delivery systems: their biochemistry, current approaches and future prospects. *Journal of Pharmacy and Pharmacology* **2014**, *66*, 1047-1061.
10. Sun, Z.; Fridrich, B.; De Santi, A.; Elangovan, S.; Barta, K., Bright side of lignin depolymerization: toward new platform chemicals. *Chemical reviews* **2018**, *118*, 614-678.
11. Wu, X.; Luo, N.; Xie, S.; Zhang, H.; Zhang, Q.; Wang, F.; Wang, Y., Photocatalytic transformations of lignocellulosic biomass into chemicals. *Chemical Society Reviews* **2020**, *49*, 6198-6223.

12. Giardino, G. J.; Wang, H.; Niu, J.; Wang, D., From technical lignin to native lignin: Depolymerization, functionalization, and applications. *Chemical Physics Reviews* **2024**, *5*, No. 2.
13. Vanholme, R.; De Meester, B.; Ralph, J.; Boerjan, W., Lignin biosynthesis and its integration into metabolism. *Current opinion in biotechnology* **2019**, *56*, 230-239.
14. Abu-Omar, M. M.; Barta, K.; Beckham, G. T.; Luterbacher, J. S.; Ralph, J.; Rinaldi, R.; Román-Leshkov, Y.; Samec, J. S.; Sels, B. F.; Wang, F., Guidelines for performing lignin-first biorefining. *Energy & Environmental Science* **2021**, *14*, 262-292.
15. Vanholme, R.; Demedts, B.; Morreel, K.; Ralph, J.; Boerjan, W., Lignin biosynthesis and structure. *Plant physiology* **2010**, *153*, 895-905.
16. Kim, S.; Chmely, S. C.; Nimlos, M. R.; Bomble, Y. J.; Foust, T. D.; Paton, R. S.; Beckham, G. T., Computational study of bond dissociation enthalpies for a large range of native and modified lignins. *The Journal of Physical Chemistry Letters* **2011**, *2*, 2846-2852.
17. Pandey, M. P.; Kim, C. S., Lignin depolymerization and conversion: a review of thermochemical methods. *Chemical Engineering & Technology* **2011**, *34*, 29-41.
18. Li, T.; Takkellapati, S., The current and emerging sources of technical lignins and their applications. *Biofuels, Bioproducts and Biorefining* **2018**, *12*, 756-787.
19. Torres, L. A. Z.; Woiciechowski, A. L.; de Andrade Tanobe, V. O.; Karp, S. G.; Lorenci, L. C. G.; Faulds, C.; Soccol, C. R., Lignin as a potential source of high-added value compounds: A review. *Journal of Cleaner Production* **2020**, *263*, 121499-121516.
20. Kun, D.; Pukánszky, B., Polymer/lignin blends: Interactions, properties, applications. *European Polymer Journal* **2017**, *93*, 618-641.
21. Liu, W.-J.; Jiang, H.; Yu, H.-Q., Thermochemical conversion of lignin to functional materials: a review and future directions. *Green Chemistry* **2015**, *17*, 4888-4907.
22. Kawamoto, H., Lignin pyrolysis reactions. *Journal of Wood Science* **2017**, *63*, 117-132.
23. Tolbert, A.; Akinosho, H.; Khunsupat, R.; Naskar, A. K.; Ragauskas, A. J., Characterization and analysis of the molecular weight of lignin for biorefining studies. *Biofuels, Bioproducts and Biorefining* **2014**, *8*, 836-856.

24. Wu, X.; Xie, S.; Liu, C.; Zhou, C.; Lin, J.; Kang, J.; Zhang, Q.; Wang, Z.; Wang, Y., Ligand-controlled photocatalysis of CdS quantum dots for lignin valorization under visible light. *ACS Catalysis* **2019**, *9*, 8443-8451.
25. Li, R. J.; Gutierrez, J.; Chung, Y.-L.; Frank, C. W.; Billington, S. L.; Sattely, E. S., A lignin-epoxy resin derived from biomass as an alternative to formaldehyde-based wood adhesives. *Green chemistry* **2018**, *20*, 1459-1466.
26. Sadeghifar, H.; Venditti, R.; Jur, J.; Gorga, R. E.; Pawlak, J. J., Cellulose-lignin biodegradable and flexible UV protection film. *ACS Sustainable Chemistry & Engineering* **2017**, *5*, 625-631.
27. Henry, C.; Nejad, M., Lignin-Based Low-Density Rigid Polyurethane/Polyisocyanurate Foams. *Industrial & Engineering Chemistry Research* **2023**, *62*, 6865-6873.
28. Jedrzejczyk, M. A.; Engelhardt, J.; Djokic, M. R.; Bliznuk, V.; Van Geem, K. M.; Verberckmoes, A.; De Clercq, J.; Bernaerts, K. V., Development of lignin-based mesoporous carbons for the adsorption of humic acid. *ACS omega* **2021**, *6*, 15222-15235.
29. Liu, W.; Zhou, R.; Goh, H. L. S.; Huang, S.; Lu, X., From waste to functional additive: toughening epoxy resin with lignin. *ACS applied materials & interfaces* **2014**, *6*, 5810-5817.
30. Zheng, Y.; Liu, T.; He, H.; Lv, Z.; Xu, J.; Ding, D.; Dai, L.; Huang, Z.; Si, C., Lignin-based epoxy composite vitrimers with light-controlled remoldability. *Advanced Composites and Hybrid Materials* **2023**, *6*, No. 53.
31. Sutradhar, S.; Gao, W.; Fatehi, P., A green cement plasticizer from softwood kraft lignin. *Industrial & Engineering Chemistry Research* **2023**, *62*, 1676-1687.
32. Posoknistakul, P.; Tangkrakul, C.; Chaosuanphae, P.; Deepentham, S.; Techasawong, W.; Phonphirunrot, N.; Bairak, S.; Sakdaronnarong, C.; Laosiripojana, N., Fabrication and characterization of lignin particles and their ultraviolet protection ability in PVA composite film. *ACS omega* **2020**, *5*, 20976-20982.
33. Vishtal, A.; Kraslawski, A., Challenges in industrial applications of technical lignins. *BioResources* **2011**, *6*, 3547-3568.

34. Korányi, T. I.; Fridrich, B.; Pineda, A.; Barta, K., Development of ‘Lignin-First’ approaches for the valorization of lignocellulosic biomass. *Molecules* **2020**, *25*, 2815-2836.
35. Wu, X.; Fan, X.; Xie, S.; Lin, J.; Cheng, J.; Zhang, Q.; Chen, L.; Wang, Y., Solar energy-driven lignin-first approach to full utilization of lignocellulosic biomass under mild conditions. *Nature catalysis* **2018**, *1*, 772-780.
36. Funaoka, M.; Matsubara, M.; Seki, N.; Fukatsu, S., Conversion of native lignin to a highly phenolic functional polymer and its separation from lignocellulosics. *Biotechnology and bioengineering* **1995**, *46*, 545-552.
37. Sadeghifar, H.; Ragauskas, A., Perspective on technical lignin fractionation. *ACS Sustainable Chemistry & Engineering* **2020**, *8*, 8086-8101.
38. Helander, M.; Theliander, H.; Lawoko, M.; Henriksson, G.; Zhang, L.; Lindström, M. E., Fractionation of technical lignin: Molecular mass and pH effects. *BioResources* **2013**, *8*, 2270-2282.
39. Luo, H.; Weeda, E. P.; Alherech, M.; Anson, C. W.; Karlen, S. D.; Cui, Y.; Foster, C. E.; Stahl, S. S., Oxidative catalytic fractionation of lignocellulosic biomass under non-alkaline conditions. *Journal of the American Chemical Society* **2021**, *143*, 15462-15470.
40. Cooreman, E.; Nicolai, T.; Arts, W.; Aelst, K. V.; Vangeel, T.; den Bosch, S. V.; Aelst, J. V.; Lagrain, B.; Thiele, K.; Thevelein, J., The Future Biorefinery: The Impact of Upscaling the Reductive Catalytic Fractionation of Lignocellulose Biomass on the Quality of the Lignin Oil, Carbohydrate Products, and Pulp. *ACS Sustainable Chemistry & Engineering* **2023**, *11*, 5440-5450.
41. Jindal, M.; Uniyal, P.; Bhaskar, T., Reductive catalytic fractionation as a novel pretreatment/lignin-first approach for lignocellulosic biomass valorization: A review. *Bioresource Technology* **2023**, *385*, 129396-129409.
42. Renders, T.; Van den Bossche, G.; Vangeel, T.; Van Aelst, K.; Sels, B., Reductive catalytic fractionation: state of the art of the lignin-first biorefinery. *Current opinion in biotechnology* **2019**, *56*, 193-201.
43. Wang, Q.; Xiao, L.-P.; Lv, Y.-H.; Yin, W.-Z.; Hou, C.-J.; Sun, R.-C., Metal-organic-framework-derived copper catalysts for the hydrogenolysis of lignin into monomeric phenols. *ACS Catalysis* **2022**, *12*, 11899-11909.

44. Paone, E.; Beneduci, A.; Corrente, G.; Malara, A.; Mauriello, F., Hydrogenolysis of aromatic ethers under lignin-first conditions. *Molecular Catalysis* **2020**, *497*, 111228-111236.
45. Anderson, E. M.; Stone, M. L.; Hülsey, M. J.; Beckham, G. T.; Román-Leshkov, Y., Kinetic studies of lignin solvolysis and reduction by reductive catalytic fractionation decoupled in flow-through reactors. *ACS Sustainable Chemistry & Engineering* **2018**, *6*, 7951-7959.
46. Li, Y.; Karlen, S. D.; Demir, B.; Kim, H.; Luterbacher, J.; Dumesic, J. A.; Stahl, S. S.; Ralph, J., Mechanistic study of diaryl ether bond cleavage during palladium - catalyzed lignin hydrogenolysis. *ChemSusChem* **2020**, *13*, 4487-4494.
47. Liu, Z.; Li, H.; Gao, X.; Guo, X.; Wang, S.; Fang, Y.; Song, G., Rational highly dispersed ruthenium for reductive catalytic fractionation of lignocellulose. *Nature Communications* **2022**, *13*, 4716.
48. Subbotina, E.; Rukkijakan, T.; Marquez-Medina, M. D.; Yu, X.; Johnsson, M.; Samec, J. S., Oxidative cleavage of C–C bonds in lignin. *Nature Chemistry* **2021**, *13*, 1118-1125.
49. Thi, H. D.; Van Aelst, K.; Van den Bosch, S.; Katahira, R.; Beckham, G. T.; Sels, B. F.; Van Geem, K. M., Identification and quantification of lignin monomers and oligomers from reductive catalytic fractionation of pine wood with GC× GC–FID/MS. *Green Chemistry* **2022**, *24*, 191-206.
50. Bartling, A. W.; Stone, M. L.; Hanes, R. J.; Bhatt, A.; Zhang, Y.; Bidy, M. J.; Davis, R.; Kruger, J. S.; Thornburg, N. E.; Luterbacher, J. S., Techno-economic analysis and life cycle assessment of a biorefinery utilizing reductive catalytic fractionation. *Energy & Environmental Science* **2021**, *14*, 4147-4168.
51. Liao, Y.; Koelewijn, S.-F.; Van den Bossche, G.; Van Aelst, J.; Van den Bosch, S.; Renders, T.; Navare, K.; Nicolai, T.; Van Aelst, K.; Maesen, M., A sustainable wood biorefinery for low-carbon footprint chemicals production. *Science* **2020**, *367*, 1385-1390.
52. Koelewijn, S.-F.; Cooreman, C.; Renders, T.; Saiz, C. A.; Van den Bosch, S.; Schutyser, W.; De Leger, W.; Smet, M.; Van Puyvelde, P.; Witters, H., Promising bulk

- production of a potentially benign bisphenol A replacement from a hardwood lignin platform. *Green Chemistry* **2018**, *20*, 1050-1058.
53. O’Dea, R. M.; Pranda, P. A.; Luo, Y.; Amitrano, A.; Ebikade, E. O.; Gottlieb, E. R.; Ajao, O.; Benali, M.; Vlachos, D. G.; Ierapetritou, M., Ambient-pressure lignin valorization to high-performance polymers by intensified reductive catalytic deconstruction. *Science Advances* **2022**, *8*, No. eabj7523.
54. Stone, M. L.; Webber, M. S.; Mounfield, W. P.; Bell, D. C.; Christensen, E.; Morais, A. R.; Li, Y.; Anderson, E. M.; Heyne, J. S.; Beckham, G. T., Continuous hydrodeoxygenation of lignin to jet-range aromatic hydrocarbons. *Joule* **2022**, *6*, 2324-2337.
55. Anderson, E. M.; Katahira, R.; Reed, M.; Resch, M. G.; Karp, E. M.; Beckham, G. T.; Román-Leshkov, Y., Reductive catalytic fractionation of corn stover lignin. *ACS Sustainable Chemistry & Engineering* **2016**, *4*, 6940-6950.
56. Du, X.; Tricker, A. W.; Yang, W.; Katahira, R.; Liu, W.; Kwok, T. T.; Gogoi, P.; Deng, Y., Oxidative catalytic fractionation and depolymerization of lignin in a one-pot single-catalyst system. *ACS Sustainable Chemistry & Engineering* **2021**, *9*, 7719-7727.
57. Schutyser, W.; Kruger, J. S.; Robinson, A. M.; Katahira, R.; Brandner, D. G.; Cleveland, N. S.; Mittal, A.; Peterson, D. J.; Meilan, R.; Román-Leshkov, Y., Revisiting alkaline aerobic lignin oxidation. *Green chemistry* **2018**, *20*, 3828-3844.
58. Nguyen, S. T.; Murray, P. R.; Knowles, R. R., Light-driven depolymerization of native lignin enabled by proton-coupled electron transfer. *ACS Catalysis* **2019**, *10*, 800-805.
59. Liu, Y.; Li, C.; Miao, W.; Tang, W.; Xue, D.; Li, C.; Zhang, B.; Xiao, J.; Wang, A.; Zhang, T., Mild redox-neutral depolymerization of lignin with a binuclear Rh complex in water. *ACS Catalysis* **2019**, *9*, 4441-4447.
60. Meng, G.; Lan, W.; Zhang, L.; Wang, S.; Zhang, T.; Zhang, S.; Xu, M.; Wang, Y.; Zhang, J.; Yue, F., Synergy of Single Atoms and Lewis Acid Sites for Efficient and Selective Lignin Disassembly into Monolignol Derivatives. *Journal of the American Chemical Society* **2023**, *145*, 12884-12893.
61. Zhu, Q.; Nocera, D. G., Catalytic C (β)-O bond cleavage of lignin in a one-step reaction enabled by a spin-center shift. *ACS Catalysis* **2021**, *11*, 14181-14187.

62. Bosque, I.; Magallanes, G.; Rigoulet, M.; Kärkäs, M. D.; Stephenson, C. R.,
Redox catalysis facilitates lignin depolymerization. *ACS central science* **2017**, *3*, 621-628.

CHAPTER 2: PHOTOCATALYTIC DEPOLYMERIZATION OF NATIVE LIGNIN TOWARD CHEMICALLY RECYCLABLE POLYMER NETWORKS

2.1 INTRODUCTION

As an important component of lignocellulose, lignin is an attractive feedstock. However, existing biomass processing technologies prioritize cellulose and hemicellulose when lignin has been significantly underutilized.¹⁻³ As discussed in Chapter 1, this can be attributed to both the complication of lignin chemical structure and industrial delignification methods. The delignification methods in traditional paper producing industry converted native lignin to a byproduct called technical lignin, which means undesired side reactions (e.g., condensation) damage the integrity of native lignin chemical structure and make the subsequent chemical utilization even more challenging. Recently, an alternative lignin-first strategy has emerged to directly convert native lignin in lignocellulose into value-added chemicals.⁴⁻⁶ For instance, reductive catalytic fractionation (RCF) as a lignin-first approach produces a mixture of low molecular weight compounds from native lignin.⁷⁻¹¹ However, the mixture produced by RCF is often difficult to separate, which limits its application to platform chemicals.

To circumvent issues connected to separating lignin monomers discussed above, and to take advantage of lignin oligomers that accounting for a large proportion in the

fractionation product mixture, we limit the degree of depolymerization and focus on producing oligomers with high-value functional groups. Without further separation, the lignin oligomer products can then be readily re-polymerized to yield DPNs that can be easily recycled.¹⁻³ Although partial depolymerization of lignin has started to show its promise for the construction of functional materials, such as thermoset plastics,¹²⁻¹⁵ elastomers,¹⁶ or vitrimers,¹⁷ these initial materials are mainly constructed from technical lignins, which have already undergone significant unwanted chemical modifications in the pulping process that affects its chemical integrity, limiting their application in reversible products. From the discussion above, we see the significance of a lignin-first approach, by which native lignin is selectively partially depolymerized for subsequent repolymerization. Here, we report a proof of this concept (**Figure 2.1**). Our work is inspired by previous reports on the cleavage of the β -O-4 motif in lignin via HAT.¹⁸⁻²⁴ To achieve the intricate balance between depolymerization and the introduction of functional groups necessary for the subsequent repolymerization, we employ an earth-abundant photocatalyst (namely, tetrabutylammonium decatungstate, or TBADT)²⁵ that enables HAT under mild conditions. The reaction can be guided through either a bond-scission or an oxidation pathway through exogenous electron mediators or electron scavengers, respectively, thereby regulating the degree of depolymerization and introducing carbonyl functionality into the resulting oligomers (**Figure 2.2**). Repolymerization of the oligomers readily produced dynamic polymer networks (DPNs) that are capable of closed-loop chemical recycling toward a biomass-based circular plastic economy.

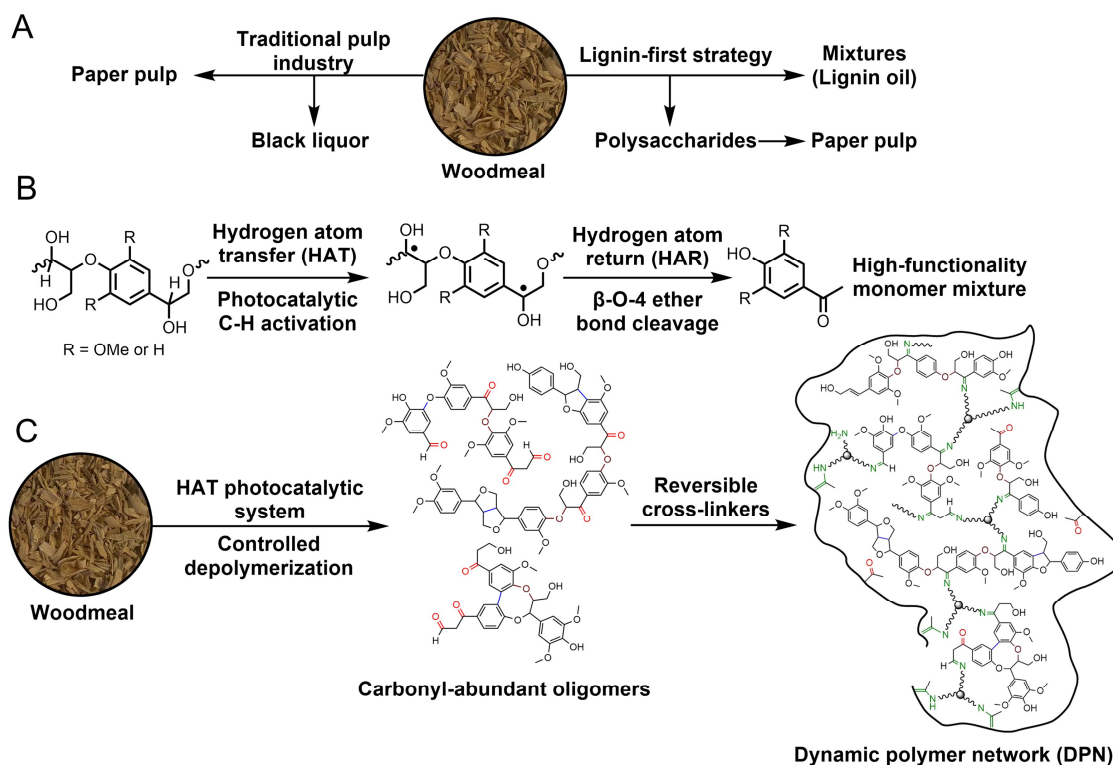


Figure 2.1 Schematic illustration of different strategies to process lignocellulose. (a)

Two industrial routes of processing woodmeal, namely, the pulp industry or the lignin oil industry. (b) Mechanisms of HAT to break the β -O-4 motif, which is abundant in native lignin. (c) Overview of our strategy to first depolymerize native lignin and then repolymerize the resulting oligomers using dynamic covalent cross-linkers.

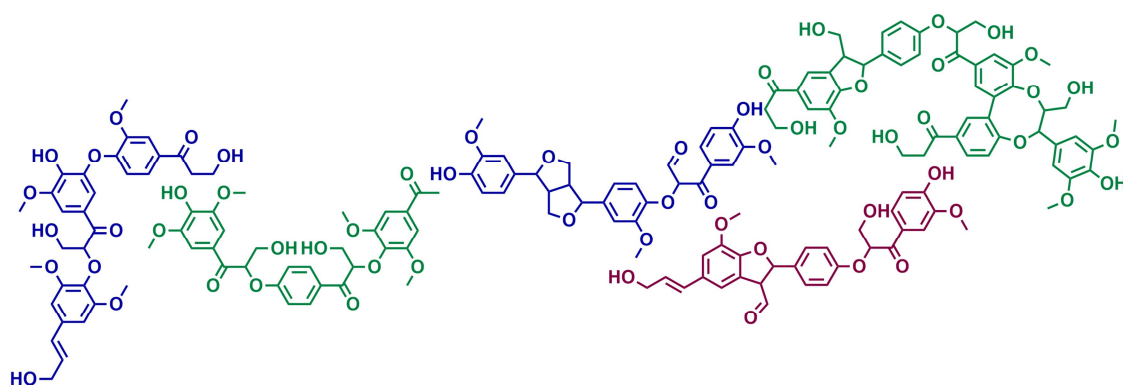


Figure 2.2 Hypothesized partial depolymerization toward lignin oligomer molecules on the lignin schematic structure in **Figure 1.2**.

2.2 METHODS

Materials

All reactions were carried out under a nitrogen atmosphere unless otherwise stated. Nitrogen and oxygen gasses were purchased from Airgas. Beech wood sawdust was purchased from Blegwood. All solvents including ethanol, acetone (AC), anhydrous acetonitrile (AN), dichloromethane (DCM), dioxane, ethyl acetate (EA), hexane (Hex), methanol (MeOH), and tetrahydrofuran (THF) were purchased from commercial sources and used without further purification unless otherwise stated. Dioxane was further dried with a drying column of a solvent system from Pure Process Technologies. NMR solvents including dimethyl sulfoxide (DMSO- d_6) and chloroform ($CDCl_3$) were purchased from Cambridge Isotope Laboratories or ACROS organics. Sodium tungstate dihydrate and tetrabutylammonium bromide (TBAB) were purchased from ACROS organics. Diphenyl anthracene (DPA) was purchased from Alfa Aesar. 2-phenoxy-1-phenylethanol (PPol) and 4-Cyano-4-(dodecylsulfanylthiocarbonyl)sulfanylpentanoic acid were purchased from Ambeed. Methyl 2-methylprop-2-enoate (MMA) and *n*-butylamine were purchased from TCI. (2-acetoacetoxy)ethyl methacrylate (AAEMA), azobisisobutyronitrile (AIBN) (recrystallized from methanol prior to use), cellulose, hemicellulose, 4-(trifluoromethyl)phenylhydrazine, and tris(2-aminoethyl)amine (TAEA) were purchased from Sigma Aldrich. MMA and AAEMA were passed through a basic aluminum oxide plug prior to use. SiliaFlash (P60 40-63 μ M (230-400 mesh)) silica gel was purchased from SiliCycle and used for column chromatography. Basic aluminum oxide (Brockmann I 50-200 μ m, 60A) was used for reagent purification. Neutral aluminum oxide (150 mesh) was used for oligomer purification. Thin Layer Chromatography (TLC) Silica Gel 60 F254: Glass Plates 20 x 20 cm were used for TLC analysis. The polytetrafluoroethylene (PTFE) mold used for creating tensile test and DMA samples had the following measurements, respectively:



Characterization

All ^1H , ^{13}C , and ^{19}F NMR spectra were obtained using a Varian 600 MHz, Varian 500 MHz, Bruker 500 MHz equipped with a X nuclei optimized 5 mm double resonance BBO H&F CryoProbe Prodigy, or Bruker 500 MHz equipped with a CryoProbe (He) BBFO 5mm BBF/ ^1H X nuclei optimized 5 mm double resonance BBFO, NMR spectrometer. Size exclusion chromatography (SEC) was carried out on a Tosoh's high-performance SEC system HLC-8320GPC containing TSKgel Alpha-M columns at 50 °C and a flow rate of 0.6 mL/min. The eluent was HPLC grade DMF with 0.01 M LiBr. Polystyrene standards (ReadyCal Kit, Sigma-Aldrich #81434) were used to determine the molecular weight and molecular weight distribution of the polymers. Prior to injection into the SEC, polymers were dissolved in DMF and filtered through a 0.20 μm PTFE filter. Differential scanning calorimetry (DSC) was performed using Tzero hermetic pans and lids on a TA Instrument Discovery DSC 250. Scans were performed from -50-200 °C over three cycles at a rate of 10 °C/min. An isotherm step for 5 minutes was used at both -50 and 200 °C. Tensile test was performed on an Instron 5543 universal testing system that was equipped with a 100 N load cell. The strain rate was set at 2 strain/min. Dynamic mechanical analysis (DMA) was carried out on a TA Instruments Discovery Dynamic Mechanical Analyzer 850.

Light Reactor Specifications and Setup

The light source was a 200 W UV LED light centered at 365 nm, from Howsuper, with the source number H6015-S-6868-LG-365nm.



Figure 2.3: Light setup used for photocatalysis.

TBADT Catalyst Synthesis

TBADT catalyst was synthesized according to a literature procedure with minor modifications.²⁶ TBAB (4.8 g, 15 mmol) and $\text{Na}_2\text{WO}_4 \cdot 2\text{H}_2\text{O}$ (10.0 g, 30 mmol) were dissolved in separate deionized (DI) water (50 mL and 100 mL, respectively) solutions. The solutions were acidified to pH 2 with concentrated hydrochloric acid. After heating to 90 °C, the solutions were mixed together. Precipitation was observed immediately, indicating the formation of TBADT. The slurry was stirred for 30 minutes in a 90 °C water bath, cooled to room temperature, and filtered with a Büchner funnel. The solid phase was washed with DI water and THF (3 x 30 mL), and dried in a vacuum oven at 90 °C overnight. The crude TBADT was further purified by recrystallization. The crude TBADT was refluxed in DCM (1 g: 20 mL) for 2 hours. The mixture was cooled on an ice bath, and then filtered to obtain pure TBADT as a transparent crystal with a light yellow color (4.02 g, 40.0% based on W).

Photocatalysis of PPol

For a typical photocatalytic reaction of PPol, PPol (10.7 mg, 50 μmol), TBADT (5.3 mg, 1.6 μmol), DPA (varied amount), and AN (1 mL) were added to a 10 mL Schlenk tube. The solution was degassed by the freeze-pump-thaw method 3 times, filling the atmosphere of the schlenk tube with 1 atm nitrogen (or mixed gas with different oxygen content). The solution was then heated to 50 °C in a water bath and irradiated with UV

light for 2 hours. The products were then identified by GC-MS, and quantified by ¹H NMR.

Wood Sawdust (Native Lignin) Pretreatment

Beech wood sawdust was pretreated according to a literature procedure⁴ with minor modifications. The wood sawdust (1 g: 10 mL) was suspended in an ethanol-water solution (4:1) and sonicated for 2 hours to remove most of the extractives. The solution was filtered, and the solid was washed with acetone (3x100 mL), and dried in a vacuum oven at 45 °C for a minimum of 48 hours. The solid was then oven-dried in 2 hour intervals at 105 °C until the weight change was <5% indicating a <5% moisture content. The dry sawdust was then knife-milled through a 1 mm screen. The wood powder was sealed and stored at 0 °C.

Klason Lignin Information

Klason lignin content was measured according to a literature procedure²⁷ in order to calculate the yield of lignin oligomers. In a typical experiment, woodmeal (0.2 g) and 72% sulfuric acid (1.5 mL) were mixed in a glass vial, and stirred for 1 hour at 30 °C in a water bath. The mixture was diluted to 42 mL with DI water and transferred to an autoclave reactor. The solution was heated to 121 °C for 1 hour. After cooling to room temperature, the brown precipitate (Klason lignin) was separated by filtration. The solid was washed with DI water (3 x 20 mL). The Klason lignin was dried at 105 °C for 24 hours to afford the product (16.1 ± 0.1%).

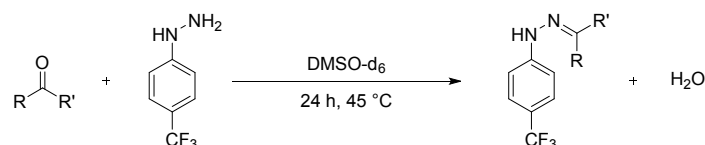
$$\text{Klason lignin content (\%)} = \frac{\text{Klason lignin product (g)}}{\text{Total biomass weight (g)}} \times 100\%$$

Photocatalysis of Native Lignin

For a typical photocatalytic reaction of native lignin, woodmeal (2.50 g), TBADT (250 mg, 75 μmol), DPA (varied amount), and AC:AN (30 mL 2:1) were mixed together in a 3 oz pressure reaction vessel. The system was degassed by freeze-pump-thaw in the same manner as the photocatalysis of PPol. The reactor was heated in a water bath to 50 °C and stirred for 48 hours under UV light irradiation. The oligomer solution was then collected by filtering the resulting slurry. The solution was concentrated under reduced pressure and the residue was resuspended in THF and sonicated for 5 minutes. The solution was then passed through a syringe filter (PET-45/25 polyester membrane with

pore diameter of 0.45 μm , and membrane diameter of 25 mm) to remove the precipitated TBADT. The crude oligomers were purified with silica gel column chromatography. A mixture of Hex and EA (8:2) was used to remove non-polar impurities. The gradient was then switched to DCM and MeOH (1:0-0:1) to obtain the remaining oligomers. The collected oligomers were then subjected to a neutral aluminum oxide plug (DCM:MeOH 1:0-0:1) to further purify the oligomers.

Carbonyl Quantification Experiments



Scheme 2.1 The hydrazone derivatization of lignin oligomers for ¹⁹F NMR carbonyl quantitative analysis.

To calculate the amount of carbonyls in the lignin oligomers, a published method about using 4-(trifluoromethyl)phenylhydrazine to derivatize carbonyls to the corresponding hydrazone was applied.²⁸ For a typical quantification reaction, lignin oligomers (15 mg), 100 μL p-trifluoromethyl toluene (Internal standard, IS) in DMSO-d₆ solution (0.1682 $\mu\text{mol}/\text{mg}$, accurately weighed), 200 μL 4-(trifluoromethyl)phenylhydrazine in DMSO-d₆ solution (containing 70.5 mg 4-(trifluoromethyl)phenylhydrazine, 0.40 mmol), and 400 μL pure DMSO-d₆ were mixed in a 4 mL vial, and then homogenized in a vortex mixer. The mixture was then transferred to a NMR tube, and heated to 45 °C for 24 hours. Before NMR analysis, 100 μL of relaxation agent solution in DMSO-d₆ (containing 2.8 mg chromium acetylacetonate) was added and homogenized. ¹⁹F NMR was carried out with the following acquisition parameters: 90° pulse angle, relaxation delay = 3 sec, scans = 64, region = -50~-70 ppm. IS was used as a reference peak set to -60.9 ppm, with the unreacted hydrazine peak at -59 ppm.

Preparation of Organosolv Lignin

Organosolv lignin for 2D-HSQC NMR was synthesized according to the literature.²⁹ Pretreated woodmeal (5 g), 80% ethanol aqueous solution (40 mL), and concentrated hydrochloric acid (0.8 mL) were added to a 100 mL round-bottom flask. The mixture was refluxed at 80 °C for 5 hours at which point the mixture was filtered. The residue was

washed with 100% ethanol (4x5 mL). The filtrate was collected and concentrated under reduced pressure. The remaining solid from the filtrate was re-dissolved in acetone (5 mL). The solution was then precipitated into DI water by dropwise addition (100 mL). Upon addition to the water, a brown-pink precipitate formed. The solution was filtered and the collected solid was dried in a vacuum oven at 45 °C overnight to afford the product (0.25 g, 5%).

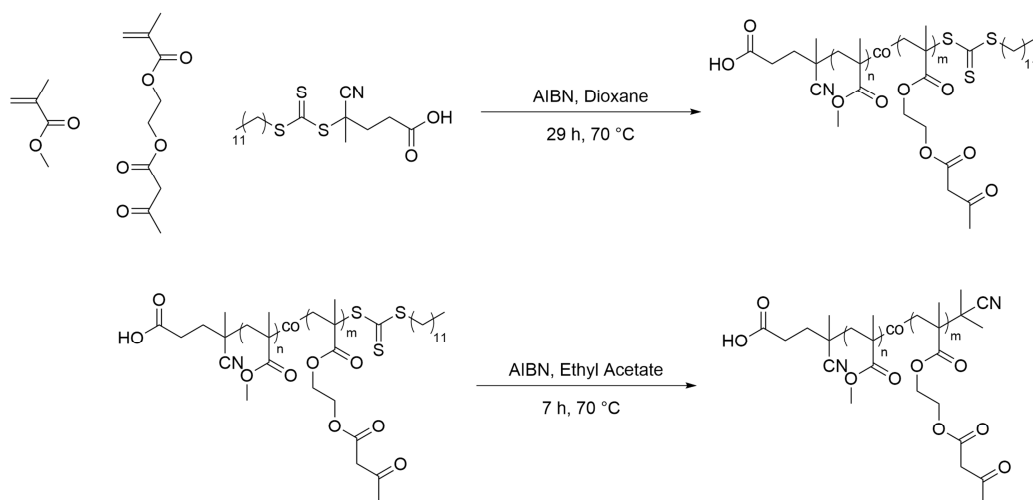
2D-HSQC NMR Experimental Details

To obtain 2D-HSQC spectra of organosolv lignin and the generated lignin oligomers, 25 mg of each sample was dissolved in 600 μ L of DMSO- d_6 . The spectra were run on a Bruker 500 MHz equipped with a CryoProbe (He) BBFO 5mm BBF/1H X nuclei optimized 5 mm double resonance BBFO. The pulse sequence selected was hsqcedetgpcisp2.3. The acquisition parameters were as follows: NS = 8, AQ = 0.08704 sec, D1 = 1 sec, 1SW = 220 ppm, O1P = 6.000, 2SW = 11.7592, O2P = 110.00, DB = 0, 1TD = 256, 2TD = 1024. The data was processed using MestReNova x64-14.1.1-24571. DMSO- d_6 was used as a reference peak set to ^1H 2.50 ppm, ^{13}C 39.52 ppm. The raw data was auto phase corrected and auto baseline corrected before integration. The contours were integrated using the following regions: Ar-OMe (^1H 3.2-4.1 ppm, ^{13}C 49.5-56.6 ppm) (internal standard), β -O-4 $_{\alpha}$ (^1H 4.6-5.0 ppm, ^{13}C 66.3-76.5 ppm), β -O-4 $_{\beta}$ / β' -O-4 $_{\beta}$ (^1H 3.8-4.5 ppm, ^{13}C 78.9-92.5 ppm), aldehyde (^1H 9.3-10.0 ppm, ^{13}C 187.5-207.7 ppm).

Control Experiments with Cellulose and Hemicellulose

The photocatalysis on cellulose and hemicellulose featured the same conditions and additives as typical woodmeal photocatalysis above, with the only difference being the reactant: using pure cellulose or hemicellulose (1.00 g) instead of woodmeal (2.50 g). After the reaction, the solution was filtered and washed with AN (3x5 mL), to remove TBADT, dried in vacuum oven overnight, and weighed to calculate the remaining percentage (weight after reaction \div weight before reaction) of each species. After photocatalysis, cellulose (95.4%) and hemicellulose (82.7%) were recovered. See Figure S9.

Synthesis of Polymer Filler



Scheme 2.2 Polymer filler synthesis process.

MMA (2.00 mL, 18.76 mmol) and AAEMA (358.14 μ L, 1.88 mmol) were added to a flask and dissolved in dioxane (15 mL). AIBN (4.62 mg, 28.14 μ mol) was added as a dioxane (1 mL) solution. The system was sealed with a septum and subjected to 3 rounds of freeze-pump-thaw to remove oxygen. The solution was heated to 70 °C for 29 hours at which point the solution was concentrated by half and precipitated into hexane (3 x 45 mL). The product was obtained as a yellow solid (2.00 g).

4-cyano-8-dodecylsulfanylcarbothioylsulfanyl-6-methoxycarbonyl-4,6,8-trimethyl-9-oxo-10-[2-(3-oxobutanoyloxy)ethoxy]decanoic acid (2.00 g, 2.73 mmol) and AIBN (30.81 mg, 187.6 μ mol) were dissolved in EA (27 mL). The system was degassed with nitrogen for 25 minutes at which point the system was sealed with a septum and heated to 70 °C for 7 hours. The solution was concentrated by half and precipitated into hexane (3 x 45 mL). The product was obtained as a white solid (1.85 g).

TAEA Crosslinking Procedure

As an example, lignin (34 mg, $f = 2.892$ mmol/g), and copolymer (52 mg, $M_n = 17.6$ kDA) were dissolved in THF (0.296 mL) in a 1.5 mL vial. From a stock solution of TAEA (10 μ L in 990 μ L of THF) was transferred (6.78 μ L, 4.53×10^{-4} mmol) to the lignin solution. The solution was mixed in a circular motion and transferred within 10 seconds to a PTFE mold via pipette, in order to avoid cross-linking in the mixing vessel. Any air bubbles were carefully removed with the tip of a needle. The solution was allowed to sit at ambient conditions and undergo solvent evaporation for 18 hours at

which point the film was carefully removed from the mold. The sample was cured under vacuum at room temperature for 24 hours to remove residual solvents.

Jeffamine Crosslinking Procedure

As an example, lignin (34 mg, $f = 2.800$ mmol/g), and copolymer (52 mg, $M_n = 17.6$ kDA) were dissolved in THF (0.250 mL) in a 1.5 mL vial. From a stock solution of Jeffamine (200 μ L in 300 μ L of THF) was transferred (44.89 μ L, 4.0×10^{-2} mmol) to the lignin solution. The solution was mixed in a circular motion and transferred within 10 seconds to a PTFE mold via pipette, in order to avoid cross-linking in the mixing vessel. Any air bubbles were carefully removed with the tip of a needle. The solution was allowed to sit at ambient conditions and undergo solvent evaporation for 18 hours at which point the film was carefully removed from the mold. The sample was cured under vacuum at room temperature for 24 hours to remove residual solvents.

Recycling Procedure

The obtained film was suspended in *n*-butylamine (4 mL) and heated to 80 °C until all solid was dissolved (4-18 hours). The solution was partially concentrated to remove about half of the *n*-butylamine. DCM and water (20 mL) were added. The aqueous phase was extracted with DCM (3 x 20 mL). The combined organic phases were washed with water (5 x 100 mL). The combined organic phases were dried over anhydrous sodium sulfate, filtered, and concentrated under reduced pressure. The residue was then subjected to the initial crosslinking conditions.

2.3 RESULTS

2.3.1 Proposed reaction mechanisms

Inspired by recent reports that show decatungstate ($[W_{10}O_{32}]^{4-}$, DT), a polyoxometalate anion, as an effective hydrogen-atom abstraction (HAA) reagent,³⁰⁻³⁴ we hypothesized that TBADT (**Figure 2.4**) can be an efficient catalyst to directly target the

abundant β -O-4 motifs in native lignin under mild conditions. Our proposed mechanism for the HAT mediated by TBADT involves hydrogen extraction from the substrate to result in an α -C radical upon irradiation, as shown in **Figure 2.5**. It can then lead to the scission of the β -C–O bond, producing an enol and an oxyl radical. The enol undergoes tautomerization to yield a ketone, and the oxyl radical receives the previously extracted hydrogen to produce an alcohol.¹⁸⁻²¹ It is noted that bond scission could also take place between the α -C–C bond, yielding an aldehyde and a methyl ether.³⁵ In either case, the overall reaction involves a hydrogen-atom return (HAR). Previous reports have shown that the presence of an electron mediator, such as 9,10-diphenylanthracene (DPA), can lend its electron to the radical³⁶⁻³⁷ and facilitate HAR to promote bond scission (**Figure 2.6-2.7**). In an alternative pathway, the α -C radical may be transformed into a stable carbonyl via oxidation, as shown in **Figure 2.8**, in which case an electron scavenger would be necessary to turn over the catalyst by extracting the hydrogen.³⁴

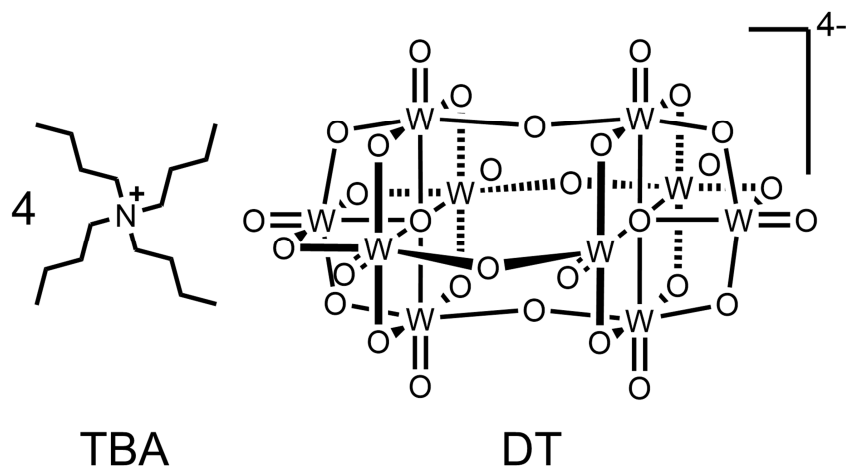


Figure 2.4 Chemical structure of the photocatalyst, TBADT.

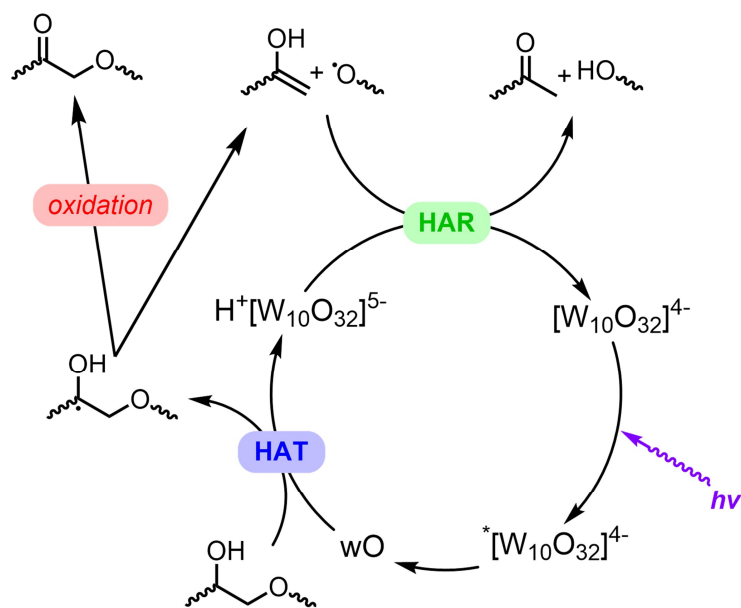


Figure 2.5 Catalytic cycles of DT-photocatalyzed conversion of the β -O-4 motif with two possible reaction pathways.

9,10-Diphenylanthracene (DPA)

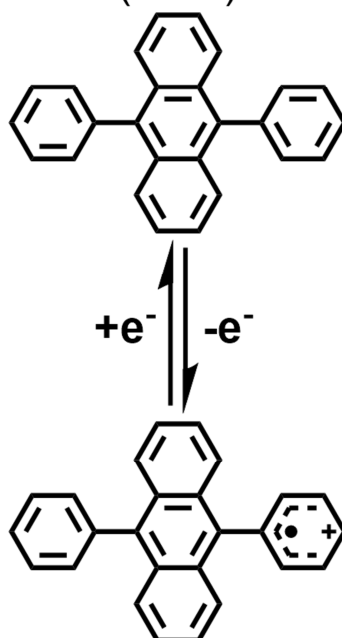


Figure 2.6 The chemical structure of DPA and the intermediate DPA^+ when its electron is lent to phenolic radicals.

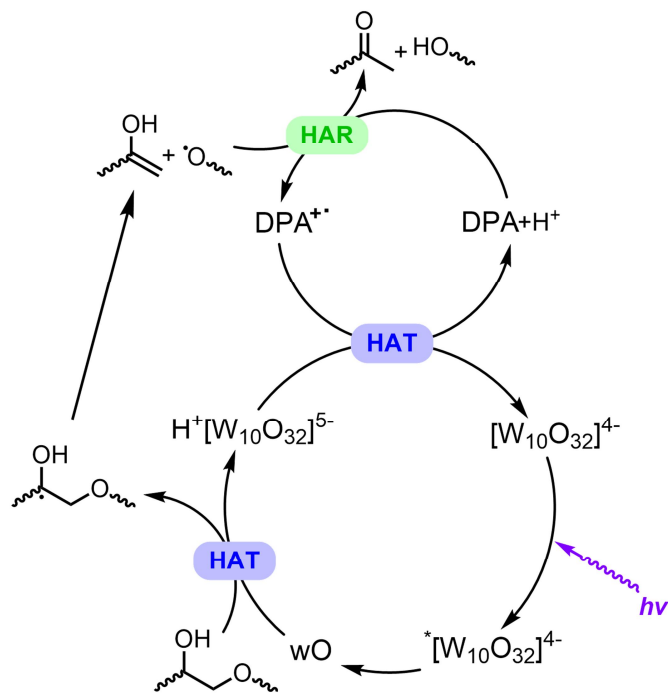


Figure 2.7 Catalytic cycle of DT in the presence of an electron mediator, DPA, which leads to the scission of the β -O-4 motif.

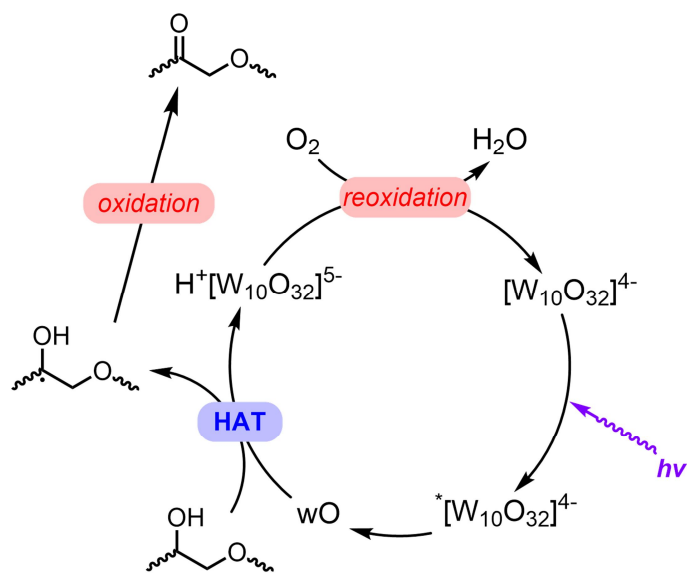


Figure 2.8 Catalytic cycle of DT in the presence of an electron scavenger, O_2 , which leads to the oxidation of the β -O-4 motif.

2.3.2 Photocatalytic depolymerization of model compounds with β -O-4 motif

To test the proposed mechanism involving the β -O-4 motif, we next carried out photocatalytic reactions on a model compound, 2-phenoxy-1-phenylethanol (PPol), which has been used as a testing platform for the study of lignin chemistry by other reports.^{18-19, 21, 38-39} As discussed above, two types of reactions are expected from this system, a redox neutral process that breaks down the β -C-O (or the α -C-C) bond or an oxidation reaction that preserves the β -O-4 motif but produces a carbonyl (**Figure 2.9**), whose products were identified by GC-MS (**Figure 2.10**). Changing the adding amount of TBADT only affected the total conversion rate of PPol, without significantly influence on the selectivity toward oxidation or bond cleavage (**Figure 2.11**).

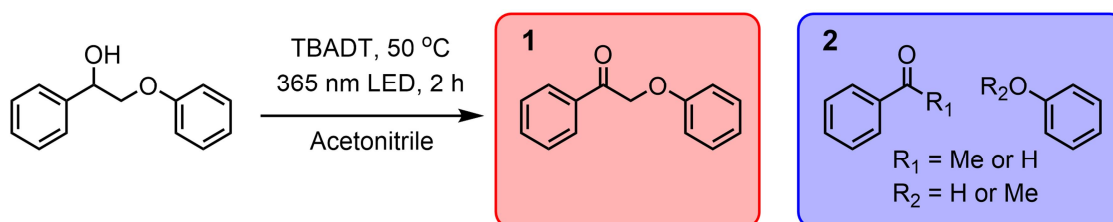


Figure 2.9 Two types of PPol reaction products in the presence of UV light: **1** oxidation and **2** bond scission.

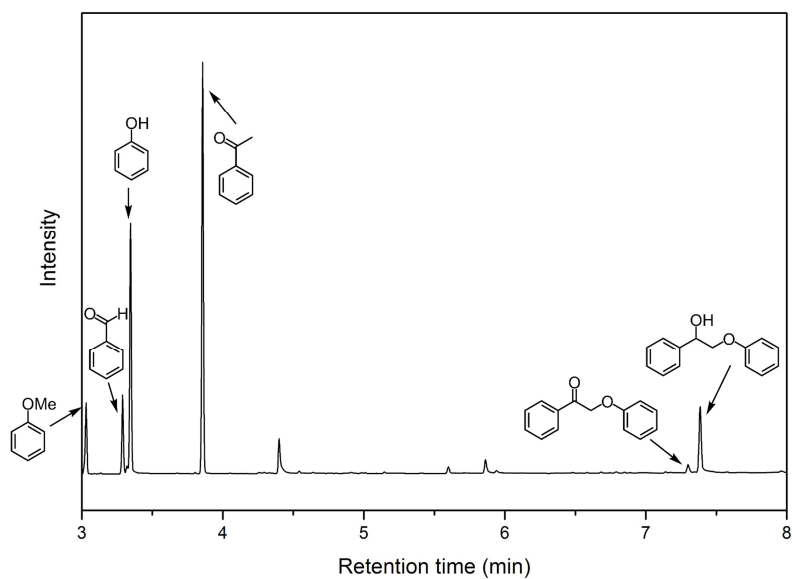


Figure 2.10 Identification of the photocatalytic cleavage and oxidation products with the PPol model reactant by GC-MS.

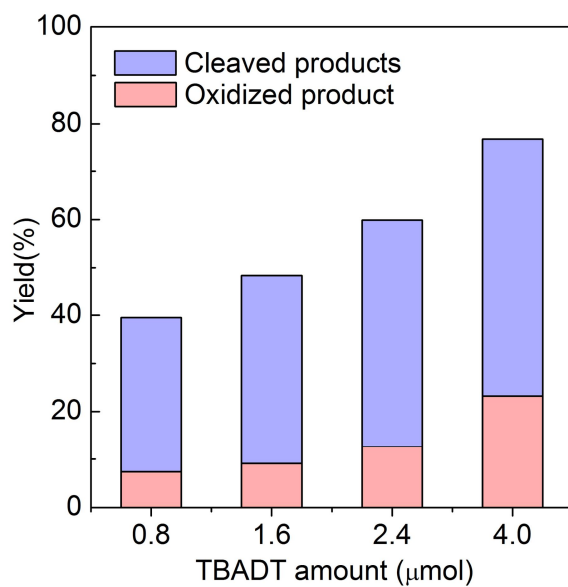


Figure 2.11 Comparison of the yields and distribution of different products with varying TBADT amount.

In a typical experiment, 50 μmol of PPol was mixed with 1.6 μmol of TBADT in 1 mL of acetonitrile, and the resulting solution was heated to 50 $^{\circ}\text{C}$ using a water bath under illuminated by a 200 W UV LED light centered at ca. 365 nm (**Figure 2.3**). The reaction was performed under 1 bar of N_2 . For a typical 2 h reaction, 4.56 μmol of 2-phenoxy-1-phenylethanone (PPone, compound **1** in **Figure 2.9**) was detected, accounting for 9.1% oxidation of the starting material (PPol). For the same reaction, 19.4 μmol of benzaldehyde or acetophenone (compounds **2** in **Figure 2.9**) or both was measured, reporting 38.9% bond scissions of the starting material. Also, 26.0 μmol of unreacted PPol was measured, which is consistent with the calculated conversion of 48.0% (**Figure 2.11**).

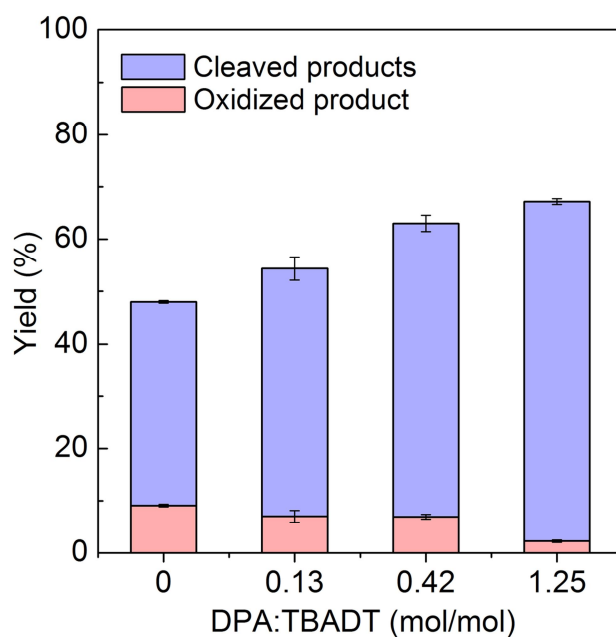


Figure 2.12 Comparison of the yields and distribution of different products with varying DPA amount.

Adding DPA as an electron mediator under otherwise identical conditions promoted the selectivity toward bond scission. Of the converted starting material, 81.0% underwent bond breaking when no DPA was added; the selectivity increased to 96.7% when 125 mol % of DPA (relative to TBADT) was used (**Figure 2.12**). Also increased was the total conversion, from 48.0% without DPA to 67.2% with 125 mol % of DPA. The increase in conversion was attributed to the improved TBADT turnover by DPA. As shown in **Figure 2.6**, when $\text{DPA}^{+\bullet}$ extracts hydrogen from the reduced TBADT, it facilitates the restoration of TBADT to the initial state, ready for the next catalytic cycle. Taken as a whole, it is concluded from this series of experiments that TBADT is effective in cleaving PPol and introducing carbonyl functional groups, and addition of electron mediators can further promote this reaction.

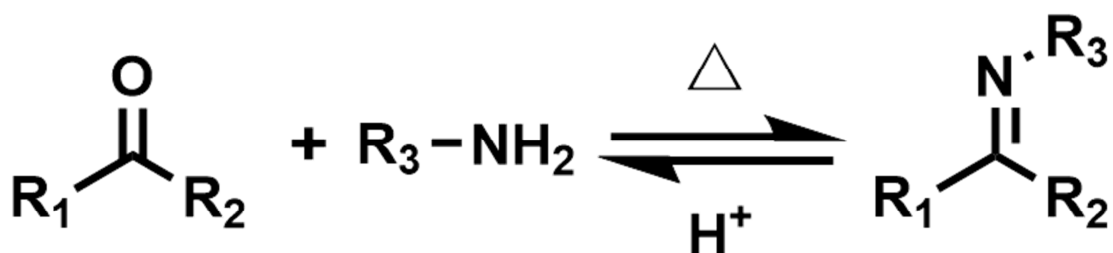


Figure 2.13 The formation of dynamic imine bonds with carbonyls as handles.

$$f = \frac{\text{Amount of carbonyls}}{\text{Amount of molecules}} = \frac{\text{Amount of carbonyls}}{\text{Weight of oligomers}} \times M_n$$

Equation 2.1 The definition and calculation of C=O stoichiometry (f).

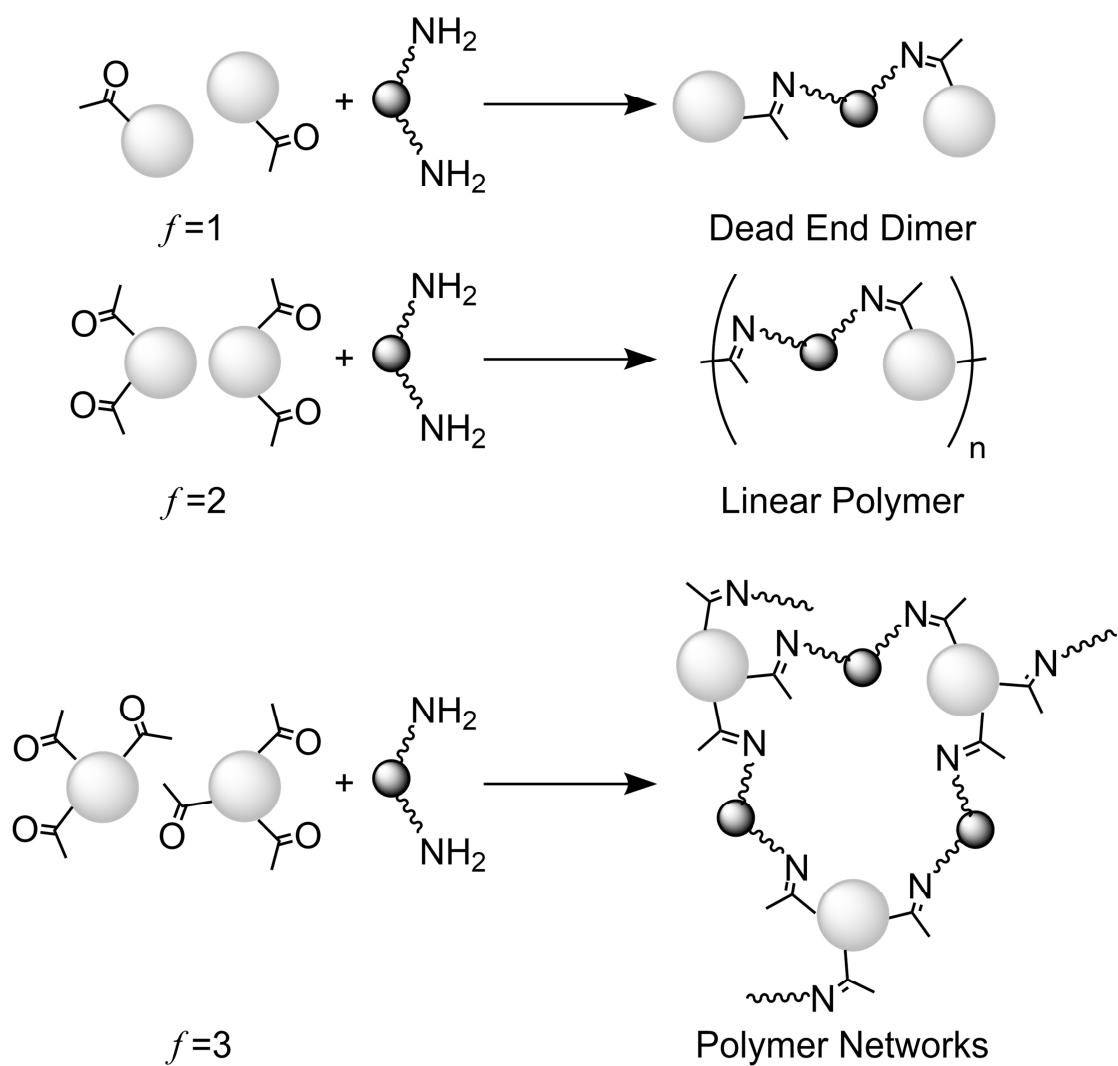


Figure 2.14 The influence of C=O stoichiometry (f) on the polymerization results.

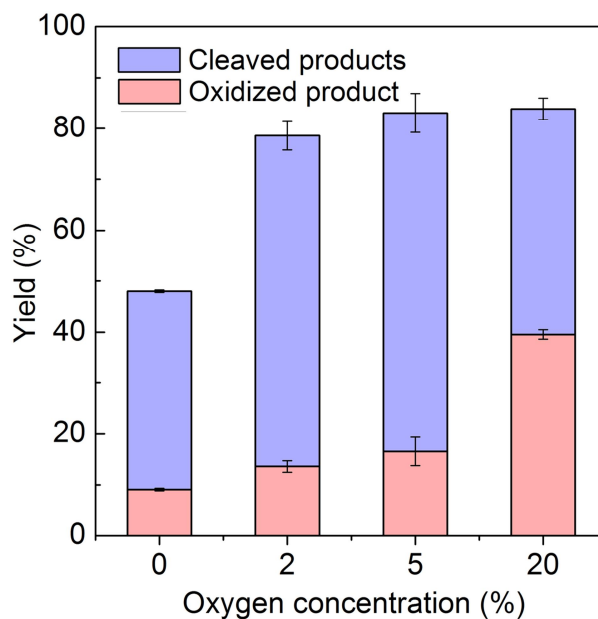


Figure 2.15 Comparison of the yields and distribution of different products with varying O₂ concentration.

For the subsequent polymerization consideration, we propose that the carbonyl (C=O) groups generating from both depolymerization and oxidation reactions can serve as a convenient reactive handle to form a dynamic imine bond by reacting with amines (**Figure 2.13**). Therefore, it is of critical importance to control the stoichiometry of C=O (**Equation 2.1**) during the depolymerization of native lignin. Too few C=O will likely make it difficult to repolymerize the resulting oligomers (**Figure 2.14**); too many C=O would mean that the reaction pathway is shunted toward the oxidation pathway, causing the lignin oligomers separation from the woodmeal challenging. A unique advantage offered by our photocatalytic depolymerization approach is the ability to control the reaction pathways by the introduction of exogenous electron scavengers, which could result in lignin oligomers with adjustable C=O stoichiometries. When the reaction

proceeds in a redox-neutral fashion, it favors the depolymerization of native lignin; when it undergoes oxidation, it is more effective in increasing C=O densities. Such a selectivity is new and significant because it will allow us to fine tune the degree of depolymerization of native lignin while controlling the density of key functional groups for subsequent repolymerization. To test this understanding, the following set of experiments was carried out on the model molecule of PPol. As shown in **Figure 2.15**, addition of O₂ as an electron scavenger to the reaction system led to increased selectivity toward oxidation, changing the selectivity toward compound **1** from 19.0% with no O₂ to 47.2% with 20% of O₂ in N₂ under otherwise identical reaction conditions. The corresponding stoichiometry of C=O increased from 2.24 mmol/g without O₂ to 3.94 mmol/g with 20% of O₂. It was observed that even without intentionally added electron scavengers, TBADT was capable of extracting electrons and protons from the substrate, acting as an effective oxidant, which helped explain why an appreciable amount of oxidation products (19.0%) was present under a pure N₂ atmosphere. Our control experiments further proved that the concentration of oxidation products scaled with the amount of TBADT used (**Figure 2.11**), while adding DPA inhibited the activity of TBADT as an oxidant (**Figure 2.12**). Replacing all N₂ with 100% O₂ led to overoxidation and diminished products of the desired compounds **1** or **2** (**Figure 2.16**). It was also observed that the addition of O₂ significantly improved the conversion of PPol. For instance, only 2% of O₂ increased the conversion from 48.0% to 78.6%. In the absence of electron mediators, the improved conversion is likely due to more TBADT turnovers, as shown in **Figure 2.8**. These experiments carried out on the model compound, PPol, established that photocatalytic transformation of the β-O-4 motif can be achieved using

TBADT following a HAT mechanism. It also showed that the reaction can be controlled between bond scission and oxidation. To further our understanding, we subjected another model system, 2-phenoxy-1-phenylpropan-1,3-diol (PPdiol), to the same conditions and found no significant difference in conversion with similar product distributions.

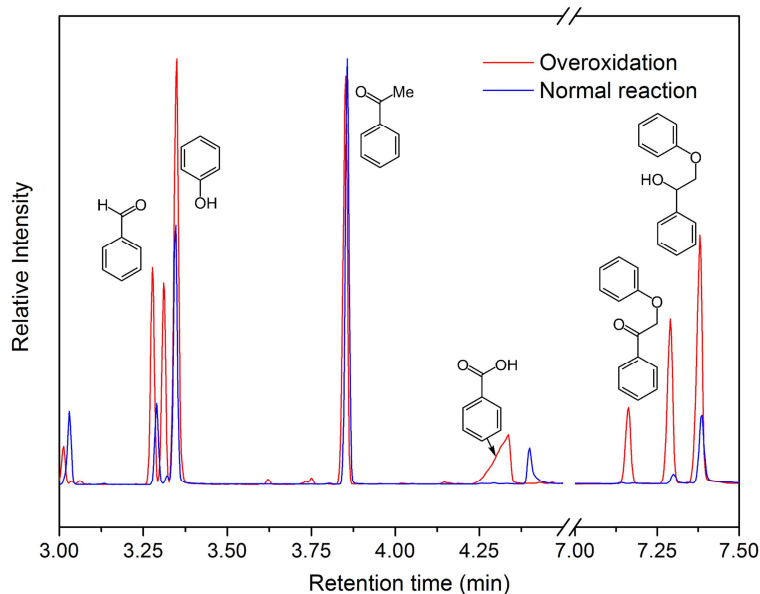


Figure 2.16: Identification of the overoxidation products under 100% O₂ atmosphere with the PPol model reactant by GC-MS.

2.3.3 Photocatalytic depolymerization of native lignin

With this knowledge in hand, we next turned our attention to the valorization of native lignin. For this purpose, we conducted experiments on beech sawdust with essential pretreatments. A typical reaction was performed with a mixture of 2.50 g of woodmeal, 75 μ mol of TBADT, and 30 mL of 2:1 acetone–acetonitrile mixture, which was then kept at 50 °C using a water bath with irradiation from the same UV LED light as noted above. The crude oligomers were purified with silica gel and neutral aluminum

oxide column chromatography to remove the remaining catalysts. In characterizing the products, attention was focused on soluble oligomer products, and two key figures of merit were quantified, namely, the yield (based on Klason lignin content) and the C=O stoichiometry. With only TBADT present, a yield of 14.5% was obtained, and the products featured a C=O stoichiometry of 2.10 mmol/g. Adding DPA as an electron mediator increased the yield but decreased the C=O stoichiometry, as expected. For instance, with 250 mol % of DPA, the yield was up to 23.3% and the C=O stoichiometry was down to 1.62 mmol/g (**Figure 2.17**). Conversely, when the reaction was carried out in different atmospheres, the presence of O₂ as an electron scavenger resulted in significant increases of the C=O stoichiometry, from 2.10 mmol/g in pure N₂ to 3.40 mmol/g in pure O₂ (**Figure 2.18**), with only modest changes to the yield (**Figure 2.19**). Importantly, the reaction could be performed in ambient air, and low concentrations of water or CO₂ did not appear to influence the process.

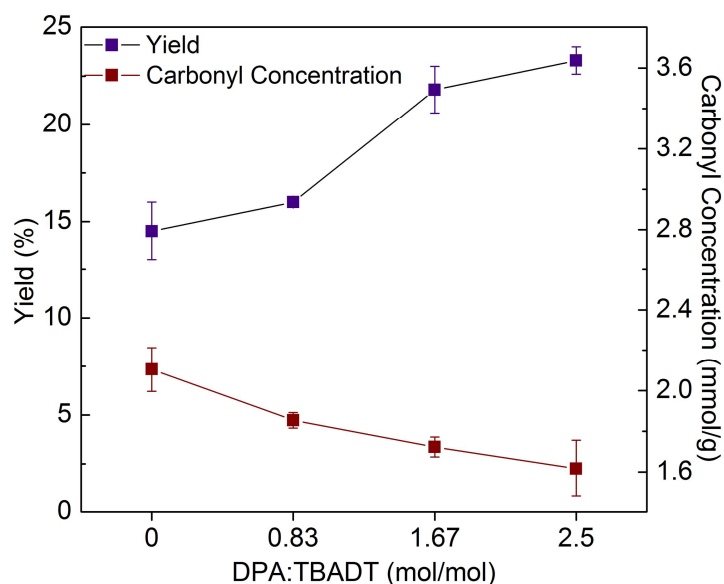


Figure 2.17 Comparison of the yield and C=O stoichiometry obtained from photocatalytic degradation of native lignin with varying DPA amount.

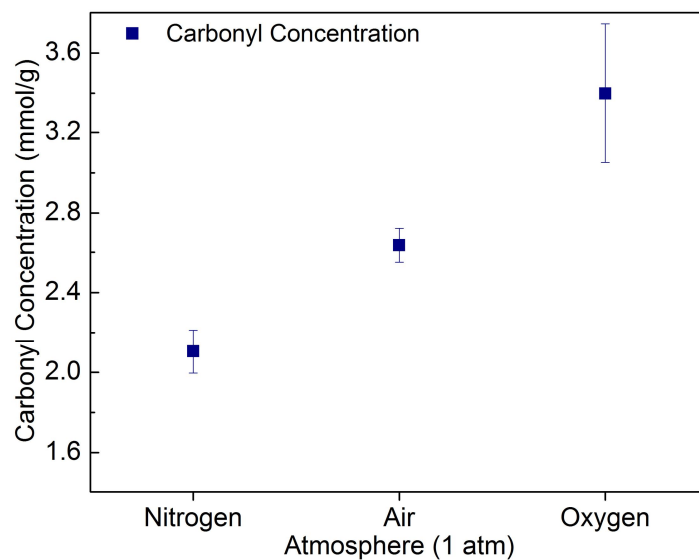


Figure 2.18 Comparison of the C=O stoichiometry obtained from photocatalytic degradation of native lignin with varying atmosphere.

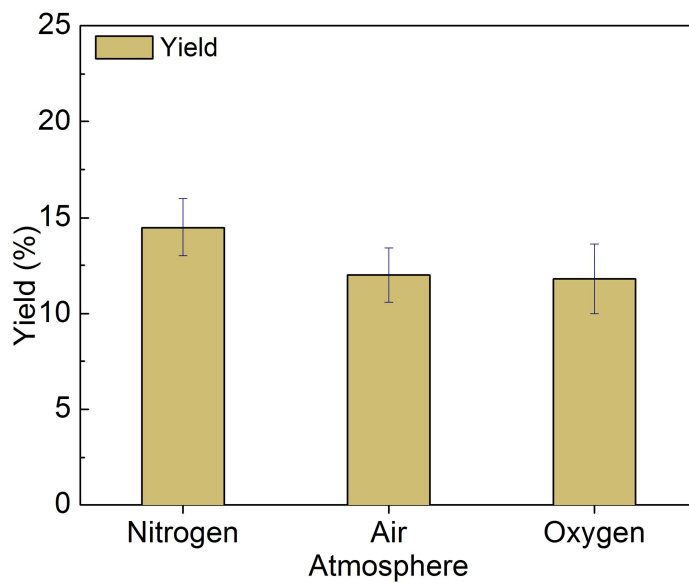


Figure 2.19 Comparison of the yield obtained from photocatalytic degradation of native lignin with varying atmosphere.

To further confirm that β -O-4 bond cleavage took place, 2-dimensional heteronuclear single-quantum coherence spectroscopy (2D-HSQC) NMR experiments were conducted using lignin oligomers generated without DPA and O₂, and mildsol lignin²⁹ as a soluble surrogate to native lignin (**Figure 2.20-Figure 2.22**). The use of organosolv lignin as a soluble surrogate of native lignin is well documented in the literature.^{22, 35} The 2D-HSQC NMR spectrum of organosolv lignin was consistent with the literature, showing the presence of β -O-4 _{α} - and β -O-4 _{β} / β' -O-4 _{β} -type bonds at ¹H 4.6–5.0 ppm, ¹³C 66.3–76.5 ppm and ¹H 3.8–4.5 ppm, ¹³C 78.9–92.5 ppm, respectively.^{29, 40-41} Similar to other reports,^{18, 29} the aryl methoxy (Ar-OMe) contours (¹H 3.2–4.1 ppm, ¹³C 49.5–56.6 ppm) were used as an internal standard for comparison of the two samples as they remained unchanged by the photocatalytic degradation. A direct comparison was made by setting the integration of the Ar-OMe peak as 1.00 and integrating the same regions of interest in both samples. After the photocatalytic degradation of native lignin to oligomers, the integration of the contours of the β -O-4 _{α} and β -O-4 _{β} / β' -O-4 _{β} bonds showed a decrease from 0.19 to 0.15 and from 0.27 to 0.17, respectively, suggesting a partial cleavage of these bonds. In addition, the increase in intensity of the contours in the aldehyde region (¹H 9.3–10.0 ppm, ¹³C 187.5–207.7 ppm) further supports the cleavage of the β -O-4 bond and the generation of the carbonyl functionalities in the resulting oligomers. The evidence strongly supports the proposed mechanisms as shown in **Figure 2.1c** and serves as a foundation to the photocatalytic lignin-first strategy. It is also noteworthy that the chemical integrity of the cellulose and hemicellulose was not significantly affected by our photocatalytic conditions and can be recycled after the reaction (**Figure 2.23**).

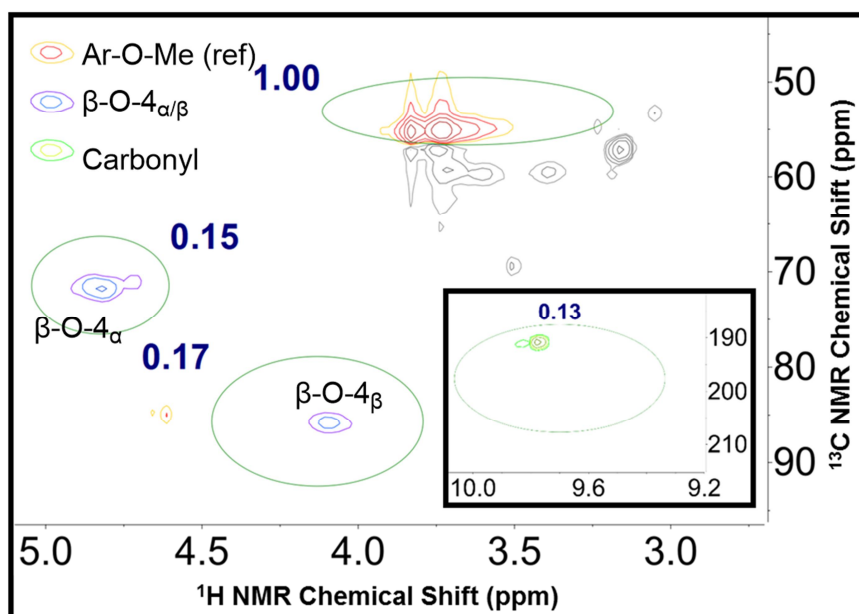


Figure 2.20 2D-HSQC spectrum of lignin oligomers showing the integration of functional groups of interest.

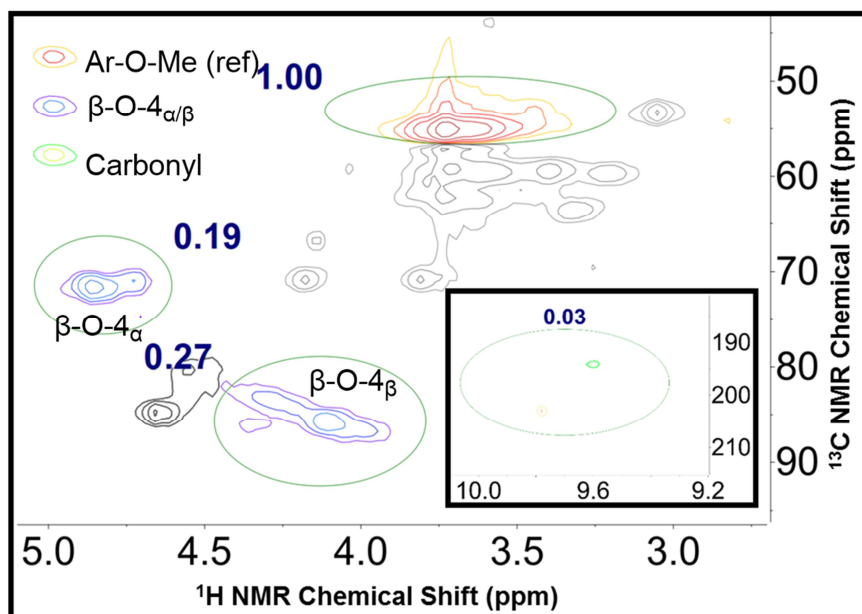


Figure 2.21 2D-HSQC spectrum of mildsol lignin showing the integration of functional groups of interest.

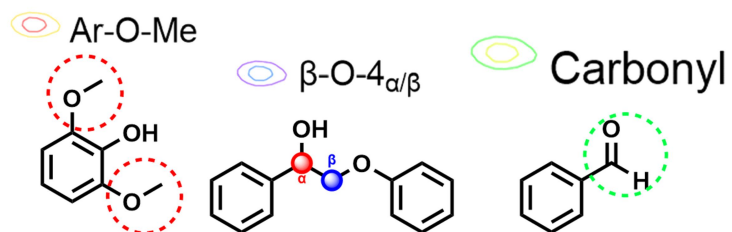


Figure 2.22 The chemical structures for the interested peaks in **Figure 2.20-Figure**

2.21 2D-HSQC spectra.

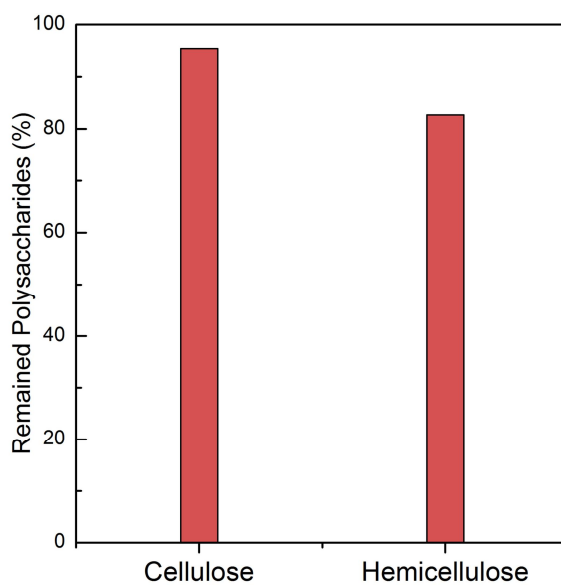


Figure 2.23 Quantification of remaining cellulose and hemicellulose after photocatalysis.

2.3.4 Polymerization of lignin oligomers

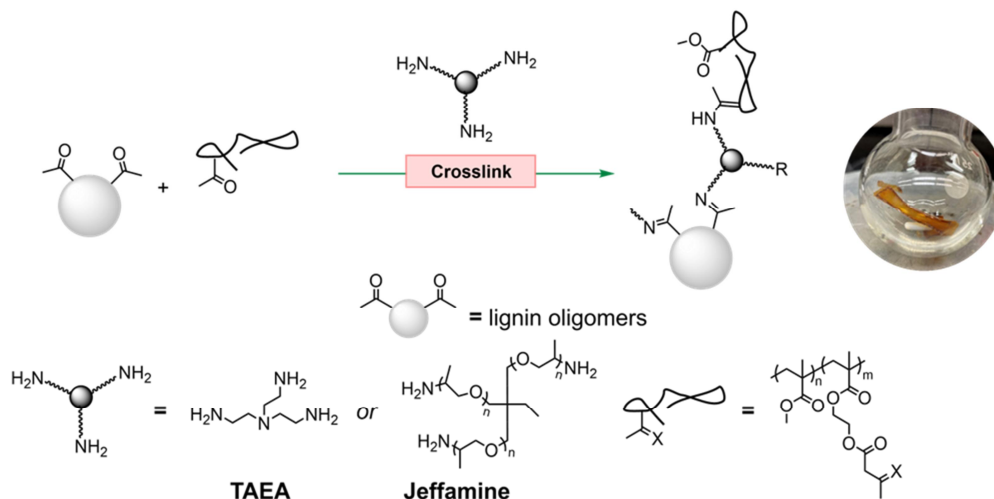


Figure 2.24 Schematic illustration of the lignin oligomer copolymerization process with dynamic crosslinker and polymer filler.

With the ability to obtain lignin oligomers rich in carbonyl functional groups, we set out to create a lignin-based polymer network material by repolymerizing the lignin oligomers with triamine cross-linkers. Inspired by the work of Sumerlin and co-workers,⁴²⁻⁴³ a copolymer of methyl methacrylate (MMA) and (2-acetoacetoxy)ethyl methacrylate (AAEMA) was used as a chemically recyclable filler to improve the mechanical strength of the network. The polymer network consisted of 40 wt % lignin oligomers and 60 wt % copolymer filler that was first cross-linked by a tris(2-aminoethyl)amine (TAEA) cross-linker (**Figure 2.24**). A substoichiometric amount (1 mol % amine groups with respect to total moles of cross-linkable carbonyls) of TAEA was found to be necessary to maintain the dynamic nature of the polymer network and avoid overhardening of the material. After curing at ambient temperature under vacuum for 24 h, tensile test revealed that the cross-linked network was brittle in nature,

exhibiting a maximum stress of 3.25 MPa and maximum strain of 15%, likely due to the short nonflexible arms of TAEA (**Figure 2.25**).

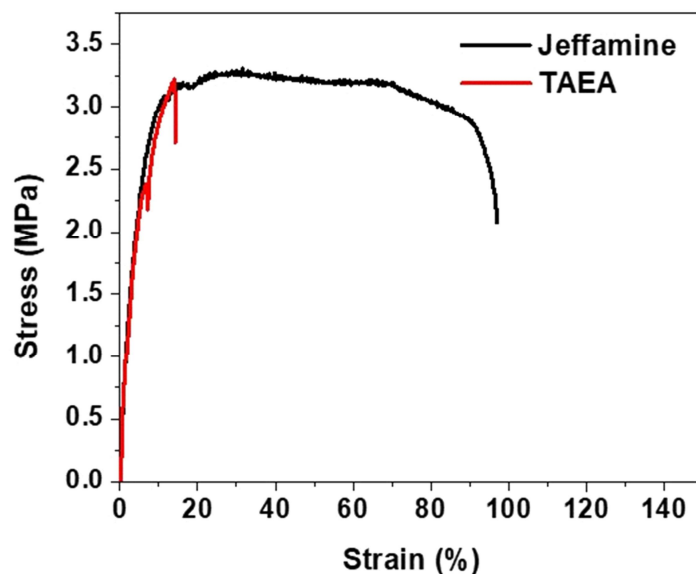


Figure 2.25 Tensile tests comparing different triamine cross-linked networks.

To overcome this challenge, a commercially available trimethylolpropane tris[poly(propylene glycol), amine terminated] ether (Jeffamine) was used as the cross-linker. Jeffamine showed the ability to create a polymer network with improved tensile properties at the stoichiometric amount (100 mol % amine groups with respect to total moles of cross-linkable carbonyls). The maximum stress of the Jeffamine network was similar to that of the TAEA network at ca. 3.25 MPa, while the strain improved to ca. 98% before breaking. The Young's modulus was similar for either the TAEA network or the Jeffamine network at 78 or 76 MPa, respectively.

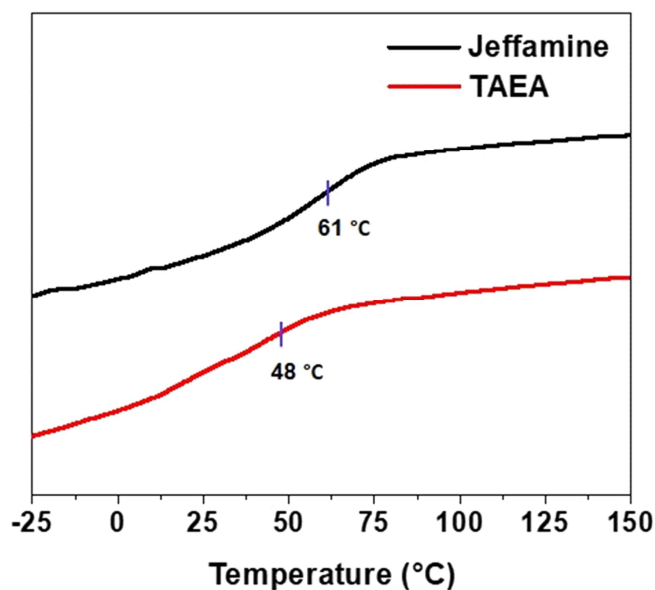


Figure 2.26 Glass transition temperatures of cross-linked networks as determined by DSC cooling curves.

Thermal analysis of the two cross-linked networks by differential scanning calorimetry (DSC) revealed the glass transition temperature (T_g) of the TAEA network to be 48 °C and the Jeffamine network to be 61 °C (**Figure 2.26**). The higher T_g of the Jeffamine cross-linked network is likely a result of a higher cross-linking density given that the initial loading of cross-linker was higher.

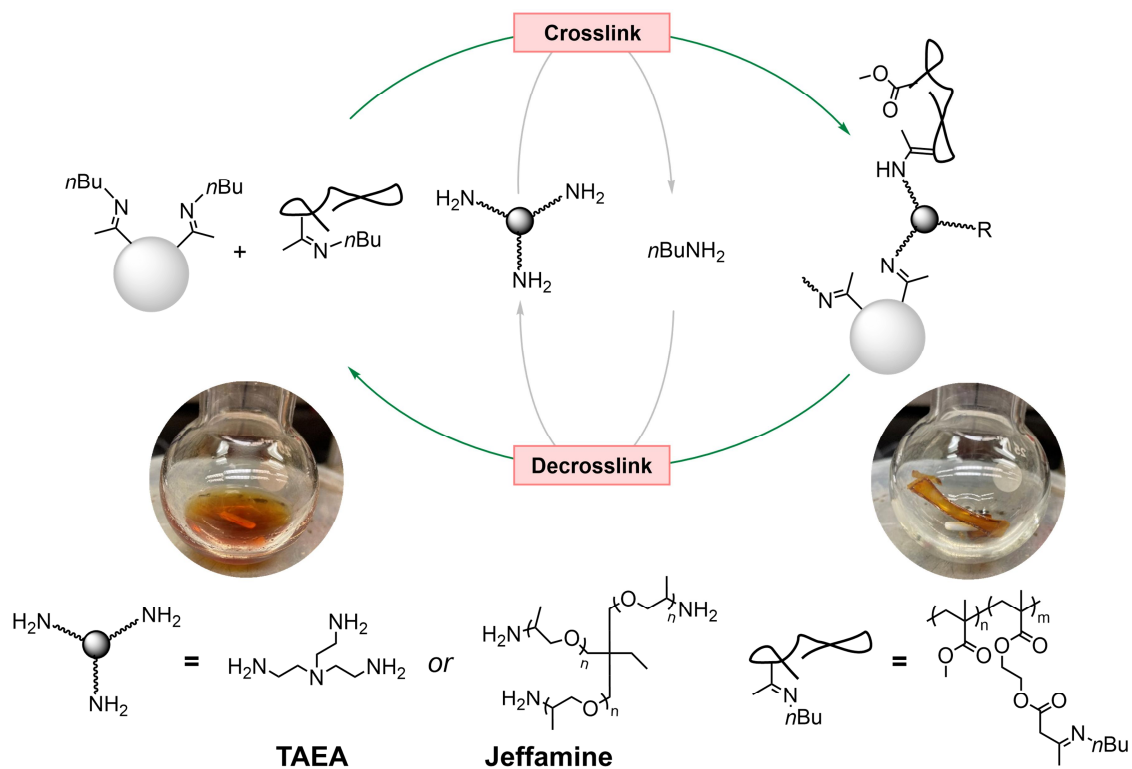


Figure 2.27 Schematic illustration of chemically recycling lignin based DPNs via *n*-butylamine.

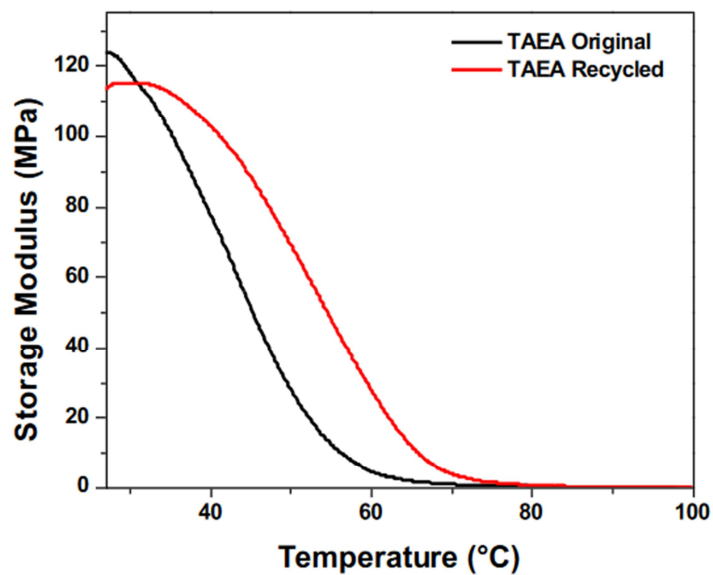


Figure 2.28 DMA analysis of original crosslinked TAEA DPNs and recycled TAEA DPNs.

Notably, the polymer network was readily depolymerized into soluble lignin oligomers and the copolymer filler by treating the film with excess n-butylamine at 80 °C. Following extraction to remove excess n-butylamine, the residues were repolymerized by simply recuring at ambient temperature followed by drying under vacuum for 24 h (**Figure 2.27**). The recured sample exhibited similar mechanical properties as the original network (**Figure 2.28**). Overall, we demonstrated that the lignin oligomers generated from the catalytic depolymerization of native lignin can be repolymerized into mechanically robust polymer networks capable of closed-loop chemical recycling.

2.4 DISCUSSION

We have developed a new approach to the direct conversion of native lignin to oligomers rich in carbonyl functionalities under photocatalytic conditions. The products were then used to prepare closed-loop, chemically recyclable DPNs. Toward this goal, TBADT as a photocatalyst made of earth-abundant elements was shown to be effective in either cleaving or oxidizing β -O-4 motifs through a HAT mechanism under conditions that would preserve cellulose and hemicellulose. The selectivity between decomposition and oxidation was controlled by adding exogenous electron mediators or electron scavengers. When applied to native lignin, the photocatalytic approach was shown to produce oligomers with up to 23.3% yield. The carbonyl stoichiometry was between 1.62 and 3.40 mmol/g, depending on the reaction conditions. 2D-HSQC results further supported that our photocatalytic system partially consumed β -O-4 motifs and generated high-value carbonyl functionalities. The produced oligomers could be repolymerized to

form chemically recyclable polymer networks via imine bond formation. The DPNs were capable of closed-loop recycling. The present work not only represents a new strategy for lignin valorization under mild conditions beyond monomerization but also provides the ability to generate closed-loop recyclable lignin-based materials with promising material properties.

2.5 REFERENCE

1. Schutyser, W.; Renders, a. T.; Van den Bosch, S.; Koelewijn, S.-F.; Beckham, G.; Sels, B. F., Chemicals from lignin: an interplay of lignocellulose fractionation, depolymerisation, and upgrading. *Chemical society reviews* **2018**, *47*, 852-908.
2. Sun, Z.; Fridrich, B.; De Santi, A.; Elangovan, S.; Barta, K., Bright side of lignin depolymerization: toward new platform chemicals. *Chemical reviews* **2018**, *118*, 614-678.
3. Wu, X.; Luo, N.; Xie, S.; Zhang, H.; Zhang, Q.; Wang, F.; Wang, Y., Photocatalytic transformations of lignocellulosic biomass into chemicals. *Chemical Society Reviews* **2020**, *49*, 6198-6223.
4. Abu-Omar, M. M.; Barta, K.; Beckham, G. T.; Luterbacher, J. S.; Ralph, J.; Rinaldi, R.; Román-Leshkov, Y.; Samec, J. S.; Sels, B. F.; Wang, F., Guidelines for performing lignin-first biorefining. *Energy & Environmental Science* **2021**, *14*, 262-292.
5. Renders, T.; Van den Bosch, S.; Koelewijn, S.-F.; Schutyser, W.; Sels, B., Lignin-first biomass fractionation: the advent of active stabilisation strategies. *Energy & environmental science* **2017**, *10*, 1551-1557.
6. Galkin, M. V.; Samec, J. S., Lignin valorization through catalytic lignocellulose fractionation: a fundamental platform for the future biorefinery. *ChemSusChem* **2016**, *9*, 1544-1558.
7. Jang, J. H.; Brandner, D. G.; Dreiling, R. J.; Ringsby, A. J.; Bussard, J. R.; Stanley, L. M.; Happs, R. M.; Kovvali, A. S.; Cutler, J. I.; Renders, T., Multi-pass flow-through reductive catalytic fractionation. *Joule* **2022**, *6*, 1859-1875.

8. Liu, Z.; Li, H.; Gao, X.; Guo, X.; Wang, S.; Fang, Y.; Song, G., Rational highly dispersed ruthenium for reductive catalytic fractionation of lignocellulose. *Nature Communications* **2022**, *13*, 4716-4726.
9. O’Dea, R. M.; Pranda, P. A.; Luo, Y.; Amitrano, A.; Ebikade, E. O.; Gottlieb, E. R.; Ajao, O.; Benali, M.; Vlachos, D. G.; Ierapetritou, M., Ambient-pressure lignin valorization to high-performance polymers by intensified reductive catalytic deconstruction. *Science Advances* **2022**, *8*, No. eabj7523.
10. Liao, Y.; Koelewijn, S.-F.; Van den Bossche, G.; Van Aelst, J.; Van den Bosch, S.; Renders, T.; Navare, K.; Nicolaï, T.; Van Aelst, K.; Maesen, M., A sustainable wood biorefinery for low-carbon footprint chemicals production. *Science* **2020**, *367*, 1385-1390.
11. Shuai, L.; Amiri, M. T.; Questell-Santiago, Y. M.; Héroguel, F.; Li, Y.; Kim, H.; Meilan, R.; Chapple, C.; Ralph, J.; Luterbacher, J. S., Formaldehyde stabilization facilitates lignin monomer production during biomass depolymerization. *Science* **2016**, *354*, 329-333.
12. Liu, G.; Jin, C.; Huo, S.; Kong, Z.; Chu, F., Preparation and properties of novel bio-based epoxy resin thermosets from lignin oligomers and cardanol. *International Journal of Biological Macromolecules* **2021**, *193*, 1400-1408.
13. Van Aelst, K.; Van Sinay, E.; Vangeel, T.; Zhang, Y.; Renders, T.; Van den Bosch, S.; Van Aelst, J.; Sels, B. F., Low molecular weight and highly functional RCF lignin products as a full bisphenol a replacer in bio-based epoxy resins. *Chemical Communications* **2021**, *57*, 5642-5645.
14. Vendamme, R.; Behaghel de Bueren, J.; Gracia-Vitoria, J.; Isnard, F.; Mulunda, M. M.; Ortiz, P.; Wadekar, M.; Vanbroekhoven, K.; Wegmann, C.; Buser, R., Aldehyde-assisted lignocellulose fractionation provides unique lignin oligomers for the design of tunable polyurethane bioresins. *Biomacromolecules* **2020**, *21*, 4135-4148.
15. Gioia, C.; Lo Re, G.; Lawoko, M.; Berglund, L., Tunable thermosetting epoxies based on fractionated and well-characterized lignins. *Journal of the American Chemical Society* **2018**, *140*, 4054-4061.

16. Cui, M.; Nguyen, N. A.; Bonnesen, P. V.; Uhrig, D.; Keum, J. K.; Naskar, A. K., Rigid oligomer from lignin in designing of tough, self-healing elastomers. *ACS Macro Letters* **2018**, *7*, 1328-1332.
17. Moreno, A.; Morsali, M.; Sipponen, M. H., Catalyst-free synthesis of lignin vitrimers with tunable mechanical properties: Circular polymers and recoverable adhesives. *ACS applied materials & interfaces* **2021**, *13*, 57952-57961.
18. Wu, X.; Fan, X.; Xie, S.; Lin, J.; Cheng, J.; Zhang, Q.; Chen, L.; Wang, Y., Solar energy-driven lignin-first approach to full utilization of lignocellulosic biomass under mild conditions. *Nature catalysis* **2018**, *1*, 772-780.
19. Wu, X.; Xie, S.; Liu, C.; Zhou, C.; Lin, J.; Kang, J.; Zhang, Q.; Wang, Z.; Wang, Y., Ligand-controlled photocatalysis of CdS quantum dots for lignin valorization under visible light. *ACS Catalysis* **2019**, *9*, 8443-8451.
20. Chen, K.; Schwarz, J.; Karl, T. A.; Chatterjee, A.; König, B., Visible light induced redox neutral fragmentation of 1, 2-diol derivatives. *Chemical Communications* **2019**, *55*, 13144-13147.
21. Zhu, Q.; Nocera, D. G., Catalytic C (β)–O bond cleavage of lignin in a one-step reaction enabled by a spin-center shift. *ACS Catalysis* **2021**, *11*, 14181-14187.
22. Bosque, I.; Magallanes, G.; Rigoulet, M.; Kärkäs, M. D.; Stephenson, C. R., Redox catalysis facilitates lignin depolymerization. *ACS central science* **2017**, *3*, 621-628.
23. Yang, C.; Karkas, M. D.; Magallanes, G.; Chan, K.; Stephenson, C. R., Organocatalytic approach to photochemical lignin fragmentation. *Organic Letters* **2020**, *22*, 8082-8085.
24. Li, S.; Wijethunga, U. K.; Davis, A. H.; Kim, S.; Zheng, W.; Sherman, B. D.; Yoo, C. G.; Leem, G., Ru (II) Polypyridyl-Modified TiO₂ Nanoparticles for Photocatalytic C–C/C–O Bond Cleavage at Room Temperature. *ACS applied nano materials* **2021**, *5*, 948-956.
25. Tzirakis, M. D.; Lykakis, I. N.; Orfanopoulos, M., Decatungstate as an efficient photocatalyst in organic chemistry. *Chemical Society Reviews* **2009**, *38*, 2609-2621.
26. Protti, S.; Ravelli, D.; Fagnoni, M.; Albin, A., Solar light-driven photocatalyzed alkylations. Chemistry on the window ledge. *Chemical communications* **2009**, *47*, 7351-7353.

27. Sluiter, A.; Hames, B.; Ruiz, R.; Scarlata, C.; Sluiter, J.; Templeton, D.; Crocker, D., Determination of structural carbohydrates and lignin in biomass. *Laboratory analytical procedure* **2008**, *1617*, 1-16.
28. Constant, S.; Lancefield, C. S.; Weckhuysen, B. M.; Bruijninx, P. C., Quantification and classification of carbonyls in industrial humins and lignins by 19F NMR. *ACS Sustainable Chemistry & Engineering* **2017**, *5*, 965-972.
29. Zijlstra, D. S.; de Santi, A.; Oldenburger, B.; de Vries, J.; Barta, K.; Deuss, P. J., Extraction of lignin with high β -O-4 content by mild ethanol extraction and its effect on the depolymerization yield. *JoVE (Journal of Visualized Experiments)* **2019**, *143*, No. e58575.
30. Wan, T.; Wen, Z.; Laudadio, G.; Capaldo, L.; Lammers, R.; Rincón, J. A.; García-Losada, P.; Mateos, C.; Frederick, M. O.; Broersma, R., Accelerated and scalable C (sp³)–H amination via decatungstate photocatalysis using a flow photoreactor equipped with high-intensity LEDs. *ACS Central Science* **2021**, *8*, 51-56.
31. Laudadio, G.; Deng, Y.; van der Wal, K.; Ravelli, D.; Nuño, M.; Fagnoni, M.; Guthrie, D.; Sun, Y.; Noël, T., C (sp³)–H functionalizations of light hydrocarbons using decatungstate photocatalysis in flow. *Science* **2020**, *369*, 92-96.
32. Sarver, P. J.; Bacauanu, V.; Schultz, D. M.; DiRocco, D. A.; Lam, Y.-h.; Sherer, E. C.; MacMillan, D. W., The merger of decatungstate and copper catalysis to enable aliphatic C (sp³)–H trifluoromethylation. *Nature chemistry* **2020**, *12*, 459-467.
33. Sarver, P. J.; Bissonette, N. B.; MacMillan, D. W., Decatungstate-catalyzed C (sp³)–H sulfonylation: rapid access to diverse organosulfur functionality. *Journal of the American Chemical Society* **2021**, *143*, 9737-9743.
34. Laudadio, G.; Govaerts, S.; Wang, Y.; Ravelli, D.; Koolman, H. F.; Fagnoni, M.; Djuric, S. W.; Noël, T., Selective C (sp³)–H aerobic oxidation enabled by decatungstate photocatalysis in flow. *Angewandte Chemie* **2018**, *130*, 4142-4146.
35. Nguyen, S. T.; Murray, P. R.; Knowles, R. R., Light-driven depolymerization of native lignin enabled by proton-coupled electron transfer. *ACS Catalysis* **2019**, *10*, 800-805.

36. Xia, P.; Raulerson, E. K.; Coleman, D.; Gerke, C. S.; Mangolini, L.; Tang, M. L.; Roberts, S. T., Achieving spin-triplet exciton transfer between silicon and molecular acceptors for photon upconversion. *Nature Chemistry* **2020**, *12*, 137-144.
37. Hu, A.; Chen, Y.; Guo, J.-J.; Yu, N.; An, Q.; Zuo, Z., Cerium-catalyzed formal cycloaddition of cycloalkanols with alkenes through dual photoexcitation. *Journal of the American Chemical Society* **2018**, *140*, 13580-13585.
38. Deng, W.; Zhang, H.; Wu, X.; Li, R.; Zhang, Q.; Wang, Y., Oxidative conversion of lignin and lignin model compounds catalyzed by CeO₂-supported Pd nanoparticles. *Green chemistry* **2015**, *17*, 5009-5018.
39. Zhou, Y.; Klinger, G. E.; Hegg, E. L.; Saffron, C. M.; Jackson, J. E., Multiple mechanisms mapped in aryl alkyl ether cleavage via aqueous electrocatalytic hydrogenation over skeletal nickel. *Journal of the American Chemical Society* **2020**, *142*, 4037-4050.
40. Wen, J.-L.; Sun, S.-L.; Yuan, T.-Q.; Xu, F.; Sun, R.-C., Structural elucidation of lignin polymers of Eucalyptus chips during organosolv pretreatment and extended delignification. *Journal of agricultural and food chemistry* **2013**, *61*, 11067-11075.
41. Wen, J.-L.; Sun, S.-L.; Xue, B.-L.; Sun, R.-C., Recent advances in characterization of lignin polymer by solution-state nuclear magnetic resonance (NMR) methodology. *Materials* **2013**, *6*, 359-391.
42. Lessard, J. J.; Garcia, L. F.; Easterling, C. P.; Sims, M. B.; Bentz, K. C.; Arencibia, S.; Savin, D. A.; Sumerlin, B. S., Catalyst-free vitrimers from vinyl polymers. *Macromolecules* **2019**, *52*, 2105-2111.
43. Lessard, J. J.; Scheutz, G. M.; Sung, S. H.; Lantz, K. A.; Epps III, T. H.; Sumerlin, B. S., Block copolymer vitrimers. *Journal of the American Chemical Society* **2019**, *142*, 283-289.

CHAPTER 3: LARGE SCALE NATIVE LIGNIN PHOTOCATALYTIC UPCYCLING TOWARD POLYIMINE NETWORKS VIA OLIGOMERS WITH ADJUSTABLE FUNCTIONALITIES

3.1 INTRODUCTION

As discussed in Chapter 1, lignin is recognized as both a useful component in the enhancement of existing materials and a promising renewable source of aromatic ring-contained platform chemicals.¹⁻³ However, the chemical heterogeneity of lignin limits the potential in development.^{1, 4} The conjugated aromatic structure is further enlarged from condensation reaction in industrial delignification, giving the technical lignin-enhanced polymers rigidity with the cost of ductility;⁵ the diverse monomer composition is also further complicated from different redox conditions in the lignin-first strategy, giving the lignin-decomposed monomers functionality with the cost of yield.⁶⁻⁷

To circumvent issues connected to the heterogeneity of lignin discussed above, there have been some efforts using abundant oxygen-containing functionalities in lignin to make lignin-based polymers, which can be a new paradigm of lignin upcycling.⁸⁻¹⁷ This route focuses on the key functional groups, mainly hydroxyls and carbonyls, as handles to form copolymers with the crosslinkers, in which the complicated separation of lignin cocktails gets bypassed.¹⁸⁻¹⁹ Recently, some promising results have been demonstrated to

use the abundant hydroxyls to construct lignin-based polymeric materials. For instance, Kraft lignin without chemical modification was added to epoxy resins,¹³ polyesters,²⁰⁻²² and polyurethane^{15-16, 23} for its abundance in hydroxyl functional groups, lending the enhanced polymeric materials extra mechanical strength while decreasing the usage of toxic chemicals, such as polyols⁸ and formaldehyde.¹¹⁻¹² Due to the high hydroxyl concentration, lignin oil from the RCF process was also valorized through polymerization. With proper modification, the lignin oil could be dimerized to an alternative of bisphenol A in polyester,²² or be functionalized by vinyl groups to generate vinyl-based polymer.²⁴ However, due to the irreversibility of the linkages in hydroxyl and vinyl based polymers, the resulting polymers are mostly not chemically recyclable, some of them are not even reversible.²⁵

Recognizing these challenges, we turned our interest toward DPNs, which feature both dimensional stability in thermosets and reprocessability in thermoplastics.²⁵ We choose imine bonds as dynamic linkages in the lignin-based DPNs because we can easily chemically recycle the material toward monomeric building blocks with the participation of external small molecular monoamines, which means the mechanical strength loss would be minimized during the recycling process.²⁵ As the second most abundant functional group in lignin, carbonyls (including aldehydes and ketones) can be used as handles to form imine dynamic bonds with crosslinkers. Very recently, we succeeded in demonstrating the concept that carbonyl-abundant lignin oligomers from lignin photocatalytic partial decomposition can produce polyimine DPNs with some recyclability.²⁶ After our concept demonstration, there are more promising results in converting chemically modified technical lignin to polyimine DPNs. For instance, the

1,3-diol structures in soda lignin reacted with terephthalic aldehyde to form an acetal, modifying this technical lignin with aldehyde functionalities.¹⁷ The polymerization reaction occurred between modified lignin and a fatty acid-based diamine crosslinker (Priamine™ 1075). Resulting copolymer containing 40% lignin showed its recyclability without significant strain loss, and its application in the wood coating was briefly talked about. In a separate study, most of the hydroxyl groups in Kraft lignin were modified by levulinic acid, which provided the lignin with ketone groups.²⁷ Diamine crosslinker bis(3-aminopropyl)-terminated polydimethylsiloxane (PDMS) was then used to make lignin polymer networks, which features a great potential to be applied for repairable, and hydrophobic coatings.

With these promising results in lignin-based imine DPNs, we found that decatungstates efficiently catalyzed the partial decomposition of β -O-4 motifs in native lignin through the HAT mechanism. However, it remained unsolved whether the molecular weight of lignin oligomers can be tuned, and how the structural factors (average molecular weight and carbonyl concentration) affect the properties of resulting DPNs. In this Chapter, we systematically study the relationship between the properties of lignin oligomers and the physical performance of lignin-based DPNs under an optimized catalytic system, and show the relationship between reaction time and average molecular weight of lignin oligomers.

3.2 METHODS

Materials

All reactions were carried out under a nitrogen atmosphere unless otherwise stated. Nitrogen and oxygen gasses were purchased from Airgas. Beech wood chips was purchased from Raeuchergold. All solvents including ethanol, acetone (AC), anhydrous acetonitrile (AN), diethyl ether, and dichloromethane (DCM) were purchased from commercial sources and used without further purification unless otherwise stated. NMR solvents including dimethyl sulfoxide (DMSO- d_6) and chloroform ($CDCl_3$) were purchased from Cambridge Isotope Laboratories and ACROS organics. Sodium tungstate dihydrate was purchased from ACROS organics. Sodium chloride, hydrochloric acid, hydrogen peroxide solution, pyridine and acetic anhydride were purchased from Thermo Fisher Scientific. 4-Trifluorophenylhydrazine, terephthalaldehyde (TPA) and sodium persulfate were purchased from Sigma Aldrich. 4-Trifluorotoluene was purchased from TCI. Dimer fatty acid with two amine end groups (PriamineTM1075) was kindly donated by Croda (now Cargill) with the amine stoichiometry of 208 mg KOH per gram. The size of polytetrafluoroethylene (PTFE) mold used for polymerization is 70 mm x 17 mm.

Characterization

All other instruments for characterizations and their parameters are the same as Chapter 2 without further clarification.

Light Reactor Specifications and Setup

The light source was the same 200 W UV LED light centered at 365 nm as Chapter 2, with all the other setup the same but changing the reactor to the 10 oz Non-Footed Starter Set w/mm scale, coupling, needle valve adaptor & SS plug purchased from Andrews Glass.

NaDT Catalyst Synthesis

NaDT photocatalyst was synthesized according to a literature procedure with minor modifications.²⁸ Concentrated hydrochloric acid (20.8 mL, 250 mmol) and $Na_2WO_4 \cdot 2H_2O$ (44.0 g, 133 mmol) were dissolved in 250 mL deionized (DI) water and heated to 90 °C separately. When the temperature reached 90 °C, the solutions were mixed together and rapidly stirred for 40 seconds. The color of mixture changed to

yellow immediately, indicating the formation of NaDT. The solution was stirred vigorously for 40 seconds, and then 180 g NaCl was added to the mixture. Then, the slurry was rapidly cooled down by 0 °C ice-water bath, and stirred for 1 hour. The solid phase was filtrated, washed with 20 mL pre-cooled DI water, ethanol, and diethyl ether. The crude NaDT precipitate was then dried with air flow for 30 minutes for subsequent purification.

Crude NaDT is purified through the solubility difference between NaDT and NaCl in hot AN. In detail, the crude NaDT was dispersed in 400 mL AN. The slurry was heated to 75 °C and stirred for 1.5 hours. After that, the mixture was centrifuged for its supernatant. The refined NaDT was then rotavaped from AN solution, dried in 90 °C vacuum oven overnight, and obtained as a yellow-white powder (16 g).

Wood Sawdust (Native Lignin) Pretreatment

Beech wood smoking chips was pretreated through a similar procedure as Chapter 2 with minor modifications. The wood sawdust (1 g: 10 mL) was suspended in an ethanol-water solution (4:1) and sonicated for 2 hours to remove most of the extractives before get filtered out. Then the wood sawdust was further washed with acetone (1 g: 10 mL) to get rid of surface extractives and extra water, and dried in a vacuum oven at 55 °C for a minimum of 48 hours, until the weight change was <5% in 105 °C 2 hour of drying, which indicating a <5% moisture content.

The dry woodmeal was then milled for 30 minutes for 6.5 grams of wood each run, on a ball mill purchased from Across International (Planetary ball mill, VQ-N, 1 kW, 1200 RPM, with 80 mL of capacity), with 2 pieces of 20mm diameter and 5 pieces of 10mm diameter stainless steel grinding balls. SEM images showed that the size of wood powder was 100-µm scale.

Klason Lignin Information

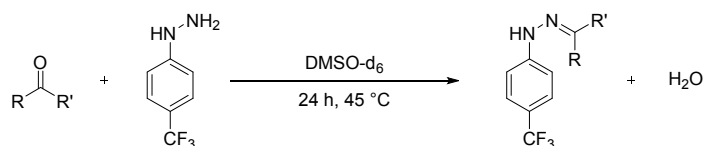
Klason lignin content was measured with the same procedure as Chapter 2, resulting in a Klason lignin content of 22.0 ± 0.1%.

$$\text{Klason lignin content (\%)} = \frac{\text{Klason lignin product (g)}}{\text{Total biomass weight (g)}} \times 100\%$$

Photocatalysis of Native Lignin

For a typical photocatalytic reaction of native lignin, woodmeal (15.0 g), NaDT (1.50 g, 600 μmol), and 80% acetone aqueous solution (150 mL) were mixed together in a 10 oz pressure reaction vessel for a larger scale. The system was purged by freeze-pump-thaw in the same manner as Chapter 2, and charged to 1 atm pressure with nitrogen (air or oxygen when dioxygen was applied as external oxidant). The reactor was then heated in a water bath to 50 $^{\circ}\text{C}$ and stirred for 24 hours under UV light irradiation without further variation. For the reaction time of less than 1.5 hours, the reactor was kept at 50 $^{\circ}\text{C}$ until passing 1.5 hours after turning off the UV light for sufficient solvent extraction. The solution containing lignin oligomers was then collected by filtering the resulting slurry, and concentrated under reduced pressure until all the acetone was removed. As a light-brown precipitate, lignin oligomers was then centrifuged and washed with water (30 mL x 3 times). Then the lignin oligomers was dried in vacuum oven overnight before subsequent acetylation and characterization.

Carbonyl Quantification Experiments



The C=O stoichiometry of lignin oligomers (and acetylated lignin oligomers) are quantified by the hydrazone derivation method with the same procedure in the Chapter 2.

Acetylation of the lignin oligomers

For a gram scale acetylation, lignin oligomers were dissolved in 4 mL of pyridine and 4 mL of acetic anhydride at room temperature and stirred for at least 18 hours. This excess amount of pyridine and acetic anhydride were briefly evaporated with air flow, then those extra reagents are removed by drying in vacuum oven overnight. Then the acetylated lignin oligomers is then dissolved in 50 mL of DCM and washed by 1 M HCl (3 x 150 mL). The organic phase was concentrated and then dried in the vacuum oven again.

Crosslinking Procedure

As an example, lignin (200 mg, 1.43 mmol/g) was dissolved in 1 mL of DCM. PriamineTM1075 (300 mg) and TPA (24 mg) were dissolved together in 1 mL of DCM. The solution of PriamineTM1075 and TPA is added to the lignin solution, and then mixed

together by pipette. The mixture was then transferred within 10 seconds to a PTFE mold on the PTFE coated petri dish purchased from Fluorolab via pipette, in order to avoid cross-linking in the mixing vessel. Then the dish was covered with a cap and allowed to slowly evaporate overnight. The polymer film was then gently removed and dried under vacuum at room temperature for at least 6 hours.

3.3 RESULTS

3.3.1 Optimization of photocatalytic system

As a compelling and trailblazing photocatalyst, DT has shown excellent effectiveness in activating C-H bonds.²⁹ Its unique oxo-structure enables a ligand-to-metal charge transfer (LMCT) transition after the tungsten centers get activated by photons, resulting in radical characteristics on the terminal oxygen centers, which enables the subsequent HAT process (**Figure 3.1**). Among all counter ions, tetrabutylammonium (TBA⁺) was commonly used in organic synthesis due to its solubility in acetonitrile, which can dissolve most of the small-molecule substrates.²⁹⁻³¹ However, it's inevitable that the C-H bonds in TBA⁺ can be activated by DT, generating 1-butene and hydrogen, which means the degradation of the catalyst.³² Besides, our previous purification methods, such as silica and alumina column chromatography, cannot remove TBA⁺ effectively, leaving TBA⁺ in the lignin oligomers as an impurity. With the water generated from lignin oxidation, TBA⁺ also catalyzes the hydration of acetonitrile to acetamide,³³ which can be another impurity that cannot be easily separated by column (**Figure 3.2-Figure**

3.3). To avoid the side reactions caused by TBA^+ , we turned our interest to NaDT (Figure 3.4).

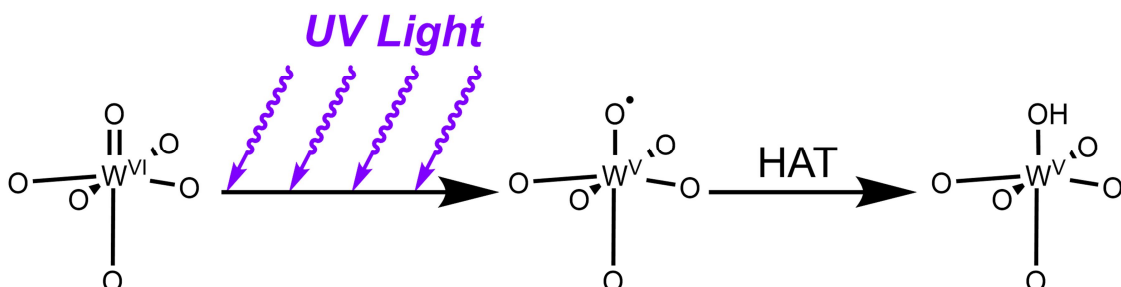


Figure 3.1 LMCT and subsequent HAT processes for the terminal W-centered octahedron indicates the photocatalytic activity for DT.

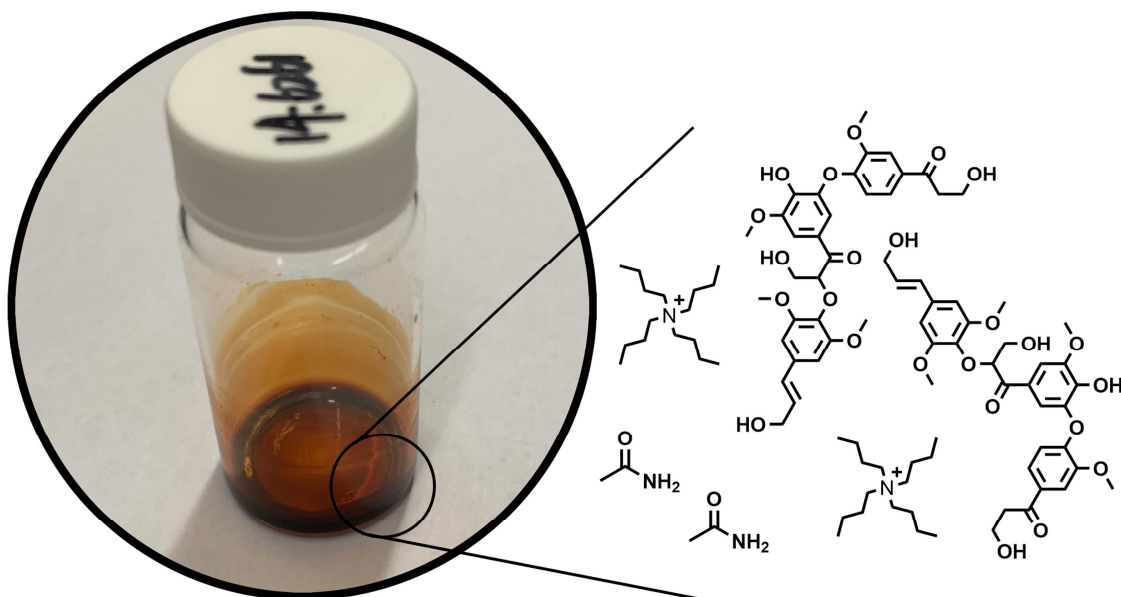


Figure 3.2 Schematic for the composition of crude lignin oligomers.

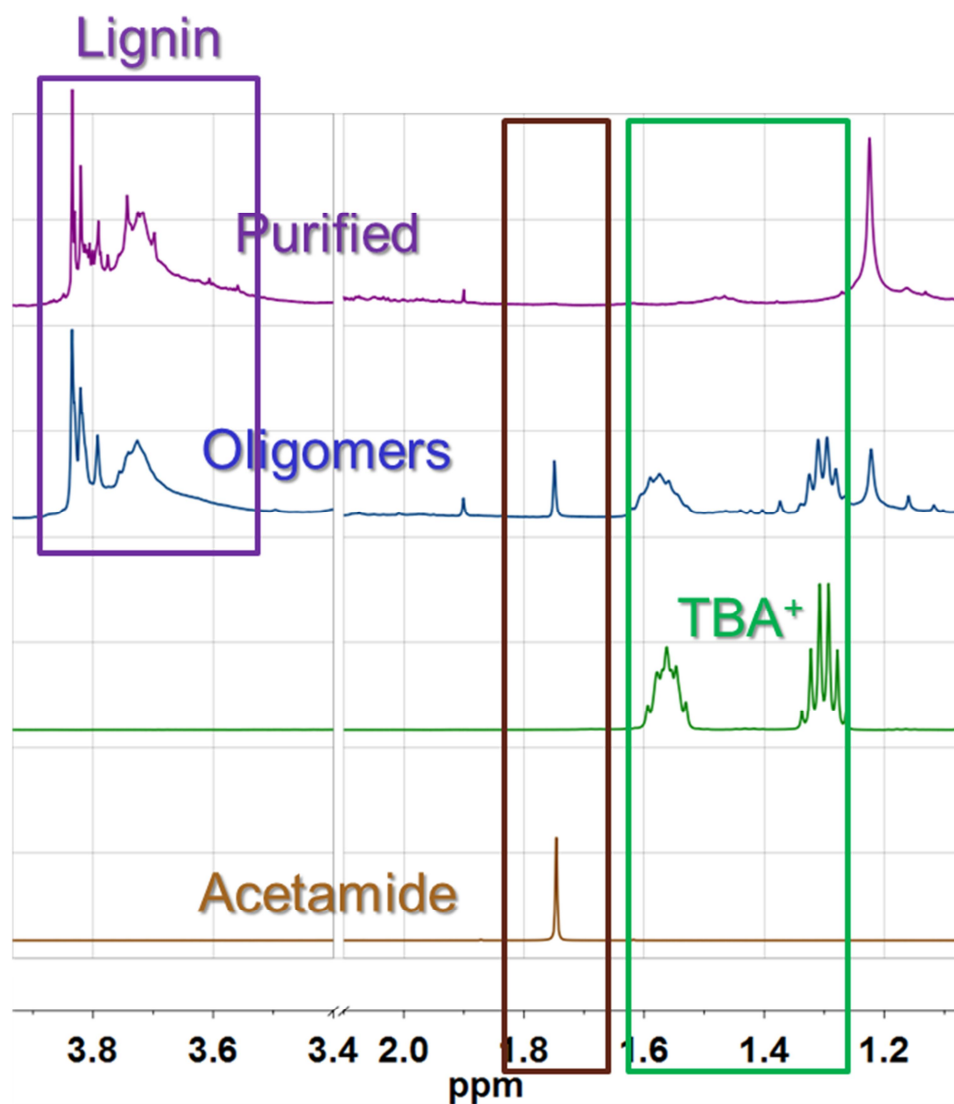


Figure 3.3 ¹H NMR results of lignin oligomers generated from different catalytic system, and the standard spectra of acetamide and TBA⁺. The peaks for acetamide (green), TBA⁺ (brown), and lignin (purple) are circled.

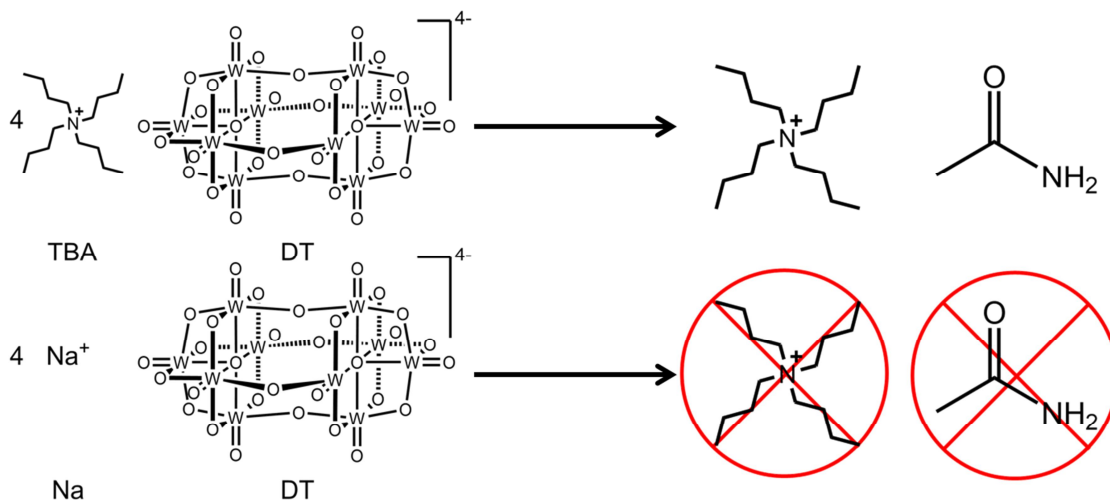


Figure 3.4 Changing the photocatalyst from TBADT to NaDT avoids the side reactions generating byproducts TBA⁺ and acetamide.

Inspired by previous studies on mild lignin extraction to organic solvents,³⁴⁻³⁶ water was found helpful in dissolving lignin with other organic solvents. Besides, adding water to the organic solvent improves the solubility of NaDT significantly. We choose the acetone-water mixture in the optimized catalytic system³⁷⁻³⁸ to minimize possible side reactions. To test the optimized composition of the solvent mixture, we performed the photocatalytic conversion of native beech lignin with different ratios between organic solvent and water (**Figure 3.5**). In a typical experiment, 15.00 g of woodmeal was mixed with 1.50 g (614 μmol) of NaDT in 150 mL of solvent, and the resulting solution was heated to 50 °C using a water bath illuminated by a 200 W UV LED light centered at ca. 365 nm for 6 hours. With the anhydrous organic solvent, 23.0 mg of lignin was separated after purification, accounting for a yield of 0.7%. The yield significantly increased to 6.4% when the 25% (v/v) water in acetone solution was used, with 212.8 mg lignin oligomers separated. It was also observed that even a small amount of water significantly improved

the extraction of lignin. For instance, only 10% of water increased the yield from 0.7% to 5.4%. With this knowledge in hand, we optimized the catalytic system to NaDT in 25% water containing acetone with maximum lignin depolymerization efficiency and minimum side reactions.

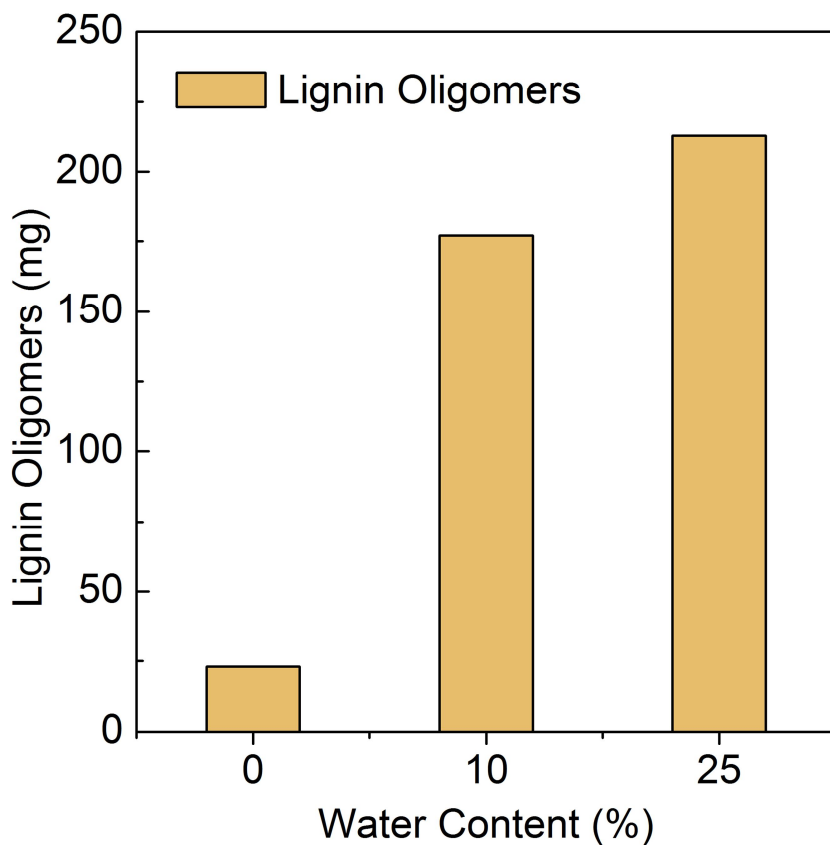


Figure 3.5 Comparison of the productivity obtained from photocatalytic degradation of native lignin with different water content in the solvent.

3.3.2 Kinetics in controllable lignin photocatalytic depolymerization

We acknowledge that the turnover of DT in both lignin model compounds and native lignin photocatalysis is a challenge. In Chapter 2, we promoted the turnover of DT

by introducing an electron mediator or electron scavenger, which also adjusted the selectivity toward cleavage and oxidation. However, the reaction kinetics without these additives is still unclear.

To test the effect of the reaction kinetics and the properties of resulting lignin oligomers, we implemented photocatalytic depolymerization on cleaned and ball-milled beech wood (purchased on Amazon, with a 22.0% Klason lignin content) with the optimized reaction conditions with different reaction time. The crude oligomers were washed with deionized water to remove the remaining catalysts. With the consideration of ruling out the solvent extraction effect, we set the control sample to 1.5 hours of stirring with light off and all other conditions the same. We accordingly extended the dark stirring time to avoid insufficient solvent extraction for the experiments with a less than 1.5 hours reaction time (**Figure 3.6**). The yield (calculated by the Klason lignin content), average molecular weight (number average, M_n , examined by gel permeation chromatography (GPC) results with polystyrene reference), and C=O stoichiometry (^{19}F NMR results of derived samples) are characterized to describe the change of water-insoluble lignin oligomer properties. Intriguingly, without photocatalysis, the acetone-water solvent mixture extracted 54.2 mg lignin with a yield of 1.64%, an M_n of 1766 g/mol, and a C=O stoichiometry of 0.83 mmol/g, showing the abundance of C=O in the native lignin and the potential for C=O based polymerization purposes.

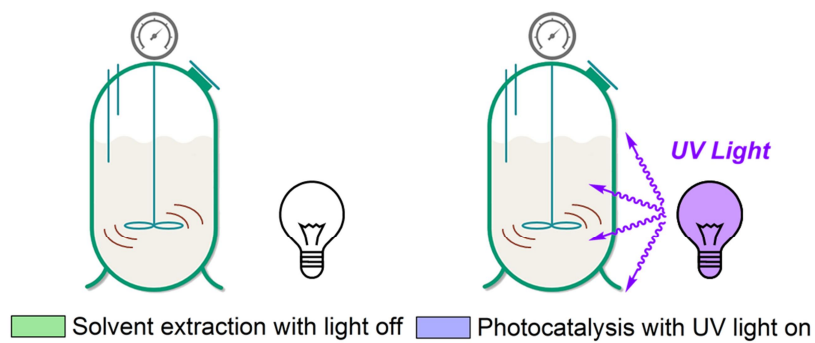
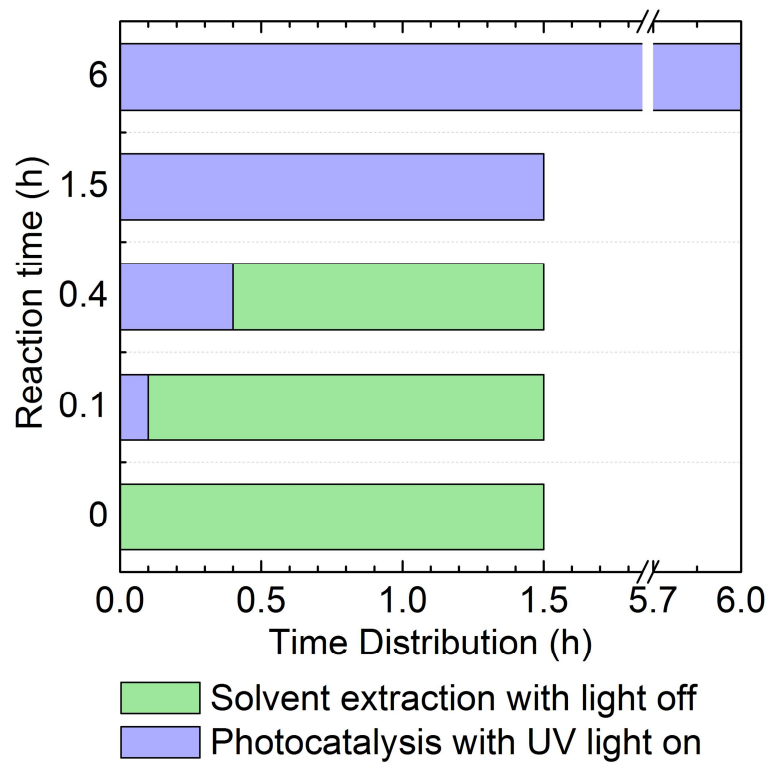


Figure 3.6 Time distribution for different reaction time with necessary solvent extraction effect for lignin.

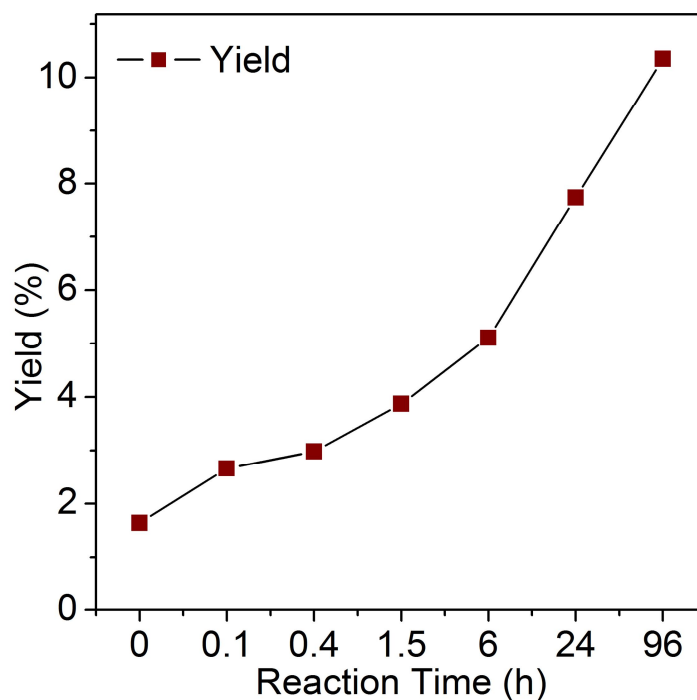


Figure 3.7 Comparison of the yield of the lignin oligomers from photocatalytic depolymerization of native lignin with different reaction time and at least 1.5 hours extraction.

Extending the reaction time significantly promoted the oligomerization of native lignin (**Figure 3.7**). With the same solvent extraction conditions, the yield of lignin oligomers significantly increased from 1.64% to 3.87% with 1.5 hours of photocatalysis. Even a 0.1-hour UV irradiation resulted in an increase of oligomer yield to 2.66%, indicating that photocatalysis is predominant in the reaction system compared with solvent extraction. Further extending reaction time to 6, 24, or 96 hours produced lignin oligomers with the yield of 5.11%, 7.74%, and 10.35%, respectively.

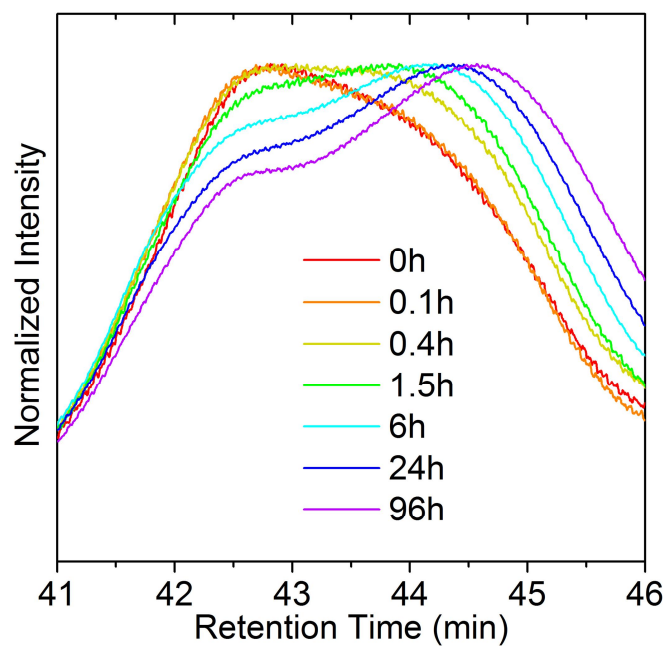


Figure 3.8 Normalized GPC results of the lignin oligomers from photocatalytic depolymerization of native lignin with different reaction time.

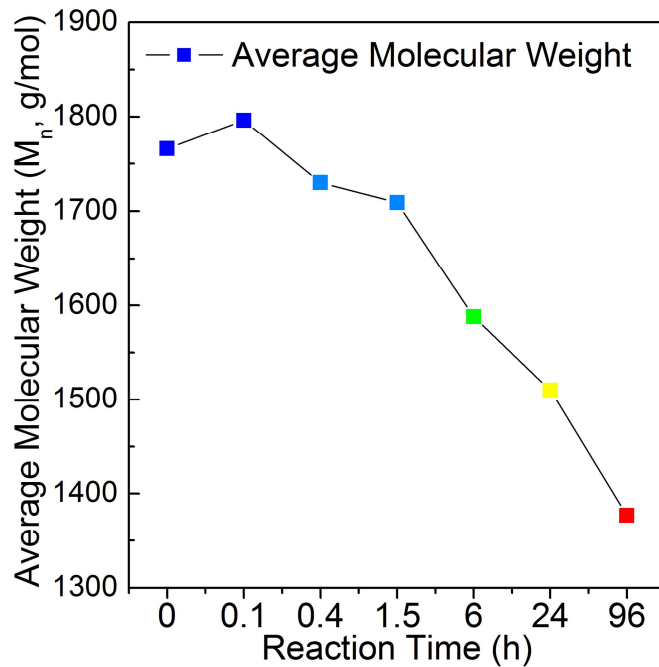


Figure 3.9 Comparison of the M_n of the lignin oligomers from photocatalytic depolymerization of native lignin with different reaction time.

As confirmed by the GPC results, extending the reaction time under otherwise identical conditions also promoted the bond scission reaction (**Figure 3.8**). In the GPC curves with a normalized intensity, there were mainly 2 fractions in the solvent-extracted lignin oligomers: a major peak located at 42.8 min of retention time, indicating large lignin oligomers with an average molecular weight of 6145 g/mol; and a shoulder peak located at 43.9 min of retention time, identified as small lignin oligomers with an average molecular weight of 1622 g/mol. When the reaction time extended, the proportion of small lignin oligomers kept increased. After 1.5 hours of photocatalysis, the large lignin oligomers lost their dominance and became a shoulder peak in the GPC results. Extending the reaction time from 1.5 hours would further decrease the content of large lignin oligomers; in the meantime, a right shift of the peak representing small lignin oligomers was observed. The retention time changed from 43.9 to 44.6 min when the reaction time extended from 1.5 to 96 hours, indicating that the average molecular weight of small lignin oligomers decreased from 1622 to 945 g/mol.

The quantitative results of M_n were calculated by integrating the GPC curves (**Figure 3.9**). Compared with lignin oligomers generated without photocatalysis, a reaction time of 96 hours decreased the M_n to 1377 g/mol, as expected. A significant decrease of M_n was observed between the reaction time of 1.5 and 96 hours, from 1709 to 1377 g/mol; however, the M_n of the resulting lignin oligomers only modestly changed between 1796 and 1709 g/mol when the reaction time varied within 1.5 hours. That trend revealed that a longer reaction time significantly promoted the bond scission reaction.

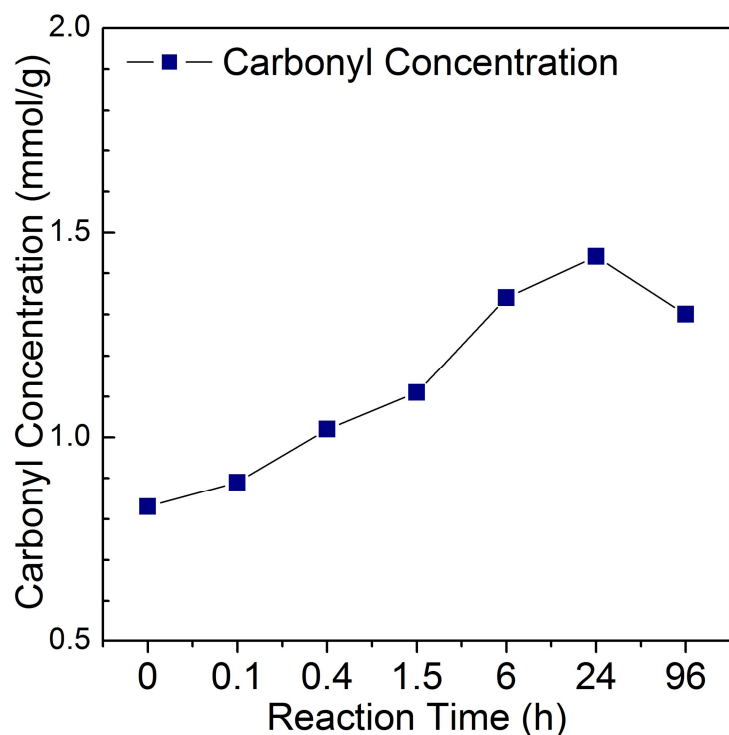


Figure 3.10 Comparison of the carbonyl concentration of the lignin oligomers from photocatalytic depolymerization of native lignin with different reaction time.

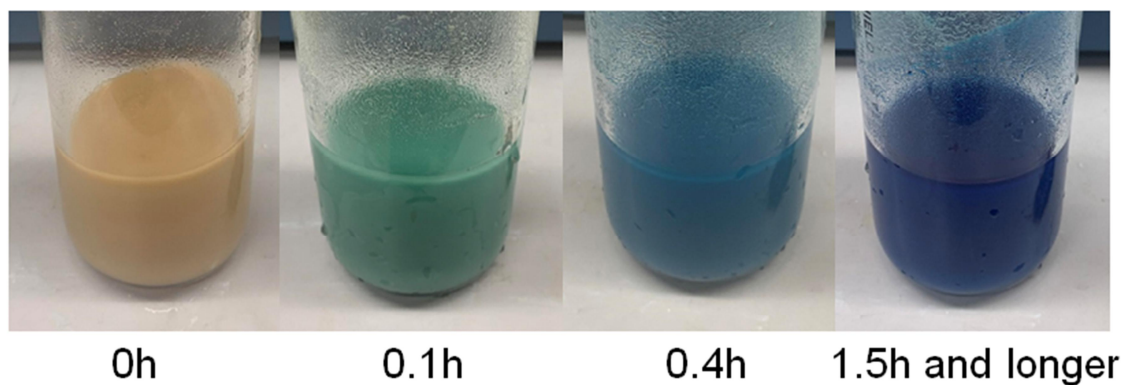


Figure 3.11 Photograph of the reactor after 1.5 hours of solvent extraction and varied time of UV irradiation. With sufficient time for HAT reaction, the blue color in UV irradiated reactors indicates the reduced state of DT, $H^+[W_{10}O_{32}]^{5-}$.

To track the reaction kinetics of oxidation reaction, the C=O stoichiometry of lignin oligomers with varied reaction time was also quantified (**Figure 3.10**). In the first 1.5 hours, different from the minor bond cleavage showed by modestly changed M_n , the C=O stoichiometry of the lignin increased from 0.83 to 1.11 mmol/g. Prolonging the reaction to 6 hours further increased the C=O stoichiometry to 1.34 mmol/g, proposing that the oxidation reaction is predominant in the early reaction. Intriguingly, after 6 hours, there was only a minor change in the C=O stoichiometry, from 1.34 to 1.44 mmol/g; it also dropped to 1.30 mmol/g when the reaction time was set to 96 hours, proposing a thorough HAR process and cleavage reaction. Taken as a whole, it can be concluded from this series of experiments that without additives, DT mainly works as an oxidant in the first 1.5 hours (**Figure 3.11**), while the cleavage reaction with DT as a photocatalyst keeps insufficient. After 6 hours, the potential of oxidation of DT has been fully exerted, with the steady state of DT changed to $H^+[W_{10}O_{32}]^{5-}$; subsequently, the bond cleavage reaction catalyzed by DT can proceed slowly and continuously without competition within 96 hours of reaction time.

3.3.3 Promotion of lignin oxidation reaction

Without an electron scavenger as an additive in the photocatalytic system, the C=O stoichiometry is limited below 1.44 mmol/g, which is far from building the dense DPNs. We acknowledged that dioxygen could promote the oxidation pathway, but it was possible that too much oxygen caused over-oxidation.²⁶ Besides, it's unrevealed whether the dioxygen promotes oxidation of the C_α -OH groups in the β -O-4 motifs by oxidizing the C_α radical or recovering the DT catalyst. Recently, sodium persulfate ($Na_2S_2O_8$), as a

water-soluble oxidant, was proven to be able to regenerate DT in the transformation of aliphatic C-H bonds to disulfides,³⁹ or oxime ethers.⁴⁰ Hydrogen peroxide was also reported to be an alternative to cocatalyze the oxidation of organic pollutants with DT.⁴¹

From both polymerization and mechanism perspectives, we chose dioxygen, sodium persulfate and hydrogen peroxide as electron scavenger candidates, and then applied the optimized photocatalytic system to native beech lignin for 24 hours. The C=O stoichiometry was focused as a direct indicator of oxidation reactions. With the knowledge that DT turnover can be promoted by these electron scavenger candidates, the M_n was also studied to determine if the cleavage reaction was also promoted.

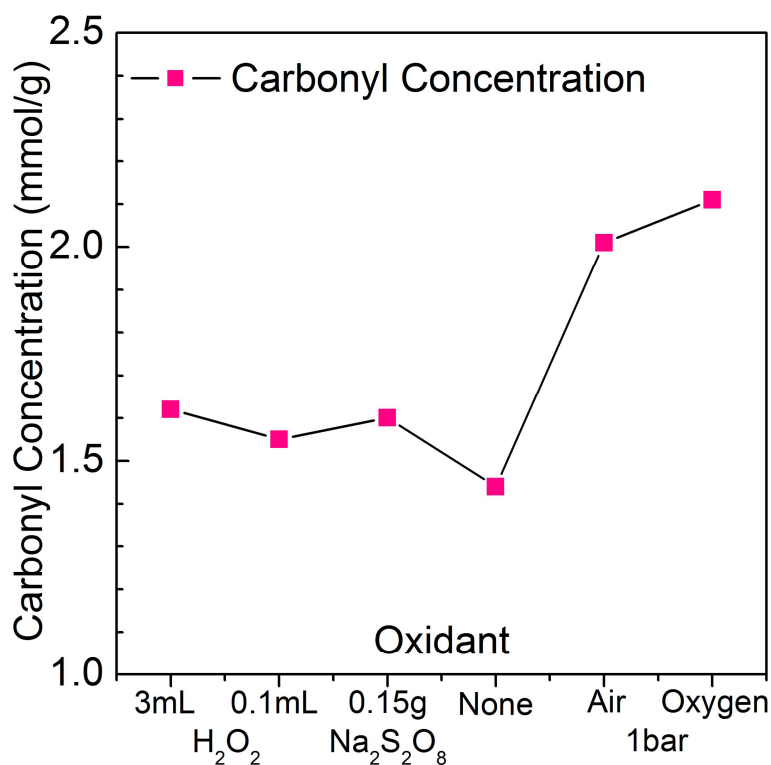


Figure 3.12 Comparison of the carbonyl concentration of the lignin oligomers from photocatalytic depolymerization of native lignin with different external electron scavengers or oxidants.

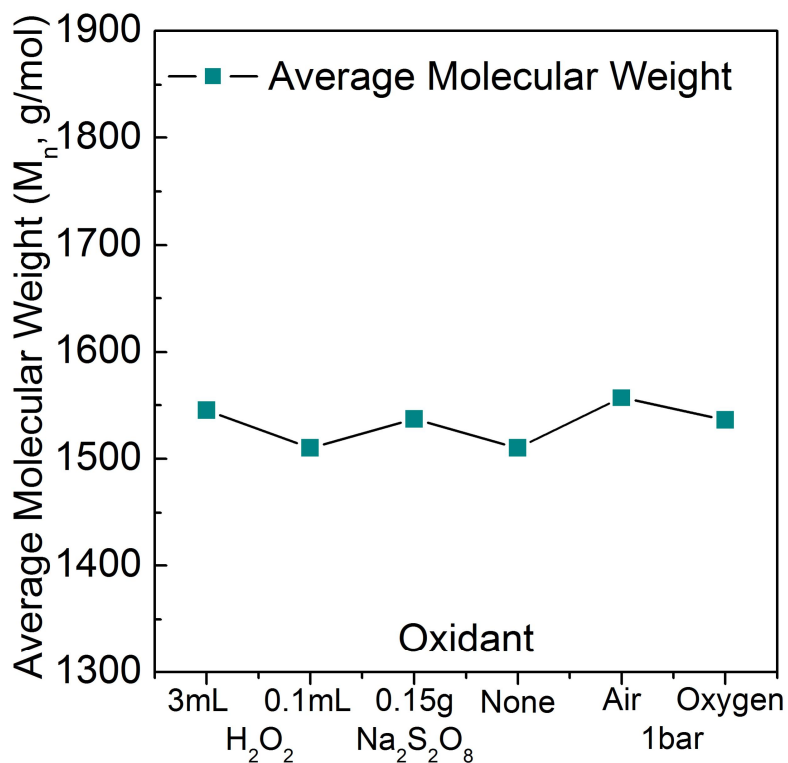


Figure 3.13 Comparison of the M_n of the lignin oligomers from photocatalytic depolymerization of native lignin with different external electron scavengers or oxidants.

Based on the C=O stoichiometry quantification results (**Figure 3.12**) of the lignin oligomers with different electron mediator candidates and varied adding amounts, we can find the uniqueness of dioxygen as an oxidant compared with hydrogen peroxide and sodium persulfate. With the same magnitude of oxidation equivalents, 1 bar air (in 20°C, 240 mL, containing 21 mmol O_2) and 30 mmol of hydrogen peroxide (from 3 ml of 10 mol/L concentrated solution, 100 equivalents calculated on DT) gave us totally different results. Adding air to the system as an oxidant significantly increased the C=O stoichiometry by 40% to 2.01 mmol/g, while using hydrogen peroxide as an electron scavenger to help DT turnover only increased the C=O stoichiometry by 12% to 1.62

mmol/g. Due to possible over-oxidation reaction, the C=O stoichiometry increase was moderate, from 2.01 to 2.11 mmol/g, when pure oxygen was used to purge the reactor. As an electron scavenger, there was no significant difference between hydrogen peroxide and sodium persulfate. With similar adding amounts (2 eq of sodium persulfate and 3.3 eq of hydrogen peroxide), there was no significant difference in the C=O stoichiometry (1.60 and 1.55 mmol/g, respectively). From the bond scission perspective, the M_n of all the other lignin oligomers were the same (**Figure 3.13**), regardless of the oxidant and the amount applied. From this, we inferred that the ameliorated DT turnover would not promote the cleavage of β -O-4 motifs. In other words, we propose that the rate-determining step (RDS) in our photocatalytic system for the cleavage pathway is the C β -O bond scission, instead of the turnover of DT. As for the exception, it could be attributed to changes in the activity of water, which was caused by a large amount of electrolytes.

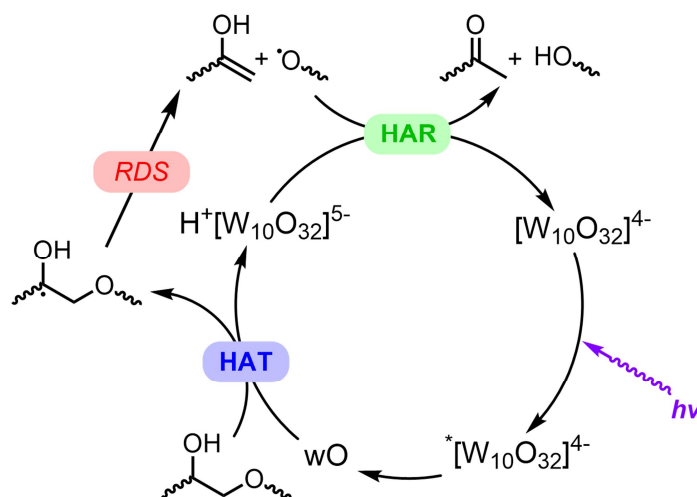


Figure 3.14 Catalytic cycle of DT in the cleavage pathway with an updated RDS.

attribute that the intermediate hydrogen superoxide radical ($\text{HO}_2\cdot$) is highly active and can further oxidize the C_α radical to a ketone (**Figure 3.16**).

3.3.4 Lignin polymerization from lignin oligomers with varied C=O stoichiometry

With a wide range of the C=O stoichiometry in the lignin oligomers intermediate, we have the ability to change the crosslinking density of the product, lignin-based DPNs. The C=O stoichiometry is the only parameter determining the crosslinking density if we use the bifunctional amine for the alternating copolymerization and avoid using macromolecular polymer filler. The relationship between the crosslinking density and the mechanical strength of the polymer networks was studied in the rubber-based products,⁴² hydrogels,⁴³ crosslinked PUR elastomers,⁴⁴ cyclodextrin-based nanosponges,⁴⁵ and inverse vulcanized sulfur-polymers.⁴⁶ However, different from theirs, our component lignin oligomer lends the lignin-based polymer rigidity by their highly conjugated structures, which is another complication for the brittleness of the polymer. To study the relationship between the crosslinking density and the resulting mechanical strength of the DPNs, we polymerized lignin oligomers with different C=O stoichiometry.

Due to the macromolecular nature of lignin oligomers, the solubility in DCM is limited without modification. To address this challenge, we acetylated all the aliphatic and aromatic hydroxyl groups for a minimum change of lignin bone structure. After the acetylation, all the C=O stoichiometry for lignin samples slightly decreased, kept the trend we observed on reaction time and oxidants the same (**Figure 3.17**).

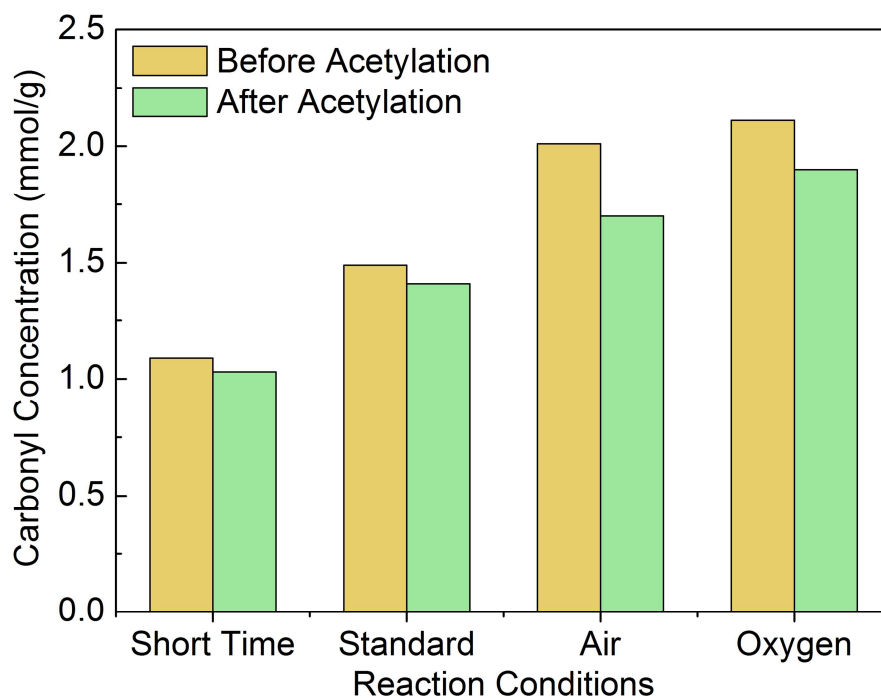


Figure 3.17 Comparison of the carbonyl concentration of the lignin oligomers before and after acetylation modification.

Inspired by the work of Bernaerts and co-workers,¹⁷ we added a small amount (5 wt%) of TPA as a plasticizer in the lignin-based polymer building. The polymer network consisted of 38 wt % lignin oligomers and 5 wt % of TPA, cross-linked 57 wt % Priamine™1075, a diamine cross-linker built from dimer fatty acid. A 5 wt % of TPA and a stoichiometric amount of cross-linker was found to be necessary to avoid overhardening and brittleness when it maintained the solid structure of the DPNs material.

3.4 DISCUSSION

In developing a new paradigm through the lignin-first strategy, we have taken a solid step forward. Compared with TBADT, NaDT brought us fewer side reactions, lower purification difficulty, and enabled us to perform the photocatalytic conversion of lignin on a larger scale. With an optimized catalytic system, we were allowed to study the reaction kinetics and the choice of external oxidant. Under insufficient reaction time, the NaDT-catalyzed lignin oxidation reaction will proceed first until the potential of the oxidation reaction fully realized. Due to the rate limitation in the C β -O bond scission step, the cleavage reaction will proceed slowly with a steady reaction rate. Applying external dioxygen as an additive promotes the oxidative pathway in the photocatalytic system, resulting in a significant increase of C=O stoichiometry. However, there's a minimum effect when only an electron scavenger is used to promote DT turnover. With the ability to continuously adjust the C=O stoichiometry from 1.03 to 1.90 mmol/g after acetylation, we successfully produced lignin-based DPNs without polymer filler.

3.5 REFERENCE

1. Galkin, M. V.; Samec, J. S., Lignin valorization through catalytic lignocellulose fractionation: a fundamental platform for the future biorefinery. *ChemSusChem* **2016**, *9*, 1544-1558.
2. Giardino, G. J.; Wang, H.; Niu, J.; Wang, D., From technical lignin to native lignin: Depolymerization, functionalization, and applications. *Chemical Physics Reviews* **2024**, *5*, No.2.

3. Vanholme, R.; De Meester, B.; Ralph, J.; Boerjan, W., Lignin biosynthesis and its integration into metabolism. *Current opinion in biotechnology* **2019**, *56*, 230-239.
4. Vanholme, R.; Demedts, B.; Morreel, K.; Ralph, J.; Boerjan, W., Lignin biosynthesis and structure. *Plant physiology* **2010**, *153*, 895-905.
5. Vishtal, A.; Kraslawski, A., Challenges in industrial applications of technical lignins. *BioResources* **2011**, *6*, 3547-3568.
6. Thi, H. D.; Van Aelst, K.; Van den Bosch, S.; Katahira, R.; Beckham, G. T.; Sels, B. F.; Van Geem, K. M., Identification and quantification of lignin monomers and oligomers from reductive catalytic fractionation of pine wood with GC× GC–FID/MS. *Green Chemistry* **2022**, *24*, 191-206.
7. Luo, H.; Weeda, E. P.; Alherech, M.; Anson, C. W.; Karlen, S. D.; Cui, Y.; Foster, C. E.; Stahl, S. S., Oxidative catalytic fractionation of lignocellulosic biomass under non-alkaline conditions. *Journal of the American Chemical Society* **2021**, *143*, 15462-15470.
8. Pappa, C.; Feghali, E.; Vanbroekhoven, K.; Triantafyllidis, K. S., Recent advances in epoxy resins and composites derived from lignin and related bio-oils. *Current Opinion in Green and Sustainable Chemistry* **2022**, *38*, 100687-100697.
9. Liu, G.; Jin, C.; Huo, S.; Kong, Z.; Chu, F., Preparation and properties of novel bio-based epoxy resin thermosets from lignin oligomers and cardanol. *International Journal of Biological Macromolecules* **2021**, *193*, 1400-1408.
10. Van Aelst, K.; Van Sinay, E.; Vangeel, T.; Zhang, Y.; Renders, T.; Van den Bosch, S.; Van Aelst, J.; Sels, B. F., Low molecular weight and highly functional RCF lignin products as a full bisphenol a replacer in bio-based epoxy resins. *Chemical Communications* **2021**, *57*, 5642-5645.
11. Li, R. J.; Gutierrez, J.; Chung, Y.-L.; Frank, C. W.; Billington, S. L.; Sattely, E. S., A lignin-epoxy resin derived from biomass as an alternative to formaldehyde-based wood adhesives. *Green chemistry* **2018**, *20*, 1459-1466.
12. Zhao, S.; Huang, X.; Whelton, A. J.; Abu-Omar, M. M., Formaldehyde-free method for incorporating lignin into epoxy thermosets. *ACS sustainable chemistry & engineering* **2018**, *6*, 10628-10636.

13. Zheng, Y.; Liu, T.; He, H.; Lv, Z.; Xu, J.; Ding, D.; Dai, L.; Huang, Z.; Si, C., Lignin-based epoxy composite vitrimers with light-controlled remoldability. *Advanced Composites and Hybrid Materials* **2023**, *6*, No. 53.
14. Liu, W.; Zhou, R.; Goh, H. L. S.; Huang, S.; Lu, X., From waste to functional additive: toughening epoxy resin with lignin. *ACS applied materials & interfaces* **2014**, *6*, 5810-5817.
15. Henry, C.; Nejad, M., Lignin-Based Low-Density Rigid Polyurethane/Polyisocyanurate Foams. *Industrial & Engineering Chemistry Research* **2023**, *62*, 6865-6873.
16. Li, S.; Zhang, Y.; Ma, X.; Qiu, S.; Chen, J.; Lu, G.; Jia, Z.; Zhu, J.; Yang, Q.; Chen, J., Antimicrobial lignin-based polyurethane/Ag composite foams for improving wound healing. *Biomacromolecules* **2022**, *23*, 1622-1632.
17. Liu, J.; Bernaerts, K. V., Preparation of lignin-based imine vitrimers and their potential application as repairable, self-cleaning, removable and degradable coatings. *Journal of Materials Chemistry A* **2024**, *12*, 2959-2973.
18. Bass, G. F.; Epps, T. H., Recent developments towards performance-enhancing lignin-based polymers. *Polymer Chemistry* **2021**, *12*, 4130-4158.
19. Agustiany, E. A.; Rasyidur Ridho, M.; Rahmi DN, M.; Madyaratri, E. W.; Falah, F.; Lubis, M. A. R.; Solihat, N. N.; Syamani, F. A.; Karungamye, P.; Sohail, A., Recent developments in lignin modification and its application in lignin - based green composites: a review. *Polymer Composites* **2022**, *43*, 4848-4865.
20. Zhou, S.-J.; Wang, H.-M.; Xiong, S.-J.; Sun, J.-M.; Wang, Y.-Y.; Yu, S.; Sun, Z.; Wen, J.-L.; Yuan, T.-Q., Technical lignin valorization in biodegradable polyester-based plastics (BPPs). *ACS Sustainable Chemistry & Engineering* **2021**, *9*, 12017-12042.
21. Xu, Y.; Odelius, K.; Hakkarainen, M., Recyclable and flexible polyester thermosets derived from microwave-processed lignin. *ACS Applied Polymer Materials* **2020**, *2*, 1917-1924.
22. Hanson, K. G.; Lin, C.-H.; Abu-Omar, M. M., Preparation and properties of renewable polyesters based on lignin-derived bisphenol. *Polymer* **2021**, *233*, 124202-124209.

23. Vendamme, R.; Behaghel de Bueren, J.; Gracia-Vitoria, J.; Isnard, F.; Mulunda, M. M.; Ortiz, P.; Wadekar, M.; Vanbroekhoven, K.; Wegmann, C.; Buser, R., Aldehyde-assisted lignocellulose fractionation provides unique lignin oligomers for the design of tunable polyurethane bioresins. *Biomacromolecules* **2020**, *21*, 4135-4148.
24. O’Dea, R. M.; Pranda, P. A.; Luo, Y.; Amitrano, A.; Ebikade, E. O.; Gottlieb, E. R.; Ajao, O.; Benali, M.; Vlachos, D. G.; Ierapetritou, M., Ambient-pressure lignin valorization to high-performance polymers by intensified reductive catalytic deconstruction. *Science Advances* **2022**, *8*, No. eabj7523.
25. Zheng, N.; Xu, Y.; Zhao, Q.; Xie, T., Dynamic covalent polymer networks: a molecular platform for designing functions beyond chemical recycling and self-healing. *Chemical Reviews* **2021**, *121*, 1716-1745.
26. Wang, H.; Giardino, G. J.; Chen, R.; Yang, C.; Niu, J.; Wang, D., Photocatalytic Depolymerization of Native Lignin toward Chemically Recyclable Polymer Networks. *ACS Central Science* **2022**, *9*, 48-55.
27. Xie, D.; Pu, Y.; Bryant, N. D.; Harper, D. P.; Wang, W.; Ragauskas, A. J.; Li, M., Synthesis of Bio-Based Repairable Polyimines with Tailored Properties by Lignin Fractionation. *ACS Sustainable Chemistry & Engineering* **2024**, *12*, 6606-6618.
28. Sarver, P. J.; Bissonnette, N. B.; MacMillan, D. W., Decatungstate-catalyzed C (sp³)–H sulfinylation: rapid access to diverse organosulfur functionality. *Journal of the American Chemical Society* **2021**, *143*, 9737-9743.
29. Hong, B.-C.; Indurmuddam, R. R., Tetrabutylammonium decatungstate (TBADT), a compelling and trailblazing catalyst for visible-light-induced organic photocatalysis. *Organic & Biomolecular Chemistry* **2024**, *22*, 3799-3842.
30. Tzirakis, M. D.; Lykakis, I. N.; Orfanopoulos, M., Decatungstate as an efficient photocatalyst in organic chemistry. *Chemical Society Reviews* **2009**, *38*, 2609-2621.
31. Nielsen, E. K.; El - Chami, K.; de Lichtenberg, C. M.; Madsen, R., Decatungstate - Catalyzed Carbon - Carbon Bond Formation Between Furfural and Electron - Deficient Olefins. *European Journal of Organic Chemistry* **2024**, *27*, No. e202400109.

32. Yamase, T.; Takabayashi, N.; Kaji, M., Solution photochemistry of tetrakis (tetrabutylammonium) decatungstate (VI) and catalytic hydrogen evolution from alcohols. *Journal of the Chemical Society, Dalton Transactions* **1984**, *5*, 793-799.
33. Veisi, H.; Maleki, B.; Hamelian, M.; Ashrafi, S. S., Chemoselective hydration of nitriles to amides using hydrated ionic liquid (IL) tetrabutylammonium hydroxide (TBAH) as a green catalyst. *RSC advances* **2015**, *5*, 6365-6371.
34. Zijlstra, D. S.; de Santi, A.; Oldenburger, B.; de Vries, J.; Barta, K.; Deuss, P. J., Extraction of lignin with high β -O-4 content by mild ethanol extraction and its effect on the depolymerization yield. *JoVE (Journal of Visualized Experiments)* **2019**, *143*, No. e58575.
35. Zijlstra, D. S.; Lahive, C. W.; Analbers, C. A.; Figueirêdo, M. B.; Wang, Z.; Lancefield, C. S.; Deuss, P. J., Mild organosolv lignin extraction with alcohols: the importance of benzylic alkoxylation. *ACS sustainable chemistry & engineering* **2020**, *8*, 5119-5131.
36. Zijlstra, D. S.; Analbers, C. A.; de Korte, J.; Wilbers, E.; Deuss, P. J., Efficient mild organosolv lignin extraction in a flow-through setup yielding lignin with high β -O-4 content. *Polymers* **2019**, *11*, 1913-1929.
37. Tanielian, C.; Cougnon, F.; Seghrouchni, R., Acetone, a substrate and a new solvent in decatungstate photocatalysis. *Journal of Molecular Catalysis A: Chemical* **2007**, *262*, 164-169.
38. Ravelli, D.; Fagnoni, M.; Fukuyama, T.; Nishikawa, T.; Ryu, I., Site-selective C–H functionalization by decatungstate anion photocatalysis: synergistic control by polar and steric effects expands the reaction scope. *ACS Catalysis* **2018**, *8*, 701-713.
39. Zhang, J.; Studer, A., Decatungstate-catalyzed radical disulfuration through direct CH functionalization for the preparation of unsymmetrical disulfides. *Nature Communications* **2022**, *13*, 3886-3893.
40. Wang, X.; Yu, M.; Song, H.; Liu, Y.; Wang, Q., Radical Transformation of Aliphatic C–H Bonds to Oxime Ethers via Hydrogen Atom Transfer. *Organic Letters* **2021**, *23*, 8353-8358.
41. Cheng, P.; Wang, Y.; Sarakha, M.; Mailhot, G., Enhancement of the photocatalytic activity of decatungstate, $W_{10}O_{32}^{4-}$, for the oxidation of

- sulfasalazine/sulfapyridine in the presence of hydrogen peroxide. *Journal of Photochemistry and Photobiology A: Chemistry* **2021**, *404*, 112890-112898.
42. Kim, D. Y.; Park, J. W.; Lee, D. Y.; Seo, K. H., Correlation between the crosslink characteristics and mechanical properties of natural rubber compound via accelerators and reinforcement. *Polymers* **2020**, *12*, 2020-2033.
43. Seo, J. W.; Shin, S. R.; Lee, M.-Y.; Cha, J. M.; Min, K. H.; Lee, S. C.; Shin, S. Y.; Bae, H., Injectable hydrogel derived from chitosan with tunable mechanical properties via hybrid-crosslinking system. *Carbohydrate Polymers* **2021**, *251*, 117036-117047.
44. Cai, Y.; Yan, L.; Wang, Y.; Ge, Y.; Liang, M.; Chen, Y.; Zou, H.; Zhou, S., A room temperature self-healing and thermally reprocessable cross-linked elastomer with unprecedented mechanical properties for ablation-resistant applications. *Chemical Engineering Journal* **2022**, *436*, 135156-135165.
45. Hoti, G.; Caldera, F.; Cecone, C.; Rubin Pedrazzo, A.; Anceschi, A.; Appleton, S. L.; Khazaei Monfared, Y.; Trotta, F., Effect of the cross-linking density on the swelling and rheological behavior of ester-bridged β -cyclodextrin nanosponges. *Materials* **2021**, *14*, 478-497.
46. Yan, P.; Zhao, W.; Zhang, B.; Jiang, L.; Petcher, S.; Smith, J. A.; Parker, D. J.; Cooper, A. I.; Lei, J.; Hasell, T., Inverse vulcanized polymers with shape memory, enhanced mechanical properties, and vitrimer behavior. *Angewandte Chemie International Edition* **2020**, *59*, 13371-13378.

CHAPTER 4: CONCLUSION

In conclusion, our effort built a new paradigm in which lignin is valorized first toward chemically recyclable polymer networks through highly functionalized lignin oligomers intermediate.

As the second most abundant natural and renewable polymers, it was unfair for lignin to get such underutilized. An important challenge is that the complicated chemical structure of lignin inhibits us from fully decomposing lignin toward monomers, which is more severe for technical lignin after pulping-caused condensation reaction. To maximize the monomerization efficiency, people chose to extract and depolymerize lignin first, when the cellulose and hemicellulose was left for paper making. The requirement to preserve the polysaccharides only allows us to use mild conditions to depolymerize lignin, so that we have to sacrifice the monomer yield (less than 40%) and accept the lignin oligomers as byproduct.

To take advantage of these lignin oligomers and maximize the atom utilization rate, we propose an alternative approach to use redox-neutral method to partially depolymerize lignin toward carbonyl-rich lignin oligomers. However, to convert this idea to a new paradigm, there are 2 key questions we have to answer: how can we effectively and selectively generate carbonyl-rich lignin oligomers, and how can we make these complicated lignin oligomers useful.

For the first question, in Chapter 2, we used TBADT photocatalytic system to depolymerize and oxidize lignin through HAT process. Cleavage pathway extracts the lignin and proposingly improves the flexibility of the resulting polymers, while the oxidation pathway increases the carbonyl stiochiometry of the lignin oligomers and subsequently increases the crosslink density, so both of these pathways are important. The photocatalytic system was first studied on lignin model compounds with high conversion rate, on which we successfully tuned the selectivity toward cleavage and oxidation pathway by adding external electron mediator or electron scavenger, respectively. With this promising preliminary results, we applied our photocatalytic system on native lignin to selectively produce highly functionalized lignin oligomers. In the meantime, we found that the effects of electron mediator and electron scavenger were similar as on model molecules, and proved that our photocatalytic system converted β -O-4 motifs to carbonyls. In chapter 3, we first optimized our photocatalyst from TBADT to NaDT, got rid of the impurities TBA⁺ and acetamide; then with an optimized solvent composition, we enlarged our scale from 30 to 300 mg lignin oligomers per day for the subsequent polymerization needs. Then we studied the kinetics for DT system with in this optimized photocatalysis, found that DT mainly worked as an oxidant before 1.5 hours and mainly worked as a catalyst after 6 hours. We also explored different electron scavenger candidates, found the uniqueness of dioxygen to directly oxidize the β -O-4 radicals instead of only promoting the DT turnover. With these knowledge in hand, we are able to tune the carbonyl concentration of lignin oligomers from 0.83 to 2.11 mmol/g for lignin-based polymers with different properties.

For the second question, we chose to focus on carbonyls instead of hydroxyl functionalities for the reversibility and recyclability to build a closed-loop economy. Among different kinds of dynamic polymers, we built a polyimine elastomer via the reaction between carbonyls and amine groups to cover the inactive ketone functionalities. Furthermore, we successfully recycled our polymer 3 times without significant loss in mechanical strength, proved the recyclability for lignin-based DPNs.

In the near future, we are working on building lignin-based polymers with differently functionalized lignin oligomers (from 1.03 to 1.90 mmol/g) to find the relationship between the C=O stoichiometry of lignin oligomers and mechanical or thermal properties of lignin-based polymers. In the far future, we expect to commercialize the lignin-based recyclable polymers built from lignin oligomer byproducts, so that we can take advantage of both lignin monomers as fine chemicals and lignin oligomers as building blocks for green polymers. Through which, the consumption of fossil fuels can be mitigated by using biomass as an alternative.